

Bioglycerol-to-propylene routes: from fundamental catalysis to process design and marketing

M. El Doukkali,^{(*)1,2} M. Bahlouri,^{1,2} S. Paul¹ F. Dumeignil,¹

¹*Univ. Lille, CNRS, Centrale Lille, Univ. Artois, UMR 8181, UCCS, Unité de Catalyse et Chimie du Solide, F-59000 Lille, France*

²*University of Sultan Moulay Slimane, Multidisciplinary Faculty of Beni-Mellal, Department of Chemistry, Av. Mghila, BP 592, 23000, Beni-Mellal, Morocco*

(*) Corresponding author. Tel.: (+33) 53 44 39 51; Fax: (+33) 03 20 43 65 61

Email: mohamed.eldoukkali@univ-lille.fr (*M. El Doukkali*)

ABSTRACT:

Bioglycerol-to-propylene (GTP) routes are undergoing major developments in terms of both fundamental catalysis and process design on the way to becoming a connecting bridge between the biorefinery and polyolefin industries. This review starts introducing some GTP routes-related market potentialities and continues discussing significant mechanistic, kinetic, and engineering developments in GTP catalysis involving high-temperature, multi-step, tandem, and single-step hydrodeoxygenation strategies. It highlights the main advances made in the design of efficient catalysts and in the elucidation of their active sites, thereby shedding light on state-of-the art preparation, functionalization, and characterization methods. The GTP mechanisms are also assessed over versatile metallic, acid, and bifunctional catalysts' surfaces to discover which C-O bond is removed and which C=C bond is formed. GTP configurations are discussed as a function of the thermodynamic and operating conditions affecting catalysts' reactivity, selectivity, and stability. They are also compared using various qualitative and quantitative criteria such as process configuration, severity of operating conditions, energy consumption, sustainability assessment, and propylene production. We thus intend to provide a broad overview of GTP catalysis for inducing new opportunities in the biorefinery-to-olefins field.

Keywords: Bioglycerol-to-propylene catalysis, catalyst design, active sites requirement, mechanisms, reaction conditions, process configurations, thermodynamics-kinetics, market potentialities.

Introduction

1.1. Background

Light olefins, especially propylene and ethylene, are the most widely used feedstocks in the chemical industry.¹⁻³ They are currently produced mainly from fossil heavy-oils, naphtha fractions, and propane/ethane using petroleum-based technologies (Scheme 1).²⁻⁵ Although they are well-developed industrial processes used worldwide, the production of propylene usually experiences a continuous shortage in availability and price fluctuations, which are mainly due to excess of market demand, changes in industrial manufacturing methods and transportation rules, political conflict, and social restrictions (*i.e.*, the ongoing war in Ukraine and COVID-19).^{1,6-8} This prompts a need for feedstock diversification to introduce some flexibility into the production of propylene and its logistical supply and distribution.

In turn, the traditional light olefins production industry is now considered, together with steel and glass manufacturing, as the most polluting and energy-intensive one.^{9,10} The environmental issues stemming from excessive energy consumption and the use of fossil-based resources pose real threats to environmental preservation.¹⁰⁻¹²

The conflation of these environmental-energy issues together with the instability of markets and the upcoming shortage of fossil-fuel reserves are driving an increasing number of countries to adopt more sustainable policies for consolidating socio-economic progress. For example, the European Union is actively following the guidelines of Directives 2018/2001/EC¹³ and 2009/28/EC,¹⁴ designed to achieve a 20% global share in bio-based products and reduce CO₂ emissions by 30%, on the way to achieve carbon neutrality by 2050.¹⁵ In turn, the United Nations has recently adopted the new “2030 Agenda for Sustainable Development”,¹⁶ aimed at promoting a circular economy with a low-carbon footprint.^{11,17} Numerous academic and industrial collaboration programs are funding research projects for advancing the recovery and upgrading of carbon sources co-generated by the production chains in olefin industries and their byproducts. The aim is to comply with global targets for future CO₂-neutral plastic manufacturing, thereby reducing its harmful impacts on health, environment, and security.

1.2. Research context

Within this aforementioned broad context, numerous specific studies have focused on the development of more eco-friendly technologies for producing sustainable C₂-C₄ olefins as an alternative to fossil-based ones or ultimately to introduce further flexibility in traditional technologies. There are such

examples as the pyrolysis of industrial-urban wastes,^{18–20} biomass fermentation to bioethanol followed by subsequent dehydration, dimerization and metathesis to propylene,^{21–23} biomass liquification to crude bio-oil followed by hydrotreatment and cracking to olefins,^{20,22,24,25} or biomass gasification to syngas followed by Fischer–Tropsch (FT) synthesis, and methanol-to-propylene (MTP) or methanol-to-olefins (MTO).^{22,26–29}

More recently, novel bio-based routes such as bioglycerol-to-propylene (GTP) catalysis ([Scheme 1](#)) are attracting a great deal of research interest focusing on the following: *i*) finding a mass application for the widely available crude bioglycerol, which is nonetheless largely considered a waste byproduct in the global biorefinery industry,^{30–32} and *ii*) introducing a new biofeedstock for the global polyolefin manufacturing industry, which is heavily exposed to the so-called “*propylene gap*”- excess of market demand over its real production. Thus, the topic of GTP catalysis dovetails perfectly with global efforts to mitigate climate change and the future depletion of fossil resources. For example, it may contribute to lowering biodiesel costs, diversifying propylene feedstock, and avoiding the reduced availability of ethylene (reference for olefin price). It may also open new perspectives for integrating GTP routes with the well-developed technology of renewable Power-to-Hydrogen, particularly, in countries where there is an excess production of solar energy, wind, electricity, etc.

Indeed, GTP routes is undergoing advances in research in terms of both fundamental catalysis and process design^{27,28,33–60,60–67} by exploring different transformation strategies from both heterogeneous and homogeneous catalysis. GTP routes are being investigated through high-temperature processes,^{28,35,35,38,41,45,56,66,67} multi-steps reactions, including triple-stage reactors,^{50,64} separate double reactors,^{53,64,65} tandem or dual-bed catalysts,^{28,42,49,53} and single-step conversion strategies.^{37,43,44,46–48,52,54,55,57–63} These studies conclude that in the future GTP catalysis may become a sustainable bridging route between the biorefinery and polyolefin industries. Nonetheless, integrating GTP routes in a unified network, from biomass to sustainable propylene, raises intrinsic challenges, such as the nature of the most efficient GTP configurations, control of the interoperability of multi-steps and/or combined bed reactors, influenced by contact states between catalyst beds, operating conditions, reaction mechanisms, and so forth.

1.3. Scope of the review

We have recently published new insights to fill some of the gaps in GTP catalysis.⁶⁰ Indeed, despite the important advances made in this field over the past decade, no attempt has been made accordingly to comprehensively examine GTP catalysis in a single review. So far, and to the best of our knowledge,

the following studies are the only ones that have in some way addressed GTP routes, albeit some time ago: three related chapters^{27,33,36} and two related mini-reviews.^{34,35} These studies are very similar and focus more on a phenomenological description of certain sustainable processes and biofeedstocks (*e.g.*, ethanol, butanol, bio-oils, and general biomass) for producing light olefins (C₂-C₄). Moreover, the information reported on specific GTP catalysis is very succinct, of a general nature, and incomplete. These studies do not cover the most recent research findings (2018-2023) or the patented information. Our review project is therefore designed to provide a balanced assessment of the current state-of-the-art by covering contributions from the earliest discoveries (5-10 years ago) through to the most recent GTP-related publications and patents. The objective is to provide the research community with an all-comprehensive analysis of the main developments in the field of GTP catalysis. The aim is to go beyond a general description and provide a timely, critical, and systematic discussion of the mechanistic, kinetic, and engineering advances in GTP routes and their market potential.

As illustrated in [Scheme 2](#), this review is organized into interconnected sections to directly introduce the contexts and potential of producing sustainable propylene from crude bioglycerol. Thus, the main advances made in the design of efficient catalysts and in the elucidation of their active sites for GTP catalysis will be critically addressed, highlighting cutting-edge preparation, functionalization, and characterization methods. Our latest report on the single-step hydrodeoxygenation (HDO) of bioglycerol-to-propylene⁶⁰ are compared with the current state-of-the-art in GTP routes for filling existing gaps and postulating future trends in the re-modulation of the target catalytic properties. The discussion focuses on how to overcome catalyst instability in aqueous media, which is still a huge challenge, and the need for cutting-edge, *in situ*, and operando techniques, allowing more precise elucidation of active sites and mechanisms. GTP catalysis is also assessed in terms of reaction pathways under versatile metallic, redox, acid, and bifunctional catalysts' surfaces to understand when the C-O bond is removed and when the C=Cone is formed, and why certain systems perform better than others. A critical comparison is made between all the GTP configurations as a function of the thermodynamic limits and operating conditions affecting catalyst reactivity, selectivity, and stability. Other qualitative and quantitative indicators, such as severity, energy consumption, cost, viability, and/or sustainability aspects (CO₂ emission) have also been considered for the GTP routes. By considering all these aspects, we aim at identifying existing research gaps in GTP catalysis and discuss novel approaches, allowing for further progresses to be made towards the development of efficient strategies for producing sustainable propylene, thereby presenting new openings in the biorefinery-to-olefins field.

Setting the scene for GTP

The following two sub-sections provide a comprehensive analysis of the technological issues and market considerations behind the need for developing novel GTP routes. The related data were gathered from open literature sources and databases to provide an overview of current GTP routes technology.

1.4. The need for sustainable propylene production: The current situation

Propylene belongs to the group of alkenes with three carbon atoms, two of which are double bonded (C=C-C). The relative weakness of this latter bond explains its easy reactivity through different processes such as (co)- and polymerization,⁶⁸⁻⁷¹ oxidation,^{72,73} halogenation,^{74,75} epoxidation,^{76,77} alkylation,^{78,79} oligomerization, and dimerization,^{80,81} etc. This useful reactivity and properties (Table 1^{82,83}) mean that propylene is one of the main platform molecules for several sectors such as the petrochemical, plastics, textile, and automotive industries. Fig. 1 A shows that propylene is used mainly for the production of polypropylene (64 %), acrylonitrile (10 %), oxo/iso alcohols (9 %), and sundry other products (17 %).⁸⁴⁻⁸⁶ This is prompting a clear growth in global economy and demand regarding the effective production capacity and the supply chain (Fig. 1 B-C).

Despite the slightly negative impact the COVID-19 pandemic has had on the demand for olefins,^{1,6,87} particularly between 2020-2021, when the demand for propylene shrank by 1.8 % (Fig. 1B), the global market for propylene was worth around \$97.6 billion in 2022, and it is expected to grow to \$117.9 billion in 2026, at a compound annual rate of 4.8 %.^{85,88} This high demand is being driven primarily by the increasing use of polypropylene and the extensive application of polymers and fibers in electronic devices and vehicles, which is being further stimulated by the growing economic development of emerging countries.^{84-86,88,89} Polypropylene is therefore projected to continue to be the dominant outlet for propylene, and its overall share among the global propylene market will increase even further through to 2029. For example, the global market volume for thermoplastic from polypropylene alone in 2022 amounted to approximately 76 million metric tons (MmT), and it is forecast to grow to almost 100 MmT by 2029, increasing at an annual rate of 3.6 %.⁹⁰ Consequently, global propylene demand has doubled over the past twenty years,^{8,85} and is expected to reach 158.1 MmT/year in 2027/28,⁹¹ at an annual growth rate of more than 5.2-6.1 %.^{85,86,91} Global industrial output is expected to rise from 144.16 MmT in 2021 to approximately 209.18 MmT by 2030,⁹² mostly due to new plants that are scheduled to come online in Asia and the Middle East.⁹³ Nonetheless, the true production of propylene remained below 125 MmT in 2022. This was due to manufacturing

problems (*i.e.*, the shift towards shale gas fracking⁸⁷), among other supply and geopolitical issues, such as trade disputes between the US and China, the war in Ukraine, and Covid-19 uncertainties.^{1,6,7,94} Moreover, these problems are ongoing and overlap, whereby the demand for propylene will continue outpacing its production, which means that the current supply cannot keep up. This gap in propylene may be further aggravated by the emergence of fracking, which is likely to lead to a shortage in some geographical areas, specifically in North America and Europe.^{6,94,95} As a result of this uncertain scenario, the average price of propylene has increased over the past three years by more than 45 %, rising from 778 \$/metric ton (mT) in 2020 to approximately 1133 \$/mT in 2022.⁹⁶ Against this backdrop, the international propylene market keeps growing yearly at an average rate of 4-6.5 %, ⁸⁴ which will put an additional burden on the supply of this key resource for the global economy.

A further aggravating problem is the fossil origin of the propylene available on international markets.⁹⁻¹² At least 80-90 % of propylene is currently produced by environmentally harmful technologies such as Steam cracking (SC), Fluidized catalytic cracking (FCC), and Propane dehydrogenation (PDH), which involve intensive energy consumption and high ecological and health hazards.^{2-5,9,10,12,33}

The largest source of propylene (~42 %) is the conventional SC of light oil fractions (naphtha, light paraffins, and middle distillate fuels) and the shale-gas used for producing ethylene,^{2,97,98} where propylene is a byproduct with a yield of 1.6-18%.^{33,34} SC is a highly endothermic process, which is carried out without a catalyst under steam at high temperatures of ~800-1200 °C. The process energy consumption in a typical SC plant generally accounts for more than 70 % of production costs,⁹ while CO₂ emissions may amount to 15 mT/ton of ethylene.⁹⁹

The second largest supply source (~39 %) is the FCC of heavy crude or vacuum gas oils to produce gasoline and light distillates, where propylene is co-produced with a yield < 15 %.^{3,4,100-106} This process provides certain flexibility operating at 500-650 °C; however, the yield is generally small at low temperatures. Hence the reason it is mainly combined with PDH plants^{87,107,108} to improve propylene yield up to 25 %. This combination involves huge facilities that consume enormous amounts of energy because the endothermic PDH reaction involves volume expansion,⁸⁷ and requires increasing the temperature to enhance the dehydrogenation rate. In turn, bespoke olefin technologies such as PDH,^{107,108} MTO,^{26,109,110} and MTP,^{111,112} make a smaller contribution due to their lower economic performance compared to the two first SC and FCC technologies.¹⁰⁸

Overall, all these processes involve *i)* significant energy consumption, *ii)* a high carbon footprint (problematic CO₂ recovery), and *iii)* fast catalyst deactivation (*e.g.*, coke formation, particle attrition, and poisoning). Some olefin conversion technologies (*i.e.*, metathesis¹¹³⁻¹¹⁵) provide more flexibility,

but their efficiency requires further development and their viability also depends on the supply of raw feedstocks (fossil-based ethylene and butylene) , which limit their contribution to bridging the gap between propylene supply and demand.

Synthetic Summary: As mentioned above, the factors destabilizing the traditional propylene market mainly involve logistical-management concerns, with the intensive energy consumption of production prompting environmental concerns. The future depletion of fossil resources and the rising costs of commodities due to political or social issues add further problems. This uncertain scenario renders it necessary to find other sustainable processes to overcome these problems.

1.5. Targeting crude bioglycerol as a renewable feedstock for propylene

The rapid technological and industrial development of the biorefinery has exponentially increased the global production of crude bioglycerol. ^{116,117} Processes such as transesterification, saponification, hydrolyzation, and even the fermentation of biomass can co-produce up to 10 wt%. of crude bioglycerol, depending to the target product (*i.e.*, biodiesel, fatty acids, bioethanol, etc.).^{30,118–120} All these bio-based resources are directly related to the market for fossil feedstocks that set the initial prices and market tendencies. ^{121,122}

Fig. 2 A illustrates the evolution of the actual figures (2010–2022) and predicted ones (2023–2030) for the world production of the main two biofuels; biodiesel and bioethanol, with which crude bioglycerol is usually co-produced. These data, taken from the recent OECD-FAO Agricultural Outlook, ^{123,124} indicate an enormous potential for growth. Thus, output of crude bioglycerol rose from 8.3 MmT in 2010 to more than 12 MmT in 2022. It is expected to grow at a rate of 4.5 wt% per year, with a projected value of 15 MmT by 2030, due mainly to the increasing use of second and third generation biomass (*i.e.*, non-edible oils, ^{125–127} waste animal fats,^{127,128} *Jatropha*, ^{129,130} and algae. ^{131,132}). This global glut in crude bioglycerol, of which the treatment as a waste is currently more of a burden than an economic opportunity, impairs the value of the entire biofuel chain. Furthermore, this ever-growing trend ^{121,126} is also causing serious environmental problems.

Despite glycerol's benign properties (Table 1^{118,133,134}), the management of crude glycerol is challenging because of its abundance and impurities (*e.g.*, methanol, water, fatty acids, unreacted glyceride, salts, sulfurs,). ^{31,32,121,135} Many smaller biorefinery plants therefore assign it zero value, and simply dispose of it as a waste to avoid costly multiprocessing. ^{118,136,137}

Medium-sized plants directly burn crude glycerol to produce energy. ^{32,137–140} These practices are not environmentally friendly due to the formation of highly toxic substances (*i.e.*, acrolein) and CO₂

emissions that increase the process's carbon footprint. Besides, the net amount of energy produced is very modest (~18-25.3 MJ/kg^{140,141}) due to glycerol's high ignition temperature (Table 1) and because crude bioglycerol contains a lot of water. Early alternatives involved long-term storage of crude bioglycerol in abandoned mines, but various studies¹⁴¹⁻¹⁴³ have revealed that its impurities (i.e. methanol, wastewater with high salinity or alkalinity, etc.) can lead to an unacceptable level of groundwater contamination and the inhibition of microbial growth. In turn, the largest biorefineries seek to refine crude bioglycerol as a treated commodity to be sold for \$0.6- \$9 per kg, depending on the target sectors.^{30,32,118,121,144-146}

In 2020, refined bioglycerol amounted to around 2.5 MmT,¹⁴⁷ which accounted for less than 23 % of the total crude glycerol generated in the world,¹²¹ but the market of main uses (Fig. 2 B) is tending to saturation. In addition, the costly multi-steps of refining are undermining the commercial viability of these strategies.^{31,32} The price of unrefined bioglycerol does not usually exceed ~\$0.11-0.33 per kg,¹¹⁸ depending on the content of glycerol and impurities.

The combination of low prices and market saturation means that around 65-77% of all crude bioglycerol is currently treated as waste.^{121,148} This situation is expected to remain unchanged at least until 2050, given the high number of new biorefinery facilities that will be opening over the coming years, particularly in East Asia and South America.^{126,146} The availability of crude bioglycerol will therefore continue to grow annually, driven by the use of non-standard bioresources for the production of second and third generation biofuels. This boom may help to repeat the success of first-generation biofuels, so bioglycerol co-generation will continue to grow annually. 50 MmT/year of biodiesel are expected to be produced from these renewable sources, meaning the availability of an even larger amount of bioglycerol in the future.^{126,146}

The combination of abundant crude bioglycerol with problematic mis-management issues is driving research to develop new upgrading strategies. Fig. 3 reveals the high number of studies published each year. These studies have used thermochemical and catalytic strategies designed to re-demodulate the high oxophilicity of glycerol.^{116,117,121,136,146} Scheme 3 shows that reactions such as esterification,¹⁴⁹⁻¹⁵¹ reforming,^{152,153} oxidation,¹⁵⁴⁻¹⁵⁶ dehydration,¹⁵⁷⁻¹⁵⁹ hydrogenolysis,^{160,161} and hydrodeoxygenation,^{34,161-163} have been explored in an attempt to convert bioglycerol into useful intermediates (i.e., mono-alcohols, hydrogen, syn-gas, acrolein, ally-alcohol, diols, and light olefins, among others). The initial idea was to convert glycerol into a platform molecule as a sustainable-based equivalent of propylene for petrochemistry.

These approaches involve mainly the activation and reactivity of C-O, O-H, C-C, and/or C-H bonds, depending on the target product. For example, breaking C-H and C-C bonds necessarily leads to CO₂ emissions.^{164,165} Even though that this bio-based CO₂ is less problematic than that the fossil-based ones, however, its capture, storage and transport are still difficult to be immediately harness in form of useful end products.

In turn, oxidation, esterification, and dehydration require a high selectivity towards the desired liquid products in order to avoid the costly multi-distillations of liquid phases. However, only a few of these processes may be economically viable (*i.e.*, glycerol to propylene glycerol,^{116,166} glycerol to acrolein^{116,157}) if the costly separation process is solved. Furthermore, the viability of these early technologies will also depend on the market prices of refined bioglycerol directly linked to the policies adopted by biofuel producing countries.^{116,117} This list of issues is clearly not exhaustive, but only indicative of the need for continuing the search for efficient upgrading strategies to directly convert crude bioglycerol into an industrial-scale intermediate. The target process should operate under moderate temperatures and pressure conditions without CO₂ emissions to maintain a low carbon footprint. These factors are important for reducing processing costs, increasing income, and minimizing the environmental impact.

Synthetic conclusion: Design an efficient GTP technology will improve not only biorefinery viability and the supply for short-chain olefins, but will also mitigate the sustainability issues affecting the global environment, thereby contributing to a greener economic future. For example, simple calculus indicates that the HDO of all surplus crude bioglycerol, which currently amounts to more than 11 MmT/year (Fig. 2 A), to sustainable propylene may theoretically replace at least ~10.5 wt% of pre-existing fossil-based propylene or provide an additional volume to the international market, thereby, contributing to mitigate "propylene gap". In addition, the current price of propylene is ~seven times higher than crude bioglycerol,^{96,118} which could boost the competitiveness of the biorefinery sector. For example, the major drawback with biodiesel is still the high cost of its industrial production, which ranges from \$0.2/kg to \$0.4/kg, without including logistical and managements issues.^{167,168} Moreover, several biorefinery plants in certain European countries (*i.e.*, France, Spain, and Italy) are not operating to their full capacity due to the low economic competitiveness of biodiesel compared to fossil fuels and foreign imports.¹⁶⁹

The state-of-the-art of GTP catalysis

1.6. Latest developments in active sites identification and catalyst design

There is still no commercialized GTP catalyst that can convert crude bioglycerol under hydrothermal conditions to produce a high propylene yield without excessive H₂ consumption. Thus, cutting-edge preparation and functionalization strategies are being explored to improve the catalyst properties for the GTP reaction in both a homo- and heterogeneous catalysis medium.^{27,28,33–61,63–65} These efforts are focusing on controlling the nature and population of active sites for efficiently eliminating C-O and controlling C-C hydrogenation.

In a homogeneous medium, the catalyst is used as a liquid or gas in full contact with the reactant,^{43,57,65} whereas in a heterogeneous catalysis, the approach involves dispersing an active species over a solid support to improve its functional characteristics.^{27,28,34,35,41,42,60} Impregnation is the most widely used method for developing a GTP catalyst because of its ease of use; however, it may lead to low metal dispersion and easy leaching in an aqueous medium, particularly when with a high loading of metals.⁴⁸ Other synthesis strategies, such as *pH*-assisted,⁶³ slurry⁶³ or sequential impregnation,^{42,49,53,63} modified impregnations,^{28,38,42,45,49,50,64} co-precipitation,^{47,48,53,55,59} homogeneous dissolution, and/or post-recrystallization,^{43,57,65} melt-infiltration,⁶⁰ physical vapor deposition (PVD),^{39,58} physical mixtures,^{41,66} or include combined methods.^{28,42,47–49,53–55,57,59} The pre-activation treatment of the catalyst, which depends on the active sites required for the target GTP reaction, involves mainly *in situ* or *ex situ* thermo-treatments under a controlled atmosphere, such as calcination,^{38,38,41,45,45,50} reduction,^{43,44,47,48,54,59,61,63} carburization,^{58,60} sulfidation,^{46,61} or include the co-feed of acids or reductive agents or hydrogen donor molecules^{43,46,49,54,57,60} With these strategies, the type and population of target active centers are subject to mainly physicochemical modulations by controlling the interactions between the centers and the environment, chemical states, site-regeneration, geometrical exposures, and dispersion, for example.

The species studied for GTP reactions are noble metals (*e.g.*, Ir,^{49,53,61,63} Ru,^{43,49,53,54,57,63} Pt,^{28,44,50,53,58,61,63} Pd,^{44,50,55,61,63} Rh,^{49,53} and Re,⁴⁹), functionalized systems based on non-noble transition metals (*e.g.*, MoO_x,^{37,45–48,55,59–63} β-Mo₂C,^{58,60} η-MoC,⁶⁰ NiMoS_x,⁴⁶ WO_x,^{42,61,63,64} Ni,^{35,38,49,54,55,61,63} Cr,^{35,38,54,61,63} Fe,^{45,47,48,55,59,61,63} Zn,^{55,61,63,64} V,^{42,61,63,64} Nb,^{45,61,63} Cu,^{28,38,42,49,51,55,58,61,63}), non-metals (*e.g.*, Li,³⁸ Ca,³⁸ Mg,³⁸ HBO₃,⁶⁴ I,⁶⁵ P,^{49,64} Br,⁴³ and Carbon,^{47,48,54,55,59,60,63,64}), oxides such as Al₂O₃,^{35,38,46,49,50,50,53,64} SiO₂,^{49,53,60,64} SiO₂-Al₂O₃,^{28,41,42,49} TiO₂,^{53,64} ZrO₂,^{53,64} and zeolites (*e.g.*, Beta, Y, USY, Mordenite, and ZSM-5).^{28,35,38,41,45,49–51,53,64} The physicochemistry of these systems (*i.e.*, element loading, geometry, location, chemical states, and acidity) have been systemically characterized by

numerous techniques (see Table 2 and abbreviations list in the supplementary information file). Density-functional theory (DFT)^{37,39} and microkinetic modeling³⁷ have also been combined to support the design of the target catalysts. Table 2 provides a summary of the preparation and activation conditions for the catalysts studied and their most relevant physiochemistry for the GTP reaction.

1.6.1. Acid systems catalyzing GTP at high temperature

For the acid surface catalysis, Corma *et al.*⁴¹ have been the first to use acid aluminosilicates for converting glycerol to light olefins at high temperatures. Among these systems, HZSM-5 records a greater affinity toward C₂₋₃ olefin formation and less tendency to coke (< 20 %), which were attributed to its significant Brønsted acid sites (Si-OH-Al) and uniform micro-porosity ~0.5 nm. The other systems tend to yield more coke (30–50 %), causing fast deactivation; USY ~ FCC > γ -Al₂O₃ > ECat. They might also undergo dealumination, mainly under hot steam.^{170,171} To attenuate deactivation, they have used a moving-bed FCC reactor for the *in situ* regeneration of coked zeolite or for replacing dealuminated catalyst.⁴¹ In addition, physically mixing ZSM-5 with FCC systems improve C₂₋₃ olefin formation from glycerol cracking because of ZSM-5's good properties and resistance to coke.

Blass *et al.*⁵⁰ have studied the effect of pore shape on GTP selectivity over combined acid H-zeolites with hydrogenating catalysts (*i.e.*, Pt or Pd-based Al₂O₃). Increasing the pore size from 10-MR in HZSM-5 to 12-MR in HBEA (Fig. 4 A) shifts the formation of ethylene and propylene to heavy C₄₊ olefins, as larger pores seem to accommodate compounds with longer carbon-chains.

Zakaria^{35,38,51} has tailored the HZSM-5 surface by impregnating ~30 wt% of different elements such as Al, Ca, Cr, Mg, Cu, Li, Ni on HZSM-5. A direct relationship has not been found between their texture and olefin formation. However, the incorporation of metal seems to balance ZSM-5 acidity, thereby improving the yield of C₂₋₄ olefins. The Cu/ZSM-5 catalyst, which has Cu²⁺/Cu⁰ species alongside a higher amount of moderate and strong acid sites, leads mainly to ethylene, while the Cr/ZSM-5 catalyst produces the highest TOF_{propylene} (Fig. 4 C). More recently, Lima *et al.*⁴⁵ have adopted a similar approach by impregnating ~2.5 wt% of Mo, Fe or Nb on HZSM-5. Despite the low loading of metals, there is a major change in the total acidity of ZSM-5 and its distribution. The Fe/ZSM-5 catalyst, which exhibits the highest increase in both the population and strength of medium and strong acid sites, leads to propylene and ethylene (selectivity ~33 % and ~19 %, respectively). However, significant surface acidity favors competitive C-C breaking events, which decrease GTP yield after a few hours. In turn, Wu *et al.*²⁸ have controlled the acidity of aluminosilicate materials by varying their Si/Al ratio, while their bi-functionalities are improved by impregnating transition metals. Pt/ZSM-5 boosts the initial hydrogenolysis of glycerol to propanol. Balancing the ratio of weak to

strong acid sites in HZSM-5 by setting Si/Al at 127 significantly improves the subsequent dehydration of propanol to propylene selectivity (~76 %).²⁸ This rationalization minimizes coke formation, extending the lifetime of the catalyst to ~500 h, which can also be associated with the H₂-rich medium used instead of an N₂ atmosphere. These findings are consistent with those reported by Xiao *et al.*⁴⁴ and Murata *et al.*⁵² whereby noble metal sites entail an additional hydrogenation bifunction for HZSM-5, increasing its pre-existing acid dehydration sites for efficient glycerol to olefins and avoids aromatization trends.^{28,44}

1.6.2. Metallic and/or multifunctional systems catalyzing GTP under typical HDO conditions

In 2009, Taher *et al.*⁵⁷ have been the first in reporting the formation of propylene during catalytic deoxygenation of glycerol under typical HDO conditions using Ru complexes based catalyst, and since 2011, an increasing number of noble and non-noble metals and oxides have been studied as catalysts for the GTP reaction.^{28,42,49,53} These systems include combined bifunctional Ir/ZrO₂⁵³ or MoO₃-Ni₂P/Al₂O₃⁴⁹ with acid HZSM-5 in tandem mode, with a good synergy between H₂-dissociation, hydrogenolysis, and dehydration events (Fig. 5 A). This cooperative effect raises propylene selectivity to 88 %, which is comparable to that obtained under simulated crude glycerol. However, H₂-transfer from methanol to glycerol leads to excessive coke deposition,^{28,49} as corroborated by comparing the spent HZSM-5 sample in the GTP reaction with the catalysts usually used in industrial MTP process,^{28,29,111,172} Sun *et al.*⁴² have also adopted a similar dual-bed approach inspired by an early tandem process⁵³ to combine metallic species with acid aluminosilicates catalysts. NH₃-TPD shows (Fig 5 B) that the population of acid sites depends heavily on the temperature of the calcination process and the content of impregnated species on the support, while H₂-treatment at 250 °C (Fig 5 C) suffices to fully reduce the Cu precursor to Cu⁰. This synchronization of metals with acid species greatly boosts the hydrogenolysis and dehydration events in glycerol and intermediates, yielding 84.8 % of propylene. However, such combination of complex catalyst mixtures with less defined active sites hinders the *in situ* regeneration of the spent catalysts because acid sites require mainly specific oxidative agents, whereas metallic or redox sites involve a reducer atmosphere.

Among the first patents, Hulteberg *et al.*⁶⁴ have used impregnation to re-modulate the properties of various metals and non-metallic systems, from which a combination of three, WO₃ (10 wt%)/ZrO₂, Cu (10 wt%)/ZnO₂ and (10 wt%)/ZrO₂ catalysts yield 46 % propylene. Fadigas *et al.*⁶³ have combined modified-*pH* and slurry impregnations to study a vast array of metals from group VIII-B (M₁= Fe, Ni, etc.) and group VI-B (M₂= Mo, W, Cr, etc.). Specific mixed phases (with atomic ratios M₁/(M₁+M₂))

= 0.2-0.4) have been reported as active sites for propylene and propane formation (with a selectivity up to ~90 %).⁵⁵ A similar synthesis approach has been explored by Shi *et al.*⁶¹ to patent hydrotreating catalysts based on bulk and supported mono-, bi- and tri- metals from groups VI-B and VIII-B or from the first three rows of the periodic table, including noble metals and single sulfides. The main GTP catalysts are bimetallic Co-Mo, Ni-Mo and Ni-W impregnated on aluminosilicates and sulfided *in situ*. In certain cases, bulk systems are recommended, as the population of active sites is much higher with the absence of metals/support interactions, which endows them with an intrinsic HDO activity. Deshpande *et al.*⁶⁵ have patented various halogen elements (*i.e.*, I₂, HI, HIO₃, LiI, and their combinations), as potential homogeneous catalysts for the complete dehydroxylation of crude glycerol in two steps. Both catalytic systems require external H₂ pressure, acetic acid, and additional solvents to dissolve the halogen formed as intermediate in the catalytic cycle, and then act as the main leaving group to start partial dehydroxylation in the first step and facilitate the final dehydroxylation in the second one. All these patents^{61,63-65} report catalyst pre-activation under a reducer atmosphere, sometimes including *in situ* synthesis; however, the physiochemistry of the catalysts has still not been examined.

More recently, Janssens *et al.*⁴³ have explored a homogeneous approach to boost one-step GTP catalysis. They have combined *in situ* dissolution synthesis and final recrystallization to manipulate RuBr₃ (as catalyst precursor), HBr-doped ionic-liquid type Bu₄PBr - tetrabutylphosphonium bromide (as a dehydrating co-catalyst) and formalin (as an additive) for enhancing the formation of Ru-CO bonds that act as hydrogenation sites. Similar Ru-C active sites have previously been reported⁵⁷ for similar homogeneous acidic conditions. They suggest initial glycerol dehydration over a Brønsted co-site, followed by further hydrogenation either via *i*) the insertion of carbonyl in the Ru-H bond and subsequent release of the substrate formed through the protonation of the resulting Ru-O or Ru-C bonds, or *ii*) direct transfer of a hydride ligand from Ru to a H⁺-substrate. Janssens *et al.*⁴³ have pre-treated the RuBr₃ salt with 1 bar of CO pressure, instead of formalin, to increase the population of Ru-CO bonds, thereby reaching a 82 % propylene yield from crude glycerol (Fig. S1 A). Comparative FTIR spectra of fresh and recycled Ru-based complex catalyst (Fig. S1 B) reveal good catalyst recyclability up to eight cycles without any significant loss in propylene selectivity. However, working with expensive noble Ru metal homogeneous catalysis poses a real challenge for the use of GTP beyond lab tests.

Di Mondo *et al.*⁵⁴ have found that the corroded surface of a 316 Stainless Steel -316SS reactor (with HOTf acid in a reducer medium) catalyzes GTP in one-step. SEM/EDX, XRF, and ICP-MS analyses reveal the formation of a thin layer (< 10 nm) of highly active mixed Cr^{3+/5+} states, which with Fe or

Ni metals contribute to HDO activity through H₂-spillover phenomena. The GTP activity is confirmed by attacking different commercial 316SS powders with an increasing concentration of an HOTf acid/glycerol mixture, which is comparable to those of the 316SS reactor itself. The reported insights may open new perspectives for designing innovative metallic reactors that can play the role of both low-cost catalyst and host reactor. For example, studying a 316SS reactor with a spongy aspect may allow overcoming its low surface per volume ratio, and so improve the geometrical exposure to the high GTP rate.

Zacharopoulou *et al.*^{34,47,48,59} have merged impregnation and co-precipitation methods to support high loading of Mo/Fe elements over carbons, albeit with low metal dispersion, which facilitates their sintering and leaching during the liquid HDO of glycerol.⁴⁸ Both effects seem to have been induced by the low interaction of these metals with a practically neutral carbon surface. They suggest that the partial substitution of Mo⁴⁺ ions by Fe in the MoO₂-based catalysts reduces Mo⁶⁺ to form Mo⁵⁺ and Mo⁴⁺ species with oxygen vacancies.^{47,48} The arrangement of these sites within redox cycles seems to contribute to the complete removal of oxygen from glycerol and the creation of the C=C bond in propylene, according to the reverse Mars-van Krevelen cycle (Fig. S1 C).⁵⁹ Mota *et al.*⁵⁵ used the same methods to support a similar loading of NiMo, ZnMo, CuMo and FeMo on activated carbon (AC), comparing them with commercial Ru/AC and Pd/AC catalysts. The noble metals and Ni/Mo-based catalysts lead to C₁₋₃ alkanes, whereas ZnMo and CuMo-based catalysts instead form oxygenates. A FeMo/AC catalyst features a propylene yield of up to ~90 % under atmospheric H₂ pressure and 300 °C. This catalyst is highly active and more selective than those used by Zacharopoulou *et al.*^{47,48,59} that require a high H₂ pressure ~80 bar to reach ~76 % propylene selectivity and ~88 % glycerol conversion. Mota *et al.*⁵⁵ attribute the best GTP performance to the formation of MoC phases and partially reduced Mo⁴⁺ species with an oxygen vacancy. A recent DFT calculation (Fig. S1 D)³⁷ indicates that the formation of a Mo oxygen vacancy is thermodynamically favored under an H₂ atmosphere. However, the exact nature of these Mo^{δ+} species, hypothesized by both groups based on *ex situ* characterization,^{47,48,55,55,59} remains unclear.

More recently, El Doukkali *et al.*⁶⁰ have combined hydrothermal, melt-infiltration, *in situ* topotactic- and non-topotactic reductive carburization (Fig. 6 A) to fine-tuning the HDO properties and protect highly reactive sub-2 nm Mo particles in hydrophobic-inert silica against leaching and sintering, which prevail under an H₂O-rich reaction medium.^{48,55} A combination of TEM-HAADF imaging (Fig. 6 B), *in situ* XRD, and *in situ* XPS analyses with kinetic GTP test data has revealed the existence of MoO_x, β-Mo₂C, and η-MoC phases with partially reduced Mo⁵⁺, Mo³⁺, and Mo²⁺-C species that play a critical role in HDO events both in glycerol and in intermediates without causing significant C-C breaking.

The single-step GTP reaction seems to effectively take place over Mo oxides via successive redox cycles of $\text{Mo}^{5+}/\text{Mo}^{6+}$ and/or $\text{Mo}^{3+}/\text{Mo}^{4+}$ states, while over Mo carbides it occurs mostly on a carbidic and oxycarbide surface. The re-oxidation of partially reduced $\text{Mo}^{\delta+}$ states either to inactive Mo^{6+} or Mo^{4+} species hinders deoxygenation-hydrogenation events, which is attributed to the surface accumulation of oxygen that is related to the co-adsorption of certain oxygenated compounds (*i.e.*, $\text{C}_x\text{H}_y\text{O}_z$). This finding complements those of Lee *et al.*¹⁷³ and Schaidle *et al.*,¹⁷⁴ attributing Mo deactivation instead to the deposition of graphitic carbon during the HDO of anisole or acetic acid.

Anderson *et al.*,⁴⁶ in turn, control the GTP activity-stability of $\text{NiMo}/\text{Al}_2\text{O}_3$ by *in situ* sulfidation. The partially reduced catalyst records a similar initial activity in C-O breaking and C-C hydrogenation to that of the sulfided one, but the latter provides a significant improvement in terms of stability under *in situ* H_2S co-feeding (Fig. S2 A-B). This improved stability, which is attributed to the persistence of a high number of MoS_x edge sites acting as active sites, is surprisingly accompanied by significant C-C cleavage activity. As revealed by the TPO and N_2 adsorption of spent $\text{NiMo}/\text{Al}_2\text{O}_3$ catalysts, deactivation is attributed to NiMo sintering and coke formation, resulting in a loss of surface area and fewer active sites.

Other authors^{37,39,58} use DFT calculation, sometimes coupled with kinetic micro-modeling or TPD-MS and HREELS analyses, to provide a better understanding of the role of the Mo surface in GTP activity. Rellán-Piñeiro *et al.*³⁷ conclude that C-O scission and C-C hydrogenation take place effectively through the formation of oxygen defects. This process starts with initial H_2 adsorption and dissociation of the H atom that reacts with the oxygen surface to form water and an oxygen vacancy (Fig. S1 D). Subsequently, glycerol (or oxygenated intermediates) is directly adsorbed on the Mo site with an undercoordinated O- environment, whereupon a selective cleavage of the C-O bond produces partial or fully deoxygenated compounds. The snatched oxygen atom remains bound to the Mo, filling the vacancy. The latter is immediately regenerated by H_2 reduction with low energy barriers, whereby H_2 pressure or an H_2 -rich medium is required for completing the HDO cycle. In turn, Wan *et al.*^{39,58} use a glycerol-saturated H_2 flow to compare the HDO reactivity-stability of Mo_2C , $\text{Cu}/\text{Mo}_2\text{C}$, $\text{Fe}/\text{Mo}_2\text{C}$, and $\text{Pt}/\text{Mo}_2\text{C}$ surfaces by evaluating the number of C-O, C-C, and C-H bonds broken during the reaction (Fig. S3 A-D). $\text{Fe}/\text{Mo}_2\text{C}$ and Mo_2C surfaces are highly active in the complete GTP cycle, while $\text{Pt}/\text{Mo}_2\text{C}$ records significant activity in C-C and C-H bonds breaking to syngas products. $\text{Cu}/\text{Mo}_2\text{C}$ has the greater hydrogenolysis ability of only one C-O bond of glycerol to hydroxyacetone. Additional HREELS data⁵⁸ indicate that specific sites from Mo_2C are responsible for the activity in C-O scission. This is explained by the fact that the high oxophilic Mo_2C surface, which has previously been revealed by DFT calculation,³⁹ interacts more strongly with the oxygen of glycerol than over

Fe/Mo₂C and Cu/Mo₂C. The coverage of Cu species, and to a lesser extent Fe, seems to slightly reduce the oxophilicity of Mo₂C. Moreover, Fe coverage also seems to improve the stability of the carbidic Mo₂C surface during the GTP reaction.⁵⁸

Synthetic Summary: Different catalytic systems may efficiently accelerate the kinetics of the GTP reaction. They require specific preparation, operating, and activation treatments to condition the chemical environment of active sites for the reactants, depending on the target reaction conditions and process configuration. Acid catalysts such as zeolites seem suitable for the high-temperature dehydration/cracking of glycerol to ethylene and to a lesser extent propylene; however, they still experience severe deactivation. Adjusting the zeolite acidity type and starching, as well as pore re-opening by post-treatments (*e.g.*, desilication and delamination) or nanoscale synthesis (*e.g.*, soft/hard templating) may also improve coke diffusion. Synergic catalysis involves combined metal and acid catalytic systems, with the tandem mode providing promising GTP rates. However, further studies should be conducted for controlling the kinetics of the GTP reaction over tandem bed zones to extend the useful life of the multi-functional catalysts used. The best homogeneous catalyst for the one-step GTP route involves Ru-complexes, providing an extremely high selectivity towards propylene and good stability.⁴³ The best heterogeneous catalyst, in turn, is based on Mo species, featuring unprecedented rates of C-O removal and C-C hydrogenation without excessive CO₂ emissions.^{48,55,60,61} These systems are still affected by the excessive surface accumulation of oxygen and oxygenates, which seems to be related to unbalanced deoxygenation-hydrogenation rates. Controlling *in situ* the coverage of oxygen on the overlayer of Mo-based catalyst during the HDO reaction or exploring structural single-atom catalysis (*e.g.*, Mo⁵⁺ or Mo³⁺) into specific 3D structure; selectively orienting Mo nanoparticles or doping few amounts of highly hydrogenating metals (*i.e.* Ir, Pd, Ru, Ni, V, Co, etc.) may improve catalytic stability by balancing H₂ activation *vs.* C-O elimination. The selective *in situ* poisoning of Mo active sites during the reaction, using specific oxygenates as probe molecules, could provide useful insights into the evolution of the most active species and how to better control the oxygen rate over the Mo^{δ+} surface. While as the *in situ* tracking of the real active sites seems difficult under practical HDO conditions (*e.g.*, high pressure and a complex reactant mixture, etc.), the operando EPR, NAP-XPS and 3D-NMR analyses should be preferred to *ex situ* explorations. This is suitable for further studies on the most efficient Mo-based catalysts because of *i)* the high oxophilicity of their Mo^{δ+} species (*e.g.*, Mo-O_x, Mo-C_x, and Mo-S_x), and *ii)* their rich chemistry (*i.e.*, multi-oxidation states) that can change radically upon contact with an air-containing environment. These cutting-edge operando studies can help to accurately identify catalytic active sites, while further

theoretical calculations (*ab initio*, DFT, etc.) may support in-depth research on the reaction mechanism and predict the most suitable architecture for robust GTP catalysts.

1.7. Reaction mechanisms for GTP routes

There are currently major discussions on the pathways through which glycerol is converted to propylene, concluding that GTP routes encompass sequential/parallel competitive *vs.* cooperative reactions, including H₂ dissociation-formation, dehydration, hydrogenolysis, deoxygenation, and hydrogenation, among others. The kinetic arrangement of these reaction intermediates to form a complete GTP route differs from one catalyst to another, depending on the reaction conditions and process configuration.

1.7.1. Acid-catalyzed mechanisms

For high-temperatures (> 400 °C), Corma *et al.*^{41,66} have been the first ones to build a complex mechanism for converting glycerol to olefins and aromatics over acid surfaces without an external H₂ supply (Scheme 4). The integral pathways towards gas products (*i.e.*, olefins, CO_x and paraffins) involve the catalytic dehydration of glycerol, cracking, and hydrogen producing-consuming reactions on acid sites at temperatures mainly higher than 450 °C.^{41,66,67} H₂ is formed mainly through C-C and C-H cleavages, water-gas shift (WGS), decarbonylation, and dehydrogenation reactions, and is then transferred to dehydrated intermediate molecules by hydrogenation and hydrogen-transfer events, thereby producing light olefins; mainly ethylene and to a lesser extent propylene.^{35,41,66,67} The latter are involved mainly in further aldol-condensation and Diels-Alder rearrangements to form heavier paraffins or even aromatics, which negatively affects the formation of propylene as target product. An optimal balance between all these reactions is therefore required to improve propylene yield. Zakaria *et al.*^{35,38} have simplified this mechanism by hypothesizing that an acidic surface leads to initial glycerol dehydration to 3-hydroxypropanal, which in turn follows two major routes, as illustrated in Scheme S1. They have discarded glycerol dehydration to hydroxyacetone, considering that the formation of 3-hydroxypropionaldehyde is a more feasible option because the latter has a major tendency to break C-C bonds for the further formation of acetaldehyde and formaldehyde, and vinyl alcohol and formaldehyde, which have been experimentally detected during the reaction.³⁸ Acetaldehyde therefore undergoes carbonyl bond dissociation (ethylidene oxo-species) to form propylene. At the same time, protonated acetaldehyde combines to undergo reductive C-C coupling to form butylene, while vinyl alcohol releases oxygen to ethylene. A high amount of coke is observed resulting from C-C bond cleavages, which affect the C₂₋₄ olefins formation. Lima *et al.*⁴⁵ have

experimentally evaluated products distribution as a function of reaction temperature for glycerol conversion over acid Fe/ HZSM-5 to coincide on some sentences with Zakaria *et al.*^{35,38} and Corma *et al.*^{41,66} The proposed mechanism (Scheme S2) has only briefly been discussed, but they consider that the -OH group of glycerol is initially dehydrated on H-acid sites to form hydroxyacetone and 3-hydroxypropanal. The first compound is then hydrogenated to acetone *via* H₂ production and transfer, whereas the second one is further dehydrated to acrolein or cracked to acetaldehyde and formaldehyde. Subsequently, acetone and acetaldehyde undergo decarbonylation and dehydration, respectively, to produce CO, H₂O, and ethylene. The latter is in turn oligomerized to propylene, but its selectivity (17-33%) is remarkably inferior to that of ethylene (up to ~ 46%). Besides, there is further surface hydrogen-transfer from acrolein to ally-alcohol and then to propanol, while the hydrogenation of formaldehyde leads to methanol that is dehydrated to methane. The simultaneous decarbonylation of acrolein, which is a highly unstable intermediate,⁴⁶ is fully possible over an acid surface, but there is no explanation as to why it has been discarded. In addition, propanol can be easily dehydrated to propylene over an acid surface such as HZSM-5, as evidenced by Corma *et al.*^{41,66} and Zakaria *et al.*^{35,38} In contrast to these two studies, Lima *et al.*⁴⁵ propose an additional ethylene-to-propylene pathway *via* simultaneous oligomerization and cracking steps (Scheme S2), which have not been kinetically proven.

1.7.2. Mechanisms involving metallic and/or multi-functional sites

For a moderate temperature ≤ 400 °C and an H₂ atmosphere, Taher *et al.* and Di Mondo *et al.*^{54,57} have been the first ones to propose pathways (Scheme 5a) for glycerol to propylene and/or propane, catalyzed in acid medium by Cr or Ru-C sites submitted to an H₂ treatment. These conditions constitute a thermodynamic sink for these sites because the C-O cleavage in glycerol seems to begin with an initial H₂ dissociation, which is prompted by spillover phenomena that favors the hydrogenation events both in glycerol and its intermediates.⁵⁴ It then progresses through glycerol dehydration and hydrogenation to 3-hydroxypropionaldehyde. The latter undergoes a secondary Brønsted acid-catalyzed dehydration to acrolein, which is then hydrogenated to *n*-propanol. A third dehydration takes place immediately to convert *n*-propanol to propylene that can be excessively hydrogenated to propane. The presence of *i*-propanol in the aqueous medium is hypothesized to be the result of water reacting to propylene *via* the Markovnikov mechanism instead of *n*-propanol isomerization. This early mechanism is overly simple and does not consider the other possible C₃ intermediates whose formation is also kinetically possible under the typical HDO conditions studied. Hydroxyacetone and C₃-diols can be formed in parallel from 3-hydroxypropionaldehyde, which is less kinetically stable, as reported

in due course by Mota *et al.*⁵⁵ (Scheme 5b). This route has been experimentally identified as the most probable one for propylene because both *1,2*-propanediol and *i*-propanol have a much higher propylene yield over the Mo-based catalyst (~57 % and ~64 %, respectively) than their respective isomers: *1,3*-propanediol (~0 %) and *n*-propanol (~4.3 %), under identical experimental conditions.⁵⁵ The formation of hydroxyacetone and *1,2*-propanediol intermediates during the GTP reaction formed over bifunctional sites and under a low temperature has been reported.^{42,59} However, the proposed GTP pathway (Scheme 5b) is still incomplete because propionaldehyde and *n*-propanol can also establish an isomerization equilibrium with allyl-alcohol and *i*-propanol, respectively.^{42,47,59} Thus, Sun *et al.*⁴² have proposed a new GTP mechanism over metals/acid sites taking into account that partial C-O and C-C breaking to additional intermediates such as propionaldehyde, propionic acid, methanol, acetaldehyde, ethanol, ethylene-glycol, ethylene, propane and CO₂ have been included in the new pathway (Scheme S3). Some of the reported intermediates, whose formation becomes prominent under an H₂ atmosphere, has been experimentally confirmed.^{46,60}

Zacharopoulou *et al.*^{34,47,59} have, in turn, proposed four pathways for GTP (as gathered in Scheme 6), which differ in the main intermediates formed over a Mo-based catalyst: *a*) allyl alcohols, *b*) acrolein, *c*) hydroxyacetone, and *d*) C₃-diols. The reported data^{34,47,47,59} indicate that all these pathways start with the cleavage of one or two C-O bonds of glycerol either by dehydration or hydrogenolysis followed by sequential hydrogenation-deoxygenation of C₃ intermediates up to propylene.

According to the first pathway (Scheme 6 a), glycerol directly undergoes the simultaneous removal of two vicinal -OH groups to form allyl-alcohol, as primary intermediate. This step is derived either by the use of a H₂-rich atmosphere or H₂ transfer events where glycerol itself is acting as H₂ donor, as reported by other groups.^{175,176} The allyl-alcohol formed is then transformed *via* the following steps: *i*) a direct hydrogenolysis of C-O bond to propylene, and *ii*) an isomerization to propionaldehyde as secondary intermediate that is hydrogenated to *l*- and *2*-propanol equilibrium and then to propylene. Further *ex situ* HDO tests with the oxygenates involved⁵⁹ indicate that the second step contributes little to propylene formation considering the very low rate of *l*-propanol to propylene (< 0.6 mmol.g_{cat}⁻¹.h⁻¹). Nevertheless, the rate of allyl-alcohol to propylene is the highest (~23 mmol.g_{cat}⁻¹.h⁻¹).⁵⁹ This might be due to the high reactivity of the C=C bond that facilitates H₂ adsorption and probably affects the dissociation energy of the C-OH bond, enabling its cleavage and simultaneous C=C isomerization. However, the proposition for simultaneous removal of two vicinal OH groups from glycerol should be re-contextualized because according to the principle of microscopic reversibility,^{177,178} the transition state for a hypothetical single step of direct glycerol-to-allyl alcohol must be also the same for the reverse incorporation of two simultaneous water into allyl alcohol at overall equilibrium. This would involve

simultaneous collision of three chemical species to form the corresponding transition state, which is unlikely from a statistical point of view. Therefore, it is more probable that the microscopic pathway of glycerol to allyl alcohols would involve more than one transient state, which means simultaneous removal of two OH groups is less likely.

Acrolein is formed as an intermediate through another totally independent (Scheme 6 b), via the protonation of the central -OH group of unstable 3-hydroxypropionaldehyde (formed by tautomerism).^{179,180} The subsequent hydrogenation of acrolein through propionaldehyde to *l*- or 2-propanol equilibrium results in propylene via final dehydration. However, acrolein is a highly unstable intermediate⁶⁰ that is detected in a small amount in these studies,^{47,48,59} particularly when an H₂ atmosphere is used. This suggests that this route does not make a significant contribution to propylene formation.

A third GTP pathway (Scheme 6 c) takes place through hydroxyacetone, which is formed through an initial protonation of terminal -OH of the glycerol and a rapid isomerization of an unstable enol intermediate.^{181,182} The dehydration of hydroxyacetone to acetone over acid sites is then favored more than the parallel hydrogenation to *l*,2-propanediol. Nonetheless, the hydrogenation of acetone to propanol upon dehydration of the latter contributes to some extent to the formation of propylene. This pathway has also been corroborated by *ex situ* propanol HDO tests, where a significant propylene rate ($\sim 14 \text{ mmol.g}_{\text{cat}}^{-1}.\text{h}^{-1}$) is observed.⁵⁹

A fourth GTP pathway (Scheme 6 d) has also been proposed, justified by the fact that the removal of primary OH in glycerol under these typical HDO conditions is easier than the secondary one.^{183,184} It involves the formation of *l*,2-propanediol and to a lesser extent *l*,3-propanediol, which undergoes dehydration to propionaldehyde, further hydrogenation to propanol, and then to propylene.

Based on their experimental findings, Rellán-Piñero *et al.*³⁷ have theoretically evaluated the energy parameters affecting both the adsorption of glycerol and H₂ dissociation over MoO₃. As gathered in Scheme S4, they have found that the GTP reaction seems to start by creating undercoordinated Mo atoms with an oxygen defect, induced by H₂ reduction, over which sequential and simultaneous dehydration, keto–enol equilibria, and hydrogenation events in glycerol and oxygenated intermediates can take place. The latter step fills the Mo oxygen vacancy and closes the catalytic cycle. This means H₂ is used as a mandatory reductive agent to re-launch the catalytic cycle. The proposed sequences occur in accordance with the reverse Mars–Van Krevelen model, thus corroborating the experimental findings already reported by Zacharopoulou *et al.*^{47,59}

As illustrated in [Scheme 7 a](#), glycerol is first dehydrated to either *1,2*- or *1,3*-enols in an identical way to the mechanism of ethanol dehydration over MoO₃ clusters.¹⁸⁵ It is adsorbed on the uncoordinated Mo–O bond, where its H⁺ is transferred to a terminal oxygen, and the β-hydrogen is stripped by oxygen and, concomitantly, the C–O bond is cleaved. This step eventually breaks C–H and C–O bonds with a weaker barrier, forming double bonds; Mo=O on the catalyst surface and C=C in the *1,2*- or *1,3*-enols. These highly unstable enols quickly transit to their respective keto tautomers,^{46,59} depending on whether the C–O cleavage is taking place from primary or secondary. Keto–enols are thus interconverted via adsorbed enolic –OH on a Mo vacancy ([Scheme 7 b](#)). This step is followed by –OH dissociation, with an H atom reacting with an O–Mo bond. This new OH–Mo bond transfers H* either to the H₂=C group of *1,2*-enol to form hydroxyacetone, or to the =CH- group of *1,3*-enol to form 3-hydroxypropionaldehyde. Subsequently, the ketone group of hydroxyacetone or hydroxypropionaldehyde interacts with the vacancy site to absorb the H* atom from the neighboring OH–Mo bond, leading to deprotonated *1,2*- or *1,3*-propanediol ([Scheme 7 c](#)). In parallel to this step, 3-hydroxypropionaldehyde can also dehydrate to acrolein, which is not feasible for hydroxyacetone because its –OH group no longer has any β-hydrogen to be cleaved. Further dehydration of *1,2*-propanediol *via* its primary OH group forms allyl alcohol, while the dehydration *via* a secondary OH group lead to 1-propenol (or allyl alcohol again), depending on whether the β-hydrogen of C₁ or of C₃ is eliminated. *1,3*-propanediol can only be dehydrated to allyl alcohol, but this step is less likely to occur experimentally.^{48,59} These modeling data also indicate that acrolein can quickly hydrogenate to unstable enols, *1*-propenol or *2*-propenol (allyl alcohol), supporting the experimental findings of Zacharopoulou *et al.*,^{47,59} discarding propylene formation *via* an acrolein intermediate. *1*- and *2*-enolates mainly enter into an equilibrium with their respective keto-tautomers, acetone and propionaldehyde. Both compounds undergo hydrogenation to form 2-propanol and *1*-propanol, respectively, which are finally dehydrated to propylene.

The allyl alcohol formed by the dehydration of C₃ diols and the hydrogenation of acrolein may undergo further hydrogenolysis over undercoordinated Mo sites ([Scheme 7 d](#)). This route involves the simultaneous hydrogenation of the H₂=C group and C–O cleavage to directly form propylene. This last route - glycerol → allyl alcohol → propylene - has been experimentally identified,^{47,59} but the modeling data discussed³⁷ consider the pathway glycerol → hydroxypropionaldehyde → acrolein → *1*-propenol → propionaldehyde → *1*-propanol → propylene to be the main GTP route. The modeling approach used³⁷ has a major drawback by considering gas-phase GTP conditions without addressing lateral effects, which provide a high conversion rate and a wide variety of products, among which 3-hydroxypropionaldehyde and hydroxyacetone are the main intermediates. However, the GTP

experiments,^{47,59} which report 1,2-propanediol and allyl alcohol as the main intermediates, have been conducted under practical liquid or mixed-phase GTP conditions.

Wan *et al.*⁵⁸ have complemented these calculations by considering the lateral interactions of reactants over the Cu/Mo₂C catalyst. These data reveal that propylene is formed specifically over the Mo₂C surface and not on the Cu one or on the Cu-Mo interface. As indicated in [Scheme S5](#) (in green) for propylene formation, each oxygen atom of glycerol strongly interacts with a Mo site located above the second carbon layer on the Mo₂C(0001) surface, forming an alkoxide through a binding energy of -2.13 eV. The energy barriers indicate that the cleavage of O-H bonds in the two alkoxides formed over Mo₂C (with 0.03 eV and 0.28 eV) is more favorable than the cleavage of their C-O bonds (with 1.11 eV and 0.98 eV). The dissociation of the third O-H bond is also favorable against the C-O bond because the activation barriers of the O-H bond is just 0.21 eV, while that of the C-O ones is in the order of 0.68 and 0.73 eV. Such preferential O-H cleavage has been reported for ethanol and ethylene-glycol conversion over carbides.^{186,187} The adsorbed CH₂O-CHO-CH₂O* intermediate may subsequently undergo the successive cleavage of the three C-O bonds, whose respective activation barriers are 0.48 eV (for the middle carbon), 0.31 eV and 0.15 eV (for the two terminal carbons) to form an CH₂-CH=CH₂* intermediate. Propylene is therefore finally formed after protonation at a terminal carbon of the last intermediate with an activation barrier of 0.56 eV. This pathway requires the least energy (-10.36 eV), with a more favorable energy performance than those based on the prior cleavage of the C-H bond or the protonation of C-C to acrolein or saturated C-C bonds, which have higher activation barriers and lower energy (-9 eV and -8.77 eV, respectively).

These findings increase our understanding of the GTP route over a Mo-based catalyst; nevertheless, this approach still has some drawbacks, such as these calculations only considers the cleavage of one C-H bond at a terminal and central C atom without any C-C bonds breaking. Furthermore, it requires the complete scission of all C-O and O-H bonds and relevant hydrogenation events to form only four C₃ compounds: hydroxyacetone, allyl alcohol, propionaldehyde, and propylene. However, in our last study,⁶⁰ we experimentally identified around twenty partially and/or fully C₁₋₃ deoxygenated compounds formed over Mo-O or Mo-C based catalysts. Some of these intermediates were also detected over a Mo-S_x-based catalyst,⁴⁶ tested under similar hydrotreating GTP conditions. At a high conversion rate, glycerol was mainly hydrodeoxygenated to propylene, propane, and 1-propanol, or cracked to ethylene, methane, CO_x, methanol, and ethanol. However, at a low conversion rate, it was mainly converted to partially deoxygenated liquid oxygenates, such as hydroxyacetone, allyl alcohol, acrolein, and acetaldehyde. The integral networks for glycerol conversion to propylene/propane and ethylene/ethane, which include two main C₃ and C₂ pathways, are summarized in [Scheme 8](#).

The C₃ pathway involves glycerol dehydration either to 3-hydroxypropionaldehyde or to hydroxyacetone without involving 1,2- or 1,3-enols, previously reported as possible starting intermediates.^{37,58} Their absence may be due to the fast-kinetic reaction at a higher temperature ~400 °C. Hydroxyacetone was identified as the major intermediate, while a smaller amount of 3-hydroxypropionaldehyde was detected. As suggested by previous DFT calculations,^{37,58} hydroxyacetone can be hydrogenated to 1,2-propanediol, which may undergo further dehydration to acetone or allyl alcohol, while 3-hydroxypropionaldehyde can be hydrogenated to 1,3-propanediol or dehydrated to acrolein. Further hydrogenation events in the last three intermediates (acetone, allyl alcohol, and acrolein) can form propanols, which subsequently dehydrate into propylene or saturate to propane. In parallel, the C₂ pathway, which was probably started by the initial C-C scission in the first adsorbed glycerol, as C-C cracking in the H₂-transfer reaction of alcohols has been experimentally proven.^{184,188} Thus, acetaldehyde was detected as the major C₂ intermediate, while a smaller amount of hydroxyacetaldehyde was observed. Both compounds could be formed through the hydrogenolysis of C-C bonds, undergoing subsequent deoxygenation-hydrogenation events until the formation of ethylene and ethane.

Synthetic Summary: The proposed mechanisms for the GTP reaction are reported according to the following two concepts; *i*) high-temperatures catalysis (T > 400 °C, atmospheric pressure, and acid catalyst), and *ii*) typical mild condition catalysis (T ≤ 400 °C, H₂ atmosphere, and metallic or bifunctional catalysts). The first GTP mechanisms involve mainly complex pathways including glycerol dehydration/cracking, H₂ producing-transfer-consuming events, and further decarbonization and/or oligomerization to C₂₋₄ olefins; mainly ethylene and to a lesser extent propylene. Further pathways towards coke, aromatics, or paraffins may be involved *via* parallel and/or sequential reactions (*e.g.*, C-C coking, Diels-Alder, and aldol-condensation), which require adjusting catalyst properties and operating conditions to improve propylene formation. The secondary GTP pathways occur mainly through sequential deoxygenation-hydrogenation events in the glycerol and intermediates, including initial dehydration or hydrogenolysis and subsequent hydrogenation, isomerization, or further dehydration to propylene. The most probable route for the formation of a C=C bond in propylene is through the hydrogen transfers from the surface -OH group to the H₂C= group, formed in allyl alcohol *via* previous hydrogenolysis and isomerization, which leads to eventual C-O breaking, according to the reverse Mars-van Krevelen mechanism.^{37,47,59} Excessive hydrogenation events lead mainly to C=C saturation in propylene and to C-C in propane.^{52,60,61}

1.8. GTP process operability and the effect of operating conditions

Our aim here is to address the influence of key operating conditions according to different GTP configurations. The most relevant GTP data, which are gathered from lab-scale experiments and/or thermodynamic simulations, are summarized in [Table 3](#).

1.8.1. Effect of temperature

Various studies^{28,41,43,48,51,53,56,60–62} report that temperature is a crucial factor that influences both glycerol conversion and product distribution, and which also depends on process configuration and the nature of the catalyst.

Indeed, total glycerol conversion is usually obtained at high temperatures (> 400 °C),^{28,33,35,38,41,45,51,56,66} as an eventual result of the reactions reported in GTP mechanisms. Furthermore, the selectivity of propylene vs. ethylene is highly sensitive to the type of reaction involved at each temperature. Corma *et al.*⁴¹ have increased the temperature in micro-reactors from 500 °C to 700 °C (with acid HZSM-5 and FCC1, for example) to promote glycerol cracking up to a 31 % yield of C₂-C₄ olefins. This temperature increase has also promoted CO and H₂ formation (up to 62 %) due to the decomposition of C-C/C-H bonds into syngas. The observed tendencies can be attributed to thermodynamic effects, predicting a smaller improvement in exothermic H₂-transfers and oligomerization at a higher temperature. In contrast, lower temperatures usually favor the parallel formation of aromatics and coke,^{41,44} leading to fast catalyst deactivation. To resolve this conundrum, Corma *et al.*⁴¹ recommend a high-temperature FCC reactor, allowing for homogeneous mixing, better energy dissipation, and the *in situ* regeneration of catalysts.

Lima *et al.*⁴⁵ report that ethylene selectivity increases proportionally with temperature from 450 °C to 600 °C (over metals/HZSM-5), while propylene decreases inversely. This change in C₂₋₃ olefin composition is due to the entropically favored ethylene formation *via* endothermic glycerol cracking. Indeed, C-H bonds decomposed to H₂ are partially used for the hydrogenation events in ethylene and CH₄ formation. This effect becomes more pronounced at certain temperatures (> 550 °C), when the selectivity for CH₄ increases sharply.⁴⁵ Similar findings²⁸ highlight the increasing selectivity of ethylene (up to 22 %) and propylene (up to 14 %) over ZSM-5 (Si/Al ~15-127) within a temperature range of 400–600 °C ([Fig. S4 A](#)). CO_x selectivity (~ 31 %, mainly CO) is also higher at 600 °C and catalyst deactivation also occurs, which is consistent with the observations reported by Corma *et al.*^{41,66} It may be concluded that the integrated *in situ* extraction of CO_x or the WGS reaction could be efficient strategies for producing additional H₂, and thus improving the GTP yield at high temperatures. Other experimental data coupled with a multi-objective genetic algorithm^{38,51,56} reveal similar trends,

indicating also that increasing temperature favors ethylene yield over acid catalysts. An optimal yield of C₂₋₃ olefins (17.7 %) is achieved at 715.9 °C, which is supported by further thermodynamic analysis,⁵⁶ indicating that the highest ethylene rate peaks at temperature higher than 700 °C (Fig. S4 B).

In a multi-step GTP reaction, Blass *et al.*⁵⁰ have tweaked the distribution of olefins and byproducts by varying the temperature of three-stage fixed-bed reactors. Operating the first dehydration reactor (*i.e.*, HZSM-5) at 400-500 °C produces mainly a mixture of acrolein (70 %) and acetaldehyde (20 %). Acrolein is then hydrogenated in the second stage (over Pt or Pd/Al₂O₃) into propionaldehyde between 100 °C and 300 °C, where a selectivity between 70-99 % was attained at 115 °C. Temperatures near to 300 °C simultaneously favor oxygen removal and hydrogenation rates, leading to all the deoxygenated intermediates being fully converted to paraffins. Furthermore, the reverse endothermic dehydrogenation of the formed paraffins to C₂₋₃ olefins under H₂-atmosphere is thermodynamically limited.^{189,190} Consequently, the conversion of glycerol to C₂₋₃ olefins cannot proceed in two steps through paraffin intermediates. The integration of a third reactor for separate propionaldehyde conversion over zeolites (*e.g.*, HBEA) increases C₂₋₃ olefin yields; 10 % and 46 %, are obtained at 400 and 500 °C, respectively (Table 3). The direct connection of the three reactors in series for continuous glycerol-to-olefins route produces only a 6% yield of ethylene + propylene at 400 °C. However, increasing the temperature of the third reactor to 500 °C improves C₂₋₃ olefin yield (from 6 % to 15 %, Table 3), while that of C₄₋₅ olefins decreases (from 13 % to 9 %, Fig. 7 A). This trend confirms that C₂₋₃ olefins are effectively produced from the cracking of C₄₋₅ olefins, formed initially by the condensation of propionaldehyde. Similar trends have been observed in the conversion of acetone, which is an isomer of propionaldehyde, to C₃₋₆ compounds.^{66,191,192} Hulteberg *et al.*⁶⁴ have also patented a similar three-step route: glycerol dehydration over WO₃/ZrO₂, acrolein hydrogenation over Cu/ZnO₂, and propanol dehydration over WO₃/ZrO₂, to produce propylene and propane. The following are the optimal temperatures for the three steps: 280 °C, 270 °C and 208 °C, respectively, yielding ~ 46 % propylene and ~10 % propane (Fig. 7 B).

Deshpande *et al.*⁶⁵ have studied the homogeneous dehydroxylation of crude glycerol in two batch reactors to boost propylene yield *vs.* byproducts. The first reactor initiates partial dihydroxylation at a temperature below 120 °C, which require reductive conditions and a molar ratio of halogen/crude glycerol between 1:4 and 1:8. However, slightly higher temperatures between 180 °C and 210 °C in the second reaction are necessary to attain 80 % propylene and 4 % propane at full conversion. The exact temperatures values depend also on other operating conditions (*e.g.*, H₂ pressure, H₂/glycerol/ratio, and glycerol/halogen ratio). Operating under inert conditions produces only 38 % propylene at 59 % glycerol conversion, even when lengthening time-on-stream (TOS) to 6.5 h.

For the heterogeneous two-step GTP route, Yu *et al.*⁵³ increase temperature to 250 °C to boost the initial hydrogenolysis of glycerol over Ir/ZrO₂ to attain ~94 % *l*-propanol yield (Fig. S5 A), because this reaction is kinetically suppressed below 200 °C. The subsequent *l*-propanol dehydration in a second step (over ZSM5, Si/Al=30) leads to a propylene selectivity of 99 % (Table 3). Similar two-step approaches, which integrate glycerol hydrogenolysis over WO_x/T317,⁴² Pt/ZSM-5,²⁸ and MoO₃-modified Ni₂P/Al₂O₃,⁴⁹ and subsequently *l*-propanol dehydration over acid aluminosilicates, have also been studied by Sun *et al.*⁴² and Wu *et al.*^{28,49} who found 242 °C and 250 °C as appropriate temperatures for the GTP reaction. Temperatures below these values shift the reaction to liquid oxygenates, while a further increase in temperatures favors the decomposition of byproducts. Furthermore, a separate two-step strategy still reduces the efficiency of the GTP process. A compact tandem GTP configuration closely integrating double-beds (Ir/ZrO₂+HZSM-5,⁵³ 9.3% WO₃/T317+ amorphous SiO₂-Al₂O₃,⁴² Pt/ HZSM-5 + HZSM-5,²⁸ or MoO₃-modified Ni₂P/Al₂O₃ + HZSM-5,⁴⁹) has been validated at the optimal temperatures identified, recording ~88 % propylene selectivity at ~73 % glycerol conversion,⁵³ ~84.8 % propylene yield,⁴² and ~76 %²⁸ and ~71-88 %⁴⁹ propylene selectivity at full conversion (Fig. S5 B-D, Table 3). The slight discrepancy in the values of propylene selectivity and glycerol conversion reported in these four studies carried out at comparable temperatures range may be due to the difference in the composition and partial pressure of glycerol, H₂ and/or solvent, space-velocity, molar ratio of H₂/glycerol, and the nature of the catalysts used. When methanol is used as solvent, Wu *et al.*²⁸ recommend a temperature of 500 °C for the reactor zone of the acid dehydration catalyst, which is similar to that usually used in the MTP/MTO process,^{111,172} with a view to the following: *i*) avoiding the excessive alkylation of C₂₋₃ olefins with methanol to long C₄₊ olefins through a dual-cycle mechanism,^{29,110} and *ii*) enhancing the cracking of the C₄₊ compounds already formed to C₂₋₃ olefins.

The influence of temperature on a single-step GTP under typical HDO conditions has also been studied.^{43,47,48,54,55,59-63} Di Mondo *et al.*⁵⁴ have increased temperatures from 175 °C to 250 °C to boost glycerol and H₂ conversion to propylene yield (96 %) over the 316SS alloy and HOTf co-catalyst, which occurs *via* the mechanism in Scheme 5a. Fadigas *et al.*^{55,63} recommend a range from 250 °C to 350 °C for the full HDO of glycerol/water (30-100 wt%) to propylene and propane. A promising yield of propylene ~ 90 % is obtained over MoFe/AC at an optimal temperature of 300 °C and space-velocity of 5.4 h⁻¹, although a high molar ratio of H₂/glycerol (120/1) is required.⁵⁵ Similar GTP findings have been patented by Shi *et al.*⁶¹ for directly hydrotreating glycerol to propylene at temperatures between 175 °C and 550 °C (most efficiently, 200 °C and 300 °C) and under a limiting H₂/glycerol molar ratio but higher total pressure (up 200 bar). Decreasing temperature from 500 °C to 316 °C or even further

to 254 °C greatly improves propylene selectivity (up to 82.1 %) despite the use of a low molar ratio for H₂/glycerol ~2.3:1 (Table 3). Consequently, this decrease leads to incomplete glycerol conversion (from 0 % to almost 15 %). However, this un-converted glycerol could easily be separated in the liquid phase because the inlet temperature (254 °C) is lower than that of the fusion of glycerol ~290 °C (Table 1). It may therefore be recycled in commercial GTP facilities thanks to excellent propylene selectivity at a lower temperature of 254 °C without detecting any appreciable content of propane, C₁₋₂, and CO_x compounds. The reported data require further reproducibility and validation tests.

Zacharopoulou *et al.*^{47,48,59,62} and El Doukkali *et al.*⁶⁰ have investigated temperatures of 240 °C, 264 °C, 280 °C, 300 °C and 318 °C, which are close to those reported by Shi *et al.*⁶¹ A comparable GTP performance requires a high molar ratio of H₂/glycerol (53:1-100:1), a low glycerol/water mixture (2-10 wt%), and lower H₂ pressure (30-80 bar).

According to Zacharopoulou *et al.*,⁴⁸ glycerol HDO over MoFe/C increases progressively with temperature from 240 °C to 300 °C, when propylene selectivity begins to noticeably improve over 280 °C to reach 71 % of propylene selectivity at glycerol conversion ~ 50 % (Fig. 8 A).⁴⁸ Over this temperature, ally-alcohol is considered the main intermediate (Fig. 8 B), which is consistent with previous studies.^{175,176} This ally-alcohol is then directly converted to propylene or isomerized to propionaldehyde and then hydrogenated to *I*-propanol, which in turn is dehydrated to propylene, as recently reported (Fig. 8 C-D).⁶⁰ A propylene yield of up to ~84.1 % was thus obtained, depending on the reaction temperature (264 °C to 318 °C), space-velocity (1.7 h⁻¹ to 4.7 h⁻¹), a molar ratio of H₂/glycerol (78/1 to 98/1), and catalyst type.⁶⁰ A higher propylene yield may potentially be achieved at around 300-318 °C, as this range seems to be ideal for balancing the exothermic hydrogenation of ally-alcohols to *I*-propanol ($\Delta H_{298}^0 \approx -132.6 \text{ kJ/mol}$) and reducing propylene to propane ($\Delta H_{298}^0 \approx -124.3 \text{ kJ/mol}$) with the endothermic intermediate dehydration of *I*-propanol to propylene ($\Delta H_{298}^0 \approx 34.24 \text{ kJ/mol}$), prompting a good GTP performance. However, poor deoxygenation and hydrogenation activities (~27.6 %) are recorded at low temperatures (264 °C, Fig. 8 D) because these promote the exothermic dehydration of glycerol to hydroxyacetone ($\Delta H_{298}^0 \approx -34 \text{ kJ/mol}$) that is subsequently hydrogenated to propyleneglycol ($\Delta H_{298}^0 \approx -59.7 \text{ kJ/mol}$), and then dehydrated to propionaldehyde, which forms an isomerization with ally-alcohols. This explains the higher amounts of ally-alcohols and propionaldehyde observed at low temperatures (264 °C, Fig. 8 D). Both compounds are unable to undergo further hydrogenation due to thermodynamic and/or kinetic restrictions, whereby propylene yield does not exceed 8.8 %. Under these conditions, both water and glycerol are fully in the liquid phase as indicated by Aspen data in Fig. 8 E, where the condensed phase seems to prevent H₂ solubility in the medium required for the hydrogenation events. This H₂ shortage

favors the dehydration and/or hydrogenolysis of glycerol, leading to partially deoxygenated compounds.

In a homogeneous catalysis medium, Janssens *et al.*⁴³ have also highlighted the importance of temperatures (210-220 °C) in balancing dehydration with the hydrogenating rate of crude glycerol over a Ru-complex catalyst to improve propylene yield (~76%, Fig. 8 F). However, an optimal value of temperature needs to be found because an excessive increase in temperature risks favoring other pathways, while the presence of noble metals mainly leads to an over-reduction of the desired propylene to propane under excess H₂.^{52,57} Therefore, at 400 °C and 18 bar of H₂-pressure, single-step GTP provides only ~26 % propylene selectivity over a Mo-based catalyst (Table 3), which is attributed to the excessive formation of propane, C-C cracking in glycerol, and coke.⁴⁶

Synthetic Summary: In the high-temperatures GTP route, a better compromise between propylene and ethylene yield requires optimal temperatures of 500-700 °C to balance glycerol dehydration, C-C cracking, and H₂ transfer events, while suppressing aromatics favored below 500 °C and excessive CO_x formation at severe temperatures. Propylene yield cannot exceed the theoretical value of ~77.7 %⁴¹ because a part of the C-C/C-H bonds in glycerol are parallelly cracked for H₂-transfer events to form C₂₋₃ olefins. Multi-step GTP routes, including tandem processes, require relatively lower temperatures for the hydrogenolysis step (≤ 250 °C), while the catalyst dehydration beds should be at a slightly higher temperature (~500 °C) to shift the equilibrium towards C₂₋₃ olefins. For the single-step GTP route, a high propylene yield can be obtained at milder temperatures; whose exact values depend on operating in a homogeneous or heterogeneous catalysis medium (Table 3). However, further optimization studies of not only temperature of reaction but should address also H₂-pressure, H₂/glycerol molar ratio, spaces-velocity, and glycerol/water mixture, etc.

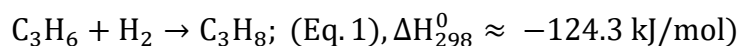
1.8.2. Effect of pressure and reaction atmosphere

The influence of the reaction atmosphere, which is directly related to the variation in the total and partial pressure of reactants and products, has also been evaluated for GTP routes.^{28,41,42,45,47-50,53,60-66}

Inert atmospheric pressure is mainly preferred for high-temperature GTP because H₂ is generated *in situ* by C-C/C-H cracking, thereby forming mainly ethylene and to a lesser extent propylene.^{35,38,41,51,56}

Moreover, a high H₂ pressure is not necessary at temperatures of more than 400 °C because excess H₂ can shift the reaction to saturated molecules, becoming particularly pronounced over noble metals (*i.e.*,

Pt or Pd) modified acid supports.⁵² For example, ethylene and propylene hydrogenation to ethane and propane, respectively, involve a decrease in volume and in moles (example in Eq. 1) so they will be favored by high H₂ pressures according to Le Chatelier's principle.^{87,193}



Unsaturated C=C bonds and allylic C–H bonds are known to be thermodynamically unstable and highly reactive under excess H₂, rapidly evolving to form alkanes, aromatics, or polymerized coke, depending on the reaction temperature.^{40,52}

For multi-step GTP routes, Blass *et al.*⁵⁰ use a continuous H₂-flow and glycerol in three separate reactors to reach a C₂₋₃ olefin yield of 46 %. However, when connecting these reactors in series, only a 15 % yield of C₂₋₃ olefins was obtained (Table 3). The last configuration requires an increase in total pressure to improve the hydrogenation rate. According to the Antoine Equation,¹³³ the temperature of this step should also be proportionally increased over 140 °C so that the vapor pressure of glycerol is always higher than its partial pressure to avoid glycerol condensation. Adopting similar three steps approach, Hulteberg *et al.*⁶⁴ have reached a better compromise between H₂ flow and total pressure (from 2 bar to 10 bar) to balance hydrogenation and dehydration rates in three successive reactors, obtaining ~46 % propylene yield at 5 bar and 400 ml/min of H₂ flow (Fig. 7 B). However, a separate control of H₂ pressure for each reactor needs to be carefully considered because H₂ benefits hydrogenation, while not necessary for the dehydration steps. Adapting it accordingly can help to reduce H₂ wastage. Also, integrate an additional reactor involving simultaneous catalytic reforming of bioglycerol to H₂-rich gas, which can be carried out under similar operating conditions,¹⁹⁴ may also help in letting go of external H₂ use or at least minimize its utilization.

Deshpande *et al.*⁶⁵ have evaluated the influence of H₂ and N₂ partial pressure on the reductive and non-reductive dehydroxylation of crude glycerol in two steps. Reductive dehydroxylation under H₂ pressure (3.45-34.5 bar), which involves a molar ratio of glycerol/halogen-catalyst (4:1-27:1), temperature (120-210 °C), and TOS (6-6.5 h), improves GTP performance, attaining a propylene selectivity from 38 % to 96 % at a conversion from 24 % to 100 %. Yu *et al.*⁵³ have adjusted total H₂ pressure between 5 and 50 bar to promote the GTP route, according to separate two-step and tandem processes (Ir/ZrO₂+ZSM-5). Working at 50 bar and 250 °C records a propylene selectivity of 67 % at full glycerol conversion (Table 3), although a high amount of propane is also detected. To overcome this drawback, total pressure is optimized at 5 bar, with a propylene selectivity of 88 %, although glycerol conversion unfortunately decreases to 73 %. Wu *et al.*²⁸ have also studied the effect that the presence or absence of H₂ has on the HDO of simulated crude glycerol (glycerol/methanol molar ratio

=1/1.28 and oxygenates/H₂O = 1/1) over double-bed catalysts under typical MTP process conditions.^{26,109} Increasing partial H₂ pressure from 0 to 95.6 kPa therefore increases propylene selectivity from 38 % to 63 %, while decreasing the optimal temperature for the highest GTP yield from 600 °C to 500 °C (Fig. 9 A-B). This H₂-rich medium probably renders it unnecessary for C-C/C-H cracking at higher temperatures to promote hydrogenation events. Sun *et al.*⁴² have modulated H₂ partial pressure by increasing atmospheric H₂ flow from 30 ml.min⁻¹ to 180 ml.min⁻¹ to promote GTP selectivity from 57.8 % in a single bed (9.3 wt% WO₃/T317) to 84.8 % in a double bed (9.3 wt% WO₃/T317+Al₂O₃-SiO₂, Fig. S5 B, Table 3). This enriched H₂ medium shifts the equilibrium in favor of propylene formation through the initial hydrogenation of hydroxyacetone to 1,2-propanediol and propionaldehyde to 1-propanol,¹⁶¹ which seems to be intensified by the final dehydration of propanols over acid aluminosilicates catalyst placed in the down-bed.⁵³ Indeed, they recommend a slightly higher H₂ pressure than an atmospheric one to balance the pressure drop in the double powdered beds. This configuration should be adjusted to better control mass transport restrictions, kinetic reaction rates and reactor obstruction.

The effect of H₂ or N₂-pressure on a single-step GTP route has also been experimentally studied in the range of 0-200 bar.^{47,48,55,60-63} This produces a propylene yield of ~ 90 %, ^{55,63} a propylene selectivity of ~71 % at a glycerol conversion of ~ 50 %, ⁴⁸ propylene selectivity of ~82.1 % at a glycerol conversion ~ 85.8 %, ⁶¹ and a propylene yield up to ~ 84.1 %, ⁶⁰ which depend to the target optimal conditions; 98 bar (H₂/glycerol molar ratio ~120 and 300 °C), ^{55,63} 80 bar (H₂/glycerol molar ratio ~53 and 300 °C), ⁴⁸ 83 bar (H₂/glycerol molar ratio ~2.3 and 254 °C)⁶¹ and 50 bar (H₂/glycerol molar ratio ~98 and 318 °C),⁶⁰ respectively, using a transition metal-based catalyst (Table 3, Fig. 9 C-F). Increasing H₂ pressure or the H₂/glycerol molar ratio generally enhances propylene selectivity, most likely by suppressing the formation of partially deoxygenated intermediates (*i.e.*, allyl-alcohols, propionaldehyde, acetone), which has also been corroborated experimentally and by modeling.^{37,62} However, an excessive increase can saturate C=C, instead forming propane.^{46,52,60,61} For example, when SHI *et al.*⁶¹ increase H₂ availability by raising the H₂/glycerol molar ratio from 2.3:1 to 6.8:1 (at constant total pressure ~ 83 bar and 316 °C), the selectivity of products shifts significantly from ~59.2 % of propylene to ~ 75.7 % of propane (Table 3). Nevertheless, no difference in glycerol conversion is observed when N₂-pressure (~ 30 bar) is used instead of H₂, but propylene selectivity decreases significantly due to the formation of oxygenates (Fig 9 D).⁴⁸ An inert or weak H₂ atmosphere mainly favors the isomerization of allyl-alcohols to unstable propionaldehyde that becomes actively involved in the subsequent polymerization and condensation with other C₃ compounds to yield undetected heavier products in CG and/or coke deposition in the catalyst surface,^{46,59} which is

manifested as a low carbon balance. Anderson *et al.*⁴⁶ co-fed H₂S (ppm) *in situ* with a glycerol/water mixture under 18 bar of H₂ pressure and 400 °C, allowing them to eradicate the formation of oxygenates and improve the catalyst stability by 6-12 times for deoxygenation-hydrogenation activities.

Fig. 9 C-E shows that lowering H₂ pressure and the H₂/glycerol molar ratio also negatively affects glycerol HDO by providing lower propylene selectivity.^{48,60,62} This lower level of hydrogenation and deoxygenation can be primarily ascribed to low H₂ solubility in the medium. Insufficient H₂ dissolved in the medium leads to poor contact between H₂ and glycerol on the redox or metallic site, which instead forms oxygenates over acid site. Thermodynamics may have an unfavorable effect. According to Le Chatelier's rules, when the total pressure is decreased, the reactions shift towards more molecules in the gas phase. This will favor the pathways that repress H₂ consumption, or at least those that consume less H₂ (used in excess) to maintain a high number of moles of gas in the overall process, partially rewarding the effect of decreasing the pressure. Specifically, the HDO of glycerol theoretically needs two or three moles of H₂ to be fully deoxygenated in one mole of propylene or propane, respectively. However, certain partially dehydrated compounds (*e.g.*, acrolein, hydroxyacetone, C₃ diols, and allyl-alcohol) can be formed *via* dehydration without external H₂ consumption or via hydrogenolysis with just one mole of H₂, maintaining a high number of moles in the gas-phase by lowering the pressure of the overall process. Consequently, the single-step GTP route is blocked when partial H₂ pressure decreases.

Synthetic Summary: An inert atmospheric pressure is used mainly during the conversion of glycerol to C₂₋₃ olefins at high temperatures. However, an H₂ atmosphere plays a critical kinetic and thermodynamic role in the GTP reaction under typical HDO conditions (mild temperature and pressure, neutral aqueous medium, etc.). An excessively H₂-rich medium is undesirable, as it favors the further hydrogenation of propylene to propane, which becomes particularly abundant over a high amount of hydrogenating metals (*e.g.*, Ir, Pt, Pd, Ni, Mo.^{46,52,53,61,62}). At low H₂ pressure, and has been corroborated by recent experimental data,^{37,48,60,62} numeric calculations³⁷ indicate weak H₂ solubility in the reaction medium and insufficient H₂ adsorption-dissociation over active site, which negatively affects C-O cleavage and C-C hydrogenation events in glycerol and oxygenates, becoming particularly pronounced when the reaction is occurring in liquid phase. Therefore, an optimized compromise between total pressure, H₂/glycerol (*mol.*) ratio and the partial pressure of the other reactants (*i.e.* glycerol, H₂O, solvent, etc.) can provide acceptable GTP rates, albeit ultimately depending on other parameters such as temperature and space-velocity, among others.

1.8.3. Influence of feed mixture and/or space-velocity

Given that the crude bioglycerol recovered in industry contains solvents and impurities (*e.g.*, H₂O, methanol, heavy organic fractions, and inorganic salts),^{121,135,137} the effect of such additives on GTP catalysis has also been studied by different authors.^{28,41,42,44,46–49,54,57,60–63}

Corma *et al.*⁴¹ have injected a glycerol/vacuum oil mixture (molar ratio $\sim 1/7-1/31$) to simulate GTP conditions (WHSV $\sim 20-60 \text{ h}^{-1}$, 500 °C, FCC1 catalyst) in near operational industrial FCC process.¹⁹⁵ The co-feeding of oils with glycerol seems to have a diluting effect because the initial calculations of heat requirements indicate that a mixture of glycerol/oil higher than 20 wt% (WHSV at 20 h⁻¹) increases the yield of C₂-C₄ olefins to 13.3 %, which is better than those yields obtained with pure glycerol or pure vacuum oil. Furthermore, the co-injection of glycerol (before mixing with oil) with extra water ($\sim 50 \text{ wt}\%$), which acts as a heat sink in the FCC unit due to its high vaporization temperature, increases the formation of small C₂-C₄ olefins to 31 %. These findings suggest that it may be suitable to combine GTP with MTP processes in tandem to intensify the production of sustainable propylene.

Hoang *et al.*⁴⁰ have adjusted the weight of catalyst (HZSM-5) per mass of glycerol feed (W/F ~ 0.05 to 8) under N₂-flow at 400 °C, finding that W/F ~ 8 yields almost $\sim 40 \%$ propylene, while W/F ≤ 4 shifts the reaction toward heavy C₆-C₁₂ aromatics (60 %). Xiao *et al.*⁴⁴ report an inverted tendency for the GTP route over Pd/HZSM-5 when using an H₂/N₂ flow instead of pure N₂ at the same temperature of 400 °C. A W/F of more than ~ 2 yields constant rates of C₂-C₃ oxygenates and C₂-C₃ olefins ($\sim 30\%$), although the yield of aromatics increases proportionally as W/F increases. This might be related to the fast conversion of oxygenates and light olefins to aromatics, which can be induced by the dissociation of excess H₂ over Pd element impregnated over HZSM-5 catalyst to generate hydrogenating sites adjacent to Brønsted and/or Lewis sites.

Yu *et al.*⁵³ inject refined glycerol and simulated crude glycerol (containing H₂O $\sim 5-50 \text{ wt}\%$ and NaCl/methanol mass ratio $\sim 4:1-15:1$) to study the effect of these impurities on two-step GTP (Ir/ZrO₂ and HZSM-5). No change in GTP performance is observed with a low content of NaCl or methanol of $\leq 4 \text{ wt}\%$: 92-94 % of *l*-propanol in the first hydrogenolysis step and 99 % of propylene in the second dehydration step. However, when a higher amount of NaCl (15 wt%) is used, the amount of Ir used as hydrogenating element in the hydrogenolysis catalyst should be increased from 0.12 mol% to 0.2 mol%, which is equivalent to dividing WHSV by 1.67, to maintain a comparable GTP performance. A similar co-feeding strategy has been used by Wu *et al.*^{28,49} over a tandem GTP system by injecting WHSV $\sim 1 \text{ h}^{-1}$ of simulated crude glycerol (glycerol/methanol = 1/1.28 and

oxygenates/ $\text{H}_2\text{O} = 1$), corresponding to 1 kPa glycerol, 1.2 kPa methanol, 2.2 kPa water, 95.6 kPa H_2 , over dual-system Pt/ZSM-5+ HZSM-5, which provides better propylene selectivity ($\sim 63.7\%$) than that usually obtained in a typical MTP process ($\sim 47.9\%$) under similar conditions (Fig. S6 A-B). A similar GTP selectivity ($\sim 71\%$), which remains constant for ~ 500 h, is obtained when feeding a similar composition of reactants over the tandem system: $\text{MoO}_3\text{-Ni}_2\text{P/Al}_2\text{O}_3\text{+ZSM-5}$ (Fig. S5 C).⁴⁹ Sun *et al.*⁴² varied the amount of glycerol in water (20-60 wt%) over the increased mass (1-4 g) of the double-bed system; 9.3 wt% $\text{WO}_x\text{/T317 + Al}_2\text{O}_3\text{-SiO}_2$. A low glycerol/water mixture (20 wt%), an increase in the mass of the first hydrogenolysis catalyst (from 1 g to 4 g) improves the formation of propylene and propane (from 48 % to 54%), while that of *l*-propanol decreases proportionally from 38 % to 31 %. This suggests that increasing the contact time over catalytic sites favors hydrogenation events, as corroborated recently.^{60,62} However, when the amount of glycerol is increased to 60 wt%, the selectivity towards more hydrogenated compounds (propylene, propane, and *l*-propanol) decreases significantly, whereas the selectivity of more oxygenates (hydroxyacetone, *l,2*-propanediol) increases proportionally. This kinetic tendency suggests the reduced availability of active-sites, which are suppressed by increasing the amount of the second dehydration catalyst ($\text{Al}_2\text{O}_3\text{-SiO}_2$, 1 g to 3 g), reaching a stable propylene selectivity of 84.8 % at total conversion for about 24 h (Fig. S5 B).

Di Mondo *et al.*⁵⁴ have correlated the single-step HDO of glycerol/water (10 wt%) with the contact time of the homogeneous co-catalyst to show that increasing the concentration of HOTf compound (up to 60 mmol/L) improves GTP yield (up to 96 %) after just 5 h TOS under 55 bar of H_2 pressure, instead of 24 h as reported for the 40 mmol/L of co-catalyst. However, when water content is increased to 50 wt%, the HDO of glycerol forms mainly *l*-propanol, including when the hydrogenating Ru-based catalyst is coupled with the HOTf co-catalyst and a high H_2 pressure (~ 75.8 bar) is applied.⁵⁷ More recently, Janssen *et al.*⁴³ have used glycerol/water mixtures (50-100 wt%) to compare GTP performance with crude glycerol under similar homogeneous conditions, (Table 3, Fig. 8 F, Fig. S1 A). For high water content, a significant decrease in both dehydration and hydrogenation rates has been observed at 210 °C, thus decreasing GTP yield from 57 % to 35 %. This has been circumvented by improving glycerol and H_2 mixing at a slightly higher temperature ~ 220 °C, which yields 76 % propylene (Fig. 8 F). Under the same operating conditions, the use of crude glycerol yields 82 % of propylene (Table 3, Fig. S1 A).

For heterogeneous GTP conditions, Fadigas *et al.*^{55,63} have studied space-velocity between 2 h^{-1} and 20 h^{-1} for the single-step HDO of glycerol/water (30-100 wt%) to propylene and propane. A high molar ratio of H_2 /glycerol up to 120/1 is required to obtain a high GTP yield ($\sim 90\%$), increasing the space-velocity to 5.4 h^{-1} and the glycerol/water mixture to 90 wt%. Zacharopoulou *et al.*^{47,48,62} have adjusted

catalyst loading to report similar GTP findings. As expected, glycerol conversion and propylene selectivity improve with an initial increase in catalyst loading, which is evidently related to the availability of additional active sites. However, a further increase in catalyst loading does not lead to a proportional increase in conversion and selectivity (Fig. S6 C-D), which suggests there may be diffusional restrictions. The amount of catalyst in a batch reactor should be carefully adjusted to the mass of reactants in order to both improve transport aspects and avoid fast catalyst deactivation.⁴⁸ Anderson *et al.*⁴⁶ report that a short contact time (~ 3 s) for the single-step HDO of a higher glycerol/water mixture (80 wt%) leads to a very low HDO activities and alkenes formation (Fig. S7 A-B), producing mainly unsaturated C₃ oxygenates, while a longer contact time (~ 360 s) improves glycerol conversion to yield $\sim 58\%$ alkanes/alkenes (i.e., propylene $\sim 26\%$). These HDO tendencies have recently been corroborated,⁶⁰ whereby a low WHSV (1.7 h^{-1}) of glycerol/water (10 wt%) seems to balance the deoxygenation-hydrogenation rates over MoO_x supported on SBA-15, with a high GTP yield (up to 84.1 %). However, increasing WHSV to 4.7 h^{-1} significantly decreases the GTP yield to 21 % (Table 3). Similar reaction trends, which seems to be mostly related to the availability of active sites, as corroborated in our recent research,⁶⁰ were also observed over bulk MoO_x catalyst (Fig. S7 C-D).

Synthetic Summary: Feed composition, space-velocity, and catalyst amount are important parameters that affect not only the HDO events in glycerol and intermediates to form the target propylene, but also catalyst stability along TOS. GTP catalysis in a homogeneous medium seems to provide more resistance to impurities, although recycling issues are still a challenge. In turn, heterogeneous GTP routes should be further studied to reach a balanced compromise between the population of active sites and the extent of deoxygenation and hydrogenation in glycerol and intermediated oxygenates, thereby avoiding the formation of partially deoxygenated compounds (i.e., C_xH_yO_z) or fully hydrogenated propane. Combine high-throughput experimentation with predictive modeling and design of experiments methodologies could be powerful tools in adjusting the partial pressure of oxidizing (C_xH_yO_z, H₂O) and reducer (i.e., H₂) agents at optimal temperature of reaction with the HDO properties of the used catalysts. This can help to overcome catalyst instability in an aqueous medium, which is due to the excessive accumulation of oxygen on the catalyst surface, as we have been confirmed.⁶⁰

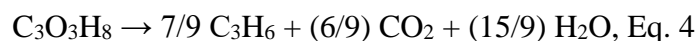
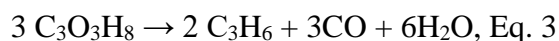
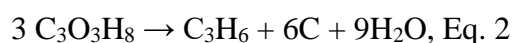
1.8.4. Thermodynamic-kinetic considerations and GTP routes comparison

As highlighted in this review, different GTP strategies (Scheme 9 a-e) have been or are being explored to link the biorefinery and polyolefin industries. We therefore compare these routes using qualitative

and/or quantitative indicators (*e.g.*, process configuration, severity of conditions, energy consumption, propylene yield, and sustainability aspects) to identify the most suitable route that can potentially produce a high yield of green propylene with minimal H₂ consumption and byproducts, as well as reducing workup facilities and investments.

High-temperature GTP^{35,38,41,45,51,56,66,67} exploits simultaneous glycerol dehydration and cracking under inert atmosphere to form propylene and ethylene at temperatures higher than 400 °C, whereas H₂ is generated *in situ* and directly activated on the catalytic sites.^{33,35,41,48} Nevertheless, the viability of this strategy is questionable because it involves the following drawbacks:

- i) Intensive energy spending on sensible and latent heats for vaporizing glycerol and water mixture,
- ii) Huge volume expansion induced by the vaporization of glycerol and water, which greatly increases the investment cost.
- iii) Low experimental yield of propylene, which in the best of cases cannot exceed the theoretical values between ~33.3 % and ~77.7 %⁴¹ because part of the glycerol is converted at high temperatures through H₂ transfer reactions and cracked in C, CO_x emission and H₂O, according to the following reactions (Eq. 2-4):



- iv) Rapid deactivation of the acid catalysts by stream dealumination or coke formed at high temperatures
- v) Instability of C=C bonds that undergo complete saturation to C₁₋₃ alkanes, which become more pronounced when external H₂ is used instead of inert gas, particularly over noble metals modified zeolites.^{28,35,52}

Multi-step GTP strategies, which apply external H₂ source either in separate steps or through cascade reactors,^{28,49,50,53,64,65} whereby the equilibrium can be shifted to form propylene under moderate operating conditions. Each reactor normally contains a specific hetero- or homogeneous catalyst for accelerating the kinetics of the target intermediate reactions: dehydration,^{50,64} hydrogenolysis,^{28,42,49,53} hydrogenation,^{50,64} aldol condensation to C₄₋₅,⁵⁰ cracking to C₂₋₃ olefins,⁵⁰ double dehydroxylation,⁶⁵ and/or further dehydration to propylene.^{28,42,49,53,64} The articulation of these reactions depends on

reactor configurations, target operating conditions, catalysts type, etc. Nonetheless, the viability of the multi-step mode also remains questionable because it requires the following:

- i) Expensive separation of value-added C₃ such as acrolein, propionaldehyde, or *l*-propanol, which cannot be viably converted into propylene. For example, the difference in the price of propylene and *l*-propanol (spread of \$400 per ton on average, 2022).⁸
- ii) Extensive H₂ consumption because hydrogenolysis or hydrogenation steps involve mainly noble metal-based catalysts (*i.e.*, Ir, Pt, Pd, ^{28,50,53}). The use of these noble metals is very expensive, reducing the financial benefits. In addition continuous H₂ use for some cascade reactions should be carefully rationalized, as the dehydration step does not require an H₂ feed. ⁵⁰

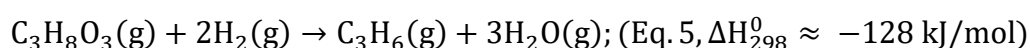
From an integration point of view, the efficiency of the multi-step approach could be improved if a continuous process combines various catalysts and active species in tandem or in close contact. ^{28,42,49,53} Various dual-bed systems have been explored accordingly: Ir (0.12 mol%)/ZrO₂ + HZM5, ⁵³ WO₃(9.3 wt%)/T317 + SiO₂-Al₂O₃, ⁴² Pt(0.3 wt%)/ZSM-5 + ZSM-5²⁸ and MoO₃/Ni₂P (20 wt%)/Al₂O₃ + ZSM-5. ⁴⁹ Propylene selectivity up to 88 % has been reported for TOS between 0.5 and 24 hours. ^{28,42,49,53} Given this short TOS, the *in situ* regeneration of spent catalysts seems difficult over such a complex mixture of active sites, where some ones require oxidative calcination and other need reducer treatment. Besides, catalysts working in tandem reaction-bed zones require an optimal kinetic control of the involved reactions for the overall GTP because the route occurs through successive reactions steps (*i.e.*, first hydrogenolysis and then dehydration) with different kinetic rates. If the GTP reaction is extended for a longer period, some active sites may be deactivated before others. Thus, successive stops of the process to unload spent catalyst and load new ones would greatly increase the cost of operation. These drawbacks would negatively affect the inter-operability of this tandem strategy.

In turn, a single-step GTP route carried out in gas, liquid or mixed phases is undergoing substantial advances. ^{43,46-48,55,59-63} It may become a truly real ecofriendly route for producing sustainable propylene, particularly if the production of H₂ from fossil-based resources is replaced by, for example, *in situ* H₂ generation from renewable sources (*i.e.*, biomass, water electrolysis, etc.). There are therefore numerous aspects to consider for continuing working on improving single-step GTP route efficiency:

- i) Oxygen elimination and hydrogen introduction, through which the GTP route takes place, are thermodynamically favorable mainly under mild HDO conditions: T ≤ 400 °C and P ≤ 83

bar, as reviewed in this work. These less-intensive energy conditions favor a better techno-economic performance and environmental impact. For example, working in liquid or mixed phases can further reduce the consumption of energy due to the unnecessary evaporation of reactants or solvents (*i.e.*, $\Delta H_{\text{Vap}}^0(\text{H}_2\text{O}) \sim 2257 \text{ kJ/kg}$, $C_p^0(\text{H}_2\text{O}) \sim 4.18 \text{ J/g/}^\circ\text{C}$), and reduce installation size and cost. The bioglycerol degradation to C_{1-2} co-products and the CO_2 emissions prevailing at severe temperatures can also be minimized.

- ii) No thermodynamic limits on the full HDO of glycerol to 100 % propylene yield from mild temperatures $\sim 200 \text{ }^\circ\text{C}$ and at any H_2 pressure (Fig. 10 A). The pressurized unit systems could be used *in situ* for the subsequent separation of propylene and H_2 using well-developed membrane technologies or pressure swing adsorption, while water can easily be recovered by condensation.
- iii) Propylene hydrogenation to propane (eq. 1) is an exothermic reaction and favored at even lower temperatures (Fig. 10 B). The formation of oxygenates (*i.e.*, hydroxyacetone and C_3 diols) is kinetically favored under a H_2 -poor medium and low temperature.^{37,47,48,59} The formation of these byproducts may be reduced by moderately increasing temperature and adjusting H_2 partial pressure accordingly, obtaining a high GTP yield over an appropriate catalyst.
- iv) Under mild HDO conditions, the one-pot HDO of glycerol theoretically requires just two moles of H_2 to produce one mole of propylene and co-generate only H_2O (eq. 5), which allows maintaining a zero carbon footprint.^{39,48,60}



However, this ideal state is still very difficult to achieve experimentally. As we have been reviewed, kinetically, and instead of completely removing oxygen from glycerol to selectively form propylene, the reaction may only contribute to partial C-O scission to form C_3 -oxygenates at a low temperature,^{48,59,60} breaking C-C and C-H bonds at a higher temperature to produce H_2 + shorter carbon chain compounds,^{28,41,46} or at the most, saturate the C=C bond of propylene to yield propane under high H_2 pressure.^{52,60,62} However, recent literature^{42,43,53,55,60,62} reports that it may draw very close to this ideal state through the application of appropriate conditions and catalysts (homogeneous Ru-complex,⁴³ and heterogeneous Mo-based catalysts^{48,55,60,62}). Although GTP in a discontinuous batch reactor^{43,47,48,57,59} is less suited to the mass production of propylene, it provides initial insights, such as proof of the single-step GTP concept. Operating in continuous systems^{46,55,60-63} provides an interesting GTP yield of up to 90 %. Nevertheless, this strategy still requires further improvements to run for a longer TOS, as catalyst instability in aqueous media is a major challenge.^{47,48,60} Therefore, stabilizing the

peak GTP yield is wholly possible by optimizing both the HDO abilities of the catalysts and the operating conditions (*i.e.*, temperature, pressure, space-velocity, feed, and composition). These propositions provide some guidance on the single-step GTP reaction, but the severity of the unselective mass/heat transfer conditions should also be considered, as the overall process is relatively exothermic (Eq. 5, -128 kJ/mol).

1.8.5. Relevance to techno-economic and environmental efficiency

To the best of our knowledge, there are no techno-economic or environmental studies specifically focused on the evaluation of GTP routes technology. The current literature deals instead with the assessment of routes integrating olefin production from industrial and urban organic wastes or general biomass, as a wider context.^{23,196–200} This might be related to the major progress in research and technology made in the field of these processes.^{18,19,21–28,197,201–204} Some of these concepts have already entered the testing stage or industrial development; *i*) SABIC technology (the Netherlands and Saudi Arabia) is based on the co-feeding of “*second generation*” animal fats and vegetable oils with petroleum feedstocks,^{205,206} *ii*) The BRASKEM approach (Brazil) involves sugarcane fermentation to bioethanol followed by dehydration to bioethylene and further dimerization and metathesis to biopropylene,^{21,23} *iii*) The MITSUI chemical route (Japan)²⁰⁷ involves second generation biomass fermentation to biobutanol, followed by dehydration to biobutylene and metathesis with ethylene to produce green propylene, for example. Furthermore, the most developed concept, which is employed by many companies (*e.g.*, ExxonMobil, TotalEnergies, and Shell Global Solutions) involves the initial gasification of second-generation biomass and urban wastes to produce syngas, followed by FTS of methanol. Conventional MTO/MTP technology is then applied to obtain relatively sustainable propylene and/or ethylene.^{196,197,205,208} As described, these technologies integrate multi-stage reactions, sometimes the co-feed of petroleum-based feedstocks, and the manufacturing chain involves unrecovered CO₂ emissions,^{196,197,208} which reduces its sustainability.

The development of a novel GTP route such as that involving only a single-step HDO of crude bioglycerol to biopropylene, where the required H₂ is produced *in situ via* simultaneous catalytic reforming of bioglycerol to H₂-rich gas, or H₂O-electrolysis or splitting using surplus electricity, solar energy or wind-powered systems with closed carbon emission cycles can convert this GTP approach into a truly ecofriendly green technology. Thus, producing sustainable propylene will obviously help to comply with the global targets for future CO₂-neutral polypropylene production, whereby the

polyolefin industries may become more ecofriendly. This viewpoint is backed by the high availability of crude bioglycerol that will continue to grow annually, as highlighted in section 2.2.

Based on the above, it seems reasonable to advise other researchers to conduct pioneering techno-economic and environmental assessments of GTP routes. This review reports sufficient data (*i.e.*, Table 2-3) in terms of feed composition, reactant conversion, product distribution, operating conditions, and catalyst efficiency for comparative studies. As described in section 3.3.5, the GTP route in a single step seems to have promising operating characteristics, which will reduce the investment in equipment and operating costs.

Comparing the efficiency of a single-step GTP route carried out in, for example, liquid or mixed phases with those undertaken fully in a gas phase via a high-temperature GTP process, multi-step reactions, or a tandem GTP process, may provide valuable insights about their technical feasibility, energy gains, and environmental benefits. For example, light may be shed on how much energy can be saved by operating in the liquid phase, and whether it would be suitably acceptable to compensate what is lost in propylene selectivity and yield, in comparison to a GTP process fully operated in the gas phase. Such insights will encourage further research into overcoming the reported GTP-related challenges, forming a sufficiently consolidated concept to move on to the next upscaling tasks.

Conclusions

In view of the stimulating market prospects for propylene and crude bioglycerol, GTP catalysis should boost research and technological progress to become an alternative for producing sustainable polypropylene. This review of the state-of-the-art of GTP catalysis provides a useful source to guide researchers towards further developments for advancing this technology.

High-temperature GTP catalysis, which involves effective teamwork between glycerol dehydration, C-C/C-H cracking to H₂ producing-transfer-consuming reactions, and further decarbonylation over acid catalysts such as zeolites, instead forms ethylene and, to a lesser extent, propylene. The multi-step GTP process, including the tandem mode that involves various successive reactions (*e.g.*, dehydration, hydrogenolysis, aldol-condensation, and further cracking) over complex multi-functional systems, is proposed to shift the conversion of glycerol and oxygenated intermediates at a low temperature to propylene instead, avoiding further alkylation or Diels-Alder rearrangements. An optimal compromise is required between acidity, size-shape diffusion, active sites synergy and kinetic reaction rates for the process configurations used for improving GTP efficiency and avoiding constant catalysts regenerations or replacements.

In turn, single-step GTP catalysis progresses mostly via sequential C–O deoxygenation and C–C hydrogenation in the glycerol and oxygenated intermediates to form a C=C bond in propylene through H₂ transfer events, according to the reverse Mars–van Krevelen mechanism. It seems to be the most promising strategy that can provide ~100 % propylene yield without thermodynamic limits, if mild operating conditions (*e.g.*, temperature, H₂-pressure, feed, space-velocity) and highly selective catalysts (*i.e.*, homogeneous Ru-complex and heterogeneous Mo-based systems) have been chosen accordingly. Further advances in optimizing GTP operating conditions is still required for balancing deoxygenation-hydrogenation events, minimizing H₂ consumption, and improving the stability of catalysts in a hydrothermal medium.

In brief, implementing an efficient ecofriendly GTP route technology will require a balanced synergy between the design of a robust HDO catalyst and the successful optimization of GTP operating conditions, which depend on the process configuration chosen for the most viable conversion strategies.

Supporting Information: Abbreviations and general terminology, stability of Ru-based catalyst under homogeneous conditions, Mo redox-sites formation, stability of NiMoS_x-based catalyst under sulfides co-feeding, temperature-programed desorption diagrams, additional glycerol-to-propylene mechanisms, glycerol-to-propylene performance as function of temperature, catalyst loading, contact time and space-velocity, and references.”

Acknowledgements:

This study is part of the CatGTP project, which is a Marie Skłodowska-Curie Actions (MSCA) grant (agreement No. 101030636), funded by the EU H2020 program. The authors are also grateful to the following for their financial supports: the Franco-Moroccan research program of PHC Toubkal 2022 (project ref. TBK22/150, 47338YM), the Moroccan CNRST’s program for excellence fellowship (No. 2USMS2022) granted to the PhD student (M. Bahlouri), the FRAPPE program of the “*Hauts-de-France*” region, and Centrale Lille Institut.

REFERENCES:

- (1) *Alpha Olefin Market- Global Industry Analysis and Forecast (2022-2029)*. MAXIMIZE MARKET RESEARCH. <https://www.maximizemarketresearch.com/market-report/alpha-olefin-market/13674/> (accessed 2022-09-19).
- (2) Fakhroeslam, M.; Sadrameli, S. M. Thermal/Catalytic Cracking of Hydrocarbons for the Production of Olefins; a State-of-the-Art Review III: Process Modeling and Simulation. *Fuel* **2019**, *252*, 553–566. <https://doi.org/10.1016/j.fuel.2019.04.127>.

- (3) Corma, A.; Corresa, E.; Mathieu, Y.; Sauvanaud, L.; Al-Bogami, S.; Al-Ghrami, M. S.; Bourane, A. Crude Oil to Chemicals: Light Olefins from Crude Oil. *Catal. Sci. Technol.* **2017**, *7* (1), 12–46. <https://doi.org/10.1039/C6CY01886F>.
- (4) Nawaz, Z. Light Alkane Dehydrogenation to Light Olefin Technologies: A Comprehensive Review. *Rev. Chem. Eng.* **2015**, *31* (5), 413–436. <https://doi.org/10.1515/revce-2015-0012>.
- (5) Akah, A.; Al-Ghrami, M. Maximizing Propylene Production via FCC Technology. *Appl. Petrochem. Res.* **2015**, *5* (4), 377–392. <https://doi.org/10.1007/s13203-015-0104-3>.
- (6) Company, T. B. R. *2020 Global Ethylene Market and Propylene Industry Research Analysis by TBRC*. <https://www.prnewswire.com/news-releases/2020-global-ethylene-market-and-propylene-industry-research-analysis-by-tbrc-301014325.html> (accessed 2022-09-19).
- (7) *To make better decisions, you need to see the big picture*. IHS Markit. <https://ihsmarkit.com/products/propylene-chemical-economics-handbook.html> (accessed 2022-11-02).
- (8) *Global propylene demand & capacity 2015-2022*. Statista. <https://www.statista.com/statistics/1246689/propylene-demand-capacity-forecast-worldwide/> (accessed 2022-09-20).
- (9) Ren, T.; Patel, M.; Blok, K. Olefins from Conventional and Heavy Feedstocks: Energy Use in Steam Cracking and Alternative Processes. *Energy* **2006**, *31* (4), 425–451. <https://doi.org/10.1016/j.energy.2005.04.001>.
- (10) Amghizar, I.; Dedeyne, J. N.; Brown, D. J.; Marin, G. B.; Geem, K. M. V. Sustainable Innovations in Steam Cracking: CO₂ Neutral Olefin Production. *React. Chem. Eng.* **2020**, *5* (2), 239–257. <https://doi.org/10.1039/C9RE00398C>.
- (11) Zhao, Z.; Chong, K.; Jiang, J.; Wilson, K.; Zhang, X.; Wang, F. Low-Carbon Roadmap of Chemical Production: A Case Study of Ethylene in China. *Renew. Sustain. Energy Rev.* **2018**, *97*, 580–591. <https://doi.org/10.1016/j.rser.2018.08.008>.
- (12) Yang, M.; You, F. Comparative Techno-Economic and Environmental Analysis of Ethylene and Propylene Manufacturing from Wet Shale Gas and Naphtha. *Ind. Eng. Chem. Res.* **2017**, *56* (14), 4038–4051. <https://doi.org/10.1021/acs.iecr.7b00354>.
- (13) *Directive 2009/28/EC of the European Parliament and of the Council of 23 April 2009 on the Promotion of the Use of Energy from Renewable Sources and Amending and Subsequently Repealing Directives 2001/77/EC and 2003/30/EC (Text with EEA Relevance)*; 2009; Vol. 140. <http://data.europa.eu/eli/dir/2009/28/oj/eng> (accessed 2022-09-19).
- (14) *Directive (EU) 2018/2001 of the European Parliament and of the Council of 11 December 2018 on the Promotion of the Use of Energy from Renewable Sources (Recast) (Text with EEA Relevance.)*; 2018; Vol. 328. <http://data.europa.eu/eli/dir/2018/2001/oj/eng> (accessed 2022-09-19).
- (15) *Stratégie à long terme à l'horizon 2050*. https://climate.ec.europa.eu/eu-action/climate-strategies-targets/2050-long-term-strategy_fr (accessed 2023-03-05).
- (16) Martin. *The Sustainable Development Agenda*. United Nations Sustainable Development. <https://www.un.org/sustainabledevelopment/development-agenda/> (accessed 2022-09-19).
- (17) Vollmer, I.; Jenks, M. J. F.; Roelands, M. C. P.; White, R. J.; van Harmelen, T.; de Wild, P.; van der Laan, G. P.; Meirer, F.; Keurentjes, J. T. F.; Weckhuysen, B. M. Beyond Mechanical Recycling: Giving New Life to Plastic Waste. *Angew. Chem. Int. Ed.* **2020**, *59* (36), 15402–15423. <https://doi.org/10.1002/anie.201915651>.
- (18) Yuan, Z.; Eden, M. R. Superstructure Optimization of Integrated Fast Pyrolysis-Gasification for Production of Liquid Fuels and Propylene. *AIChE J.* **2016**, *62* (9), 3155–3176. <https://doi.org/10.1002/aic.15337>.
- (19) Ramamurthy, K. K.; Narayanaswamy, R.; Bhotla, V. R. G.; Stanislaus, A.; GANJI, S. Conversion of Waste Plastic to Propylene and Cumene. WO2018127813A1, July 12, 2018.

<https://patents.google.com/patent/WO2018127813A1/fr?oq=WO+2018%2f127813+AI>
(accessed 2022-09-19).

- (20) Babor, M.; Tišler, Z.; Kocík, J.; Hubáček, J.; Bačiak, M.; Herrador, J. M. H. Bioethylene and Biopropylene Production from Waste Fat and Rapeseed Oil via Catalytic Hydrodeoxygenation and Hydrocracking Followed by Pyrolysis. *Chem. Eng. Technol.* **2022**, *45* (11), 2071–2079. <https://doi.org/10.1002/ceat.202200256>.
- (21) Gotro, J. *Bio-Based Polypropylene; Multiple Synthetic Routes Under Investigation*. Polymer Innovation Blog. <https://polymerinnovationblog.com/bio-based-polypropylene-multiple-synthetic-routes-under-investigation/> (accessed 2022-09-19).
- (22) Reznichenko, A.; Harlin, A. Next Generation of Polyolefin Plastics: Improving Sustainability with Existing and Novel Feedstock Base. *SN Appl. Sci.* **2022**, *4* (4), 108. <https://doi.org/10.1007/s42452-022-04991-4>.
- (23) Machado, P. G.; Walter, A.; Cunha, M. Bio-Based Propylene Production in a Sugarcane Biorefinery: A Techno-Economic Evaluation for Brazilian Conditions. *Biofuels Bioprod. Biorefining* **2016**, *10* (5), 623–633. <https://doi.org/10.1002/bbb.1674>.
- (24) Zhang, S.; Yang, X.; Zhang, H.; Chu, C.; Zheng, K.; Ju, M.; Liu, L. Liquefaction of Biomass and Upgrading of Bio-Oil: A Review. *Molecules* **2019**, *24* (12), 2250. <https://doi.org/10.3390/molecules24122250>.
- (25) Gayubo, A. G.; Valle, B.; Aguayo, A. T.; Olazar, M.; Bilbao, J. Olefin Production by Catalytic Transformation of Crude Bio-Oil in a Two-Step Process. *Ind. Eng. Chem. Res.* **2010**, *49* (1), 123–131. <https://doi.org/10.1021/ie901204n>.
- (26) Tian, P.; Wei, Y.; Ye, M.; Liu, Z. Methanol to Olefins (MTO): From Fundamentals to Commercialization. *ACS Catal.* **2015**, *5* (3), 1922–1938. <https://doi.org/10.1021/acscatal.5b00007>.
- (27) Chierigato, A.; Ochoa, J. V.; Cavani, F. Olefins from Biomass. In *Chemicals and Fuels from Bio-Based Building Blocks*; Cavani, F., Albonetti, S., Basile, F., Gandini, A., Eds.; Wiley-VCH Verlag GmbH & Co. KGaA: Weinheim, Germany, 2016; pp 1–32. <https://doi.org/10.1002/9783527698202.ch1>.
- (28) Wu, Z.; Zhao, K.; Ge, S.; Qiao, Z.; Gao, J.; Dou, T.; Yip, A. C. K.; Zhang, M. Selective Conversion of Glycerol into Propylene: Single-Step versus Tandem Process. *ACS Sustain. Chem. Eng.* **2016**, *4* (8), 4192–4207. <https://doi.org/10.1021/acssuschemeng.6b00676>.
- (29) Teketel, S.; Olsbye, U.; Lillerud, K. P.; Beato, P.; Svelle, S. Co-Conversion of Methanol and Light Alkenes over Acidic Zeolite Catalyst H-ZSM-22: Simulated Recycle of Non-Gasoline Range Products. *Appl. Catal. Gen.* **2015**, *494*, 68–76. <https://doi.org/10.1016/j.apcata.2015.01.035>.
- (30) Tan, H. W.; Abdul Aziz, A. R.; Aroua, M. K. Glycerol Production and Its Applications as a Raw Material: A Review. *Renew. Sustain. Energy Rev.* **2013**, *27*, 118–127. <https://doi.org/10.1016/j.rser.2013.06.035>.
- (31) Hájek, M.; Skopal, F. Treatment of Glycerol Phase Formed by Biodiesel Production. *Bioresour. Technol.* **2010**, *101* (9), 3242–3245. <https://doi.org/10.1016/j.biortech.2009.12.094>.
- (32) Kumar, L. R.; Yellapu, S. K.; Tyagi, R. D.; Zhang, X. A Review on Variation in Crude Glycerol Composition, Bio-Valorization of Crude and Purified Glycerol as Carbon Source for Lipid Production. *Bioresour. Technol.* **2019**, *293*, 122155. <https://doi.org/10.1016/j.biortech.2019.122155>.
- (33) Bakhtyari, A.; Makarem, M. A.; Rahimpour, M. R. 4 - Light Olefins/Bio-Gasoline Production from Biomass. In *Bioenergy Systems for the Future*; Dalena, F., Basile, A., Rossi, C., Eds.; Woodhead Publishing, 2017; pp 87–148. <https://doi.org/10.1016/B978-0-08-101031-0.00004-1>.
- (34) Zacharopoulou, V.; Lemonidou, A. A. Olefins from Biomass Intermediates: A Review. *Catalysts* **2018**, *8* (1), 2. <https://doi.org/10.3390/catal8010002>.

- (35) Zakaria, Z. Y.; Amin, N. A. S.; Linnekoski, J. A Perspective on Catalytic Conversion of Glycerol to Olefins. *Biomass Bioenergy* **2013**, *55*, 370–385. <https://doi.org/10.1016/j.biombioe.2013.02.014>.
- (36) Vasiliadou, E. S.; Lemonidou, A. A. Production of Biopropylene Using Biomass-Derived Sources. In *Encyclopedia of Inorganic and Bioinorganic Chemistry*; John Wiley & Sons, Ltd, 2016; pp 1–12. <https://doi.org/10.1002/9781119951438.eibc2454>.
- (37) Rellán-Piñeiro, M.; López, N. A Coupled Density Functional Theory–Microkinetic Modeling for the Hydrodeoxygenation of Glycerol to Propylene on MoO₃. *ACS Sustain. Chem. Eng.* **2018**, *6* (12), 16169–16178. <https://doi.org/10.1021/acssuschemeng.8b02933>.
- (38) Zakaria, Z. Y.; Linnekoski, J.; Amin, N. A. S. Catalyst Screening for Conversion of Glycerol to Light Olefins. *Chem. Eng. J.* **2012**, *207–208*, 803–813. <https://doi.org/10.1016/j.cej.2012.07.072>.
- (39) Wan, W.; Ammal, S. C.; Lin, Z.; You, K.-E.; Heyden, A.; Chen, J. G. Controlling Reaction Pathways of Selective C–O Bond Cleavage of Glycerol. *Nat. Commun.* **2018**, *9* (1), 4612. <https://doi.org/10.1038/s41467-018-07047-7>.
- (40) Hoang, T. Q.; Zhu, X.; Danuthai, T.; Lobban, L. L.; Resasco, D. E.; Mallinson, R. G. Conversion of Glycerol to Alkyl-Aromatics over Zeolites. *Energy Fuels* **2010**, *24* (7), 3804–3809. <https://doi.org/10.1021/ef100160y>.
- (41) Corma, A.; Huber, G. W.; Sauvanaud, L.; O’Connor, P. Processing Biomass-Derived Oxygenates in the Oil Refinery: Catalytic Cracking (FCC) Reaction Pathways and Role of Catalyst. *J. Catal.* **2007**, *247* (2), 307–327. <https://doi.org/10.1016/j.jcat.2007.01.023>.
- (42) Sun, D.; Yamada, Y.; Sato, S. Efficient Production of Propylene in the Catalytic Conversion of Glycerol. *Appl. Catal. B Environ.* **2015**, *174–175*, 13–20. <https://doi.org/10.1016/j.apcatb.2015.02.022>.
- (43) Janssens, K.; Stalpaert, M.; Henrion, M.; Vos, D. E. D. From Crude Industrial Waste Glycerol to Biopropene via Ru-Mediated Hydrodeoxygenation in Ionic Liquids. *Chem. Commun.* **2021**, *57* (51), 6324–6327. <https://doi.org/10.1039/D1CC01779A>.
- (44) Xiao, Y.; Varma, A. Conversion of Glycerol to Hydrocarbon Fuels via Bifunctional Catalysts. *ACS Energy Lett.* **2016**, *1* (5), 963–968. <https://doi.org/10.1021/acseenergylett.6b00421>.
- (45) Lima, D. S.; Perez-Lopez, O. W. Catalytic Conversion of Glycerol to Olefins over Fe, Mo, and Nb Catalysts Supported on Zeolite ZSM-5. *Renew. Energy* **2019**, *136*, 828–836. <https://doi.org/10.1016/j.renene.2019.01.051>.
- (46) Anderson, A. D.; Lanci, M. P.; Buchanan, J. S.; Dumesic, J. A.; Huber, G. W. The Hydrodeoxygenation of Glycerol over NiMoS_x: Catalyst Stability and Activity at Hydrolysis Conditions. *ChemCatChem* **2021**, *13* (1), 425–437. <https://doi.org/10.1002/cctc.202001289>.
- (47) Zacharopoulou, V.; Lemonidou, A. A. Novel Process for Propene Production from Biomass: Catalytic Glycerol Hydro-Deoxygenation. *Mater. Today Proc.* **2018**, *5* (14, Part 1), 27511–27516. <https://doi.org/10.1016/j.matpr.2018.09.070>.
- (48) Zacharopoulou, V.; Vasiliadou, E. S.; Lemonidou, A. A. One-Step Propylene Formation from Bio-Glycerol over Molybdena-Based Catalysts. *Green Chem.* **2015**, *17* (2), 903–912. <https://doi.org/10.1039/C4GC01307G>.
- (49) Wu, Z.; Yan, H.; Ge, S.; Gao, J.; Dou, T.; Li, Y.; Yip, A. C. K.; Zhang, M. MoO₃ Modified Ni₂P/Al₂O₃ as an Efficient Catalyst for Crude Glycerol to Propylene. *Catal. Commun.* **2017**, *92*, 80–85. <https://doi.org/10.1016/j.catcom.2017.01.009>.
- (50) Blass, S. D.; Hermann, R. J.; Persson, N. E.; Bhan, A.; Schmidt, L. D. Conversion of Glycerol to Light Olefins and Gasoline Precursors. *Appl. Catal. Gen.* **2014**, *475*, 10–15. <https://doi.org/10.1016/j.apcata.2014.01.013>.

- (51) Zakaria, Z. Y.; Amin, N. A. S.; Linnekoski, J. Optimization of Catalytic Glycerol Steam Reforming to Light Olefins Using Cu/ZSM-5 Catalyst. *Energy Convers. Manag.* **2014**, *86*, 735–744. <https://doi.org/10.1016/j.enconman.2014.06.040>.
- (52) Murata, K.; Takahara, I.; Inaba, M. Propane Formation by Aqueous-Phase Reforming of Glycerol over Pt/H-ZSM5 Catalysts. *React. Kinet. Catal. Lett.* **2008**, *93* (1), 59–66. <https://doi.org/10.1007/s11144-008-5190-0>.
- (53) Yu, L.; Yuan, J.; Zhang, Q.; Liu, Y.-M.; He, H.-Y.; Fan, K.-N.; Cao, Y. Propylene from Renewable Resources: Catalytic Conversion of Glycerol into Propylene. *ChemSusChem* **2014**, *7* (3), 743–747. <https://doi.org/10.1002/cssc.201301041>.
- (54) Di Mondo, D.; Ashok, D.; Waldie, F.; Schrier, N.; Morrison, M.; Schlaf, M. Stainless Steel As a Catalyst for the Total Deoxygenation of Glycerol and Levulinic Acid in Aqueous Acidic Medium. *ACS Catal.* **2011**, *1* (4), 355–364. <https://doi.org/10.1021/cs200053h>.
- (55) Mota, C. J. A.; Gonçalves, Valter. L. C.; Mellizo, J. E.; Rocco, A. M.; Fadigas, J. C.; Gambetta, R. Green Propene through the Selective Hydrogenolysis of Glycerol over Supported Iron-Molybdenum Catalyst: The Original History. *J. Mol. Catal. Chem.* **2016**, *422*, 158–164. <https://doi.org/10.1016/j.molcata.2015.11.014>.
- (56) Zakaria, Z. Y.; Amin, N. A. S.; Linnekoski, J. Thermodynamic Analysis of Glycerol Conversion to Olefins. *Energy Procedia* **2014**, *61*, 2489–2492. <https://doi.org/10.1016/j.egypro.2014.12.029>.
- (57) Taher, D.; Thibault, M. E.; Di Mondo, D.; Jennings, M.; Schlaf, M. Acid-, Water- and High-Temperature-Stable Ruthenium Complexes for the Total Catalytic Deoxygenation of Glycerol to Propane. *Chem. – Eur. J.* **2009**, *15* (39), 10132–10143. <https://doi.org/10.1002/chem.200901427>.
- (58) Wan, W.; Lin, Z.; Chen, J. G. Vibrational Spectroscopic Characterization of Glycerol Reaction Pathways over Metal-Modified Molybdenum Carbide Surfaces. *ChemCatChem* **2020**, *12* (1), 281–286. <https://doi.org/10.1002/cctc.201901629>.
- (59) Zacharopoulou, V.; Vasiliadou, E. S.; Lemonidou, A. A. Exploring the Reaction Pathways of Bioglycerol Hydrodeoxygenation to Propene over Molybdena-Based Catalysts. *ChemSusChem* **2018**, *11* (1), 264–275. <https://doi.org/10.1002/cssc.201701605>.
- (60) El Doukkali, M.; Dumeignil, F.; Paul, S. New Insights in Single-Step Hydrodeoxygenation of Glycerol to Propylene by Coupling Rational Catalyst Design with Systematic Analysis. *Appl. Catal. B Environ.* **2023**, *324*, 122280. <https://doi.org/10.1016/j.apcatb.2022.122280>.
- (61) Shi, T.-P.; Yao, J.; Dunn, B. C.; Sughrue, E. L. Converting Glycerol to Propylene. US20160168044A1, June 16, 2016. <https://patents.google.com/patent/US20160168044A1/en> (accessed 2022-09-20).
- (62) Ioannidou, G.; Loukia Yfanti, V. –; Lemonidou, A. A. Optimization of Reaction Conditions for Hydrodeoxygenation of Bio-Glycerol towards Green Propylene over Molybdenum-Based Catalyst. *Catal. Today* **2022**. <https://doi.org/10.1016/j.cattod.2022.09.008>.
- (63) FADIGAS, J. C. S.; Gambetta, R.; MOTA, C. J. de A.; CONCEIÇÃO, G. V. L. da. Préparation de catalyseurs hétérogènes utilisés dans l’hydrogénation sélective de glycérine en propène et procédé pour l’hydrogénation sélective de glycérine en propène. WO2009155674A1, December 30, 2009. <https://patents.google.com/patent/WO2009155674A1/fr> (accessed 2022-09-20).
- (64) Hulteberg, C.; Brandin, J. Process for Preparing Lower Hydrocarbons from Glycerol. US20110224470A1, September 15, 2011. <https://patents.google.com/patent/US20110224470A1/en> (accessed 2022-08-25).
- (65) Deshpande, R.; Davis, P.; Pandey, V.; Kore, N. Dehydroxylation of Crude Alcohol Streams Using a Halogen-Based Catalyst, June 20, 2013. <https://patentscope.wipo.int/search/en/detail.jsf?docId=WO2013090076> (accessed 2022-09-20).

- (66) Corma, A.; Huber, G. W.; Sauvanaud, L.; O'Connor, P. Biomass to Chemicals: Catalytic Conversion of Glycerol/Water Mixtures into Acrolein, Reaction Network. *J. Catal.* **2008**, *257* (1), 163–171. <https://doi.org/10.1016/j.jcat.2008.04.016>.
- (67) Gujar, J. P.; Modhera, B. A Review on Catalytic Conversion of Biodiesel Derivative Glycerol to Bio-Olefins. *Mater. Today Proc.* **2023**, *72*, 2723–2730. <https://doi.org/10.1016/j.matpr.2022.09.418>.
- (68) Buehler, C. K.; Masino, A. 5610246 Process for Polymerizing Propylene Using a Silica-Supported Catalyst. *J. Mol. Catal. Chem.* **1997**, *125* (2), 168–169. [https://doi.org/10.1016/S1381-1169\(98\)80069-1](https://doi.org/10.1016/S1381-1169(98)80069-1).
- (69) Fink, G.; Steinmetz, B.; Zechlin, J.; Przybyla, C.; Tesche, B. Propene Polymerization with Silica-Supported Metallocene/MAO Catalysts. *Chem. Rev.* **2000**, *100* (4), 1377–1390. <https://doi.org/10.1021/cr9804689>.
- (70) Kulajanpeng, K.; Sheibat-Othman, N.; Tanthapanichakoon, W.; McKenna, T. F. L. Multiscale Modelling of Multizone Gas Phase Propylene (Co)Polymerization Reactors—A Comprehensive Review. *Can. J. Chem. Eng.* **2022**, *100* (9), 2505–2545. <https://doi.org/10.1002/cjce.24471>.
- (71) Nakano, R.; Nozaki, K. Copolymerization of Propylene and Polar Monomers Using Pd/IzQO Catalysts. *J. Am. Chem. Soc.* **2015**, *137* (34), 10934–10937. <https://doi.org/10.1021/jacs.5b06948>.
- (72) Ghosh, S.; Acharyya, S. S.; Tiwari, R.; Sarkar, B.; Singha, R. K.; Pendem, C.; Sasaki, T.; Bal, R. Selective Oxidation of Propylene to Propylene Oxide over Silver-Supported Tungsten Oxide Nanostructure with Molecular Oxygen. *ACS Catal.* **2014**, *4* (7), 2169–2174. <https://doi.org/10.1021/cs5004454>.
- (73) Khatib, S. J.; Oyama, S. T. Direct Oxidation of Propylene to Propylene Oxide with Molecular Oxygen: A Review. *Catal. Rev.* **2015**, *57* (3), 306–344. <https://doi.org/10.1080/01614940.2015.1041849>.
- (74) Martin, G. A. G.; Erich, H.; Kurt, R. K. G.; Wilhelm, G. E.; Ludwig, O.; Horst, H. Process for Preparing Halogenated and Sulfohalogenated Copolymers of Lower Olefins. US3206444A, September 14, 1965. <https://patents.google.com/patent/US3206444A/en> (accessed 2022-09-20).
- (75) Lin, R.; Amrute, A. P.; Pérez-Ramírez, J. Halogen-Mediated Conversion of Hydrocarbons to Commodities. *Chem. Rev.* **2017**, *117* (5), 4182–4247. <https://doi.org/10.1021/acs.chemrev.6b00551>.
- (76) Teržan, J.; Huš, M.; Likozar, B.; Djinović, P. Propylene Epoxidation Using Molecular Oxygen over Copper- and Silver-Based Catalysts: A Review. *ACS Catal.* **2020**, *10* (22), 13415–13436. <https://doi.org/10.1021/acscatal.0c03340>.
- (77) Lu, J.; Zhang, X.; Bravo-Suárez, J. J.; Tsubota, S.; Gaudet, J.; Oyama, S. T. Kinetics of Propylene Epoxidation Using H₂ and O₂ over a Gold/Mesoporous Titanosilicate Catalyst. *Catal. Today* **2007**, *123* (1), 189–197. <https://doi.org/10.1016/j.cattod.2007.02.005>.
- (78) Degnan, T. F.; Smith, C. M.; Venkat, C. R. Alkylation of Aromatics with Ethylene and Propylene: Recent Developments in Commercial Processes. *Appl. Catal. Gen.* **2001**, *221* (1), 283–294. [https://doi.org/10.1016/S0926-860X\(01\)00807-9](https://doi.org/10.1016/S0926-860X(01)00807-9).
- (79) Prokešová, P.; Žilková, N.; Mintova, S.; Bein, T.; Čejka, J. Catalytic Activity of Micro/Mesoporous Composites in Toluene Alkylation with Propylene. *Appl. Catal. Gen.* **2005**, *281* (1), 85–91. <https://doi.org/10.1016/j.apcata.2004.11.016>.
- (80) Li, X.; Han, D.; Wang, H.; Liu, G.; Wang, B.; Li, Z.; Wu, J. Propene Oligomerization to High-Quality Liquid Fuels over Ni/HZSM-5. *Fuel* **2015**, *144*, 9–14. <https://doi.org/10.1016/j.fuel.2014.12.005>.
- (81) Olivier-Bourbigou, H.; Breuil, P. A. R.; Magna, L.; Michel, T.; Espada Pastor, M. F.; Delcroix, D. Nickel Catalyzed Olefin Oligomerization and Dimerization. *Chem. Rev.* **2020**, *120* (15), 7919–7983. <https://doi.org/10.1021/acs.chemrev.0c00076>.

- (82) *Propene*. <https://webbook.nist.gov/cgi/cbook.cgi?Name=propylene&Units=SI> (accessed 2022-09-20).
- (83) *1,3-Butadiene, Ethylene Oxide and Vinyl Halides (Vinyl Fluoride, Vinyl Chloride and Vinyl Bromide): This Publication Represents the Views and Expert Opinions of an IARC Working Group on the Evaluation of Carcinogenic Risks to Humans, Which Met in Lyon, 5 - 12 June 2007*; International Agency for Research on Cancer, Ed.; IARC monographs on the evaluation of carcinogenic risks to humans; IARC: Lyon, 2008.
- (84) *Propylene: 2022 World Market Outlook and Forecast up to 2031*. <https://mcgroup.co.uk/researches/propylene>, (accessed 2022-09-20).
- (85) *Propylene Market Size, Share, Growth, Analysis, Price, Segmentation, & Industrial Trends By 2029*. <https://www.databridgemarketresearch.com/reports/global-propylene-market> (accessed 2022-10-31).
- (86) Ltd, B. C. and R. P. *Global Propylene Market to Boost In Coming Years – Projected To Reach 132.1 Metric Tons In 2028, at a CAGR of 6.1% During Forecast Period | BlueWeave Consulting*. GlobeNewswire News Room. <https://www.globenewswire.com/en/news-release/2022/03/31/2414083/0/en/Global-Propylene-Market-to-Boost-In-Coming-Years-Projected-To-Reach-132-1-Metric-Tons-In-2028-at-a-CAGR-of-6-1-During-Forecast-Period-BlueWeave-Consulting.html> (accessed 2022-10-31).
- (87) Monai, M.; Gambino, M.; Wannakao, S.; M. Weckhuysen, B. Propane to Olefins Tandem Catalysis: A Selective Route towards Light Olefins Production. *Chem. Soc. Rev.* **2021**, *50* (20), 11503–11529. <https://doi.org/10.1039/D1CS00357G>.
- (88) *Propylene-Petrochemicals Market Size 2022 And Growth Analysis*. <https://www.thebusinessresearchcompany.com/report/propylene-petrochemicals-global-market-report> (accessed 2022-09-20).
- (89) *Propylene Market Capacity and Capital Expenditure (CapEx) Forecast by Region, Top Countries and Companies, Feedstock, Key Planned and Announced Projects, 2022-2030*. Market Research Reports & Consulting | GlobalData UK Ltd. <https://www.globaldata.com/store/report/propylene-capacity-and-capital-expenditure-market-analysis/> (accessed 2022-10-31).
- (90) *Polypropylene global market volume 2015-2029*. Statista. <https://www.statista.com/statistics/1245169/polypropylene-market-volume-worldwide/> (accessed 2022-10-31).
- (91) ReportLinker. *Global Propylene Market to Reach 158.4 Million Metric Tons by 2027*. GlobeNewswire News Room. <https://www.globenewswire.com/news-release/2022/10/21/2539376/0/en/Global-Propylene-Market-to-Reach-158-4-Million-Metric-Tons-by-2027.html> (accessed 2022-11-02).
- (92) *Propylene Market Capacity and Capital Expenditure (CapEx) Forecast by Region, Top Countries and Companies, Feedstock, Key Planned and Announced Projects, 2022-2030*. https://www.reportlinker.com/p06358879/Propylene-Market-Capacity-and-Capital-Expenditure-CapEx-Forecast-by-Region-Top-Countries-and-Companies-Feedstock-Key-Planned-and-Announced-Projects.html?utm_source=GNW (accessed 2022-11-01).
- (93) *Asia dominates global propylene capacity additions by 2026*. Offshore Technology. <https://www.offshore-technology.com/comment/asia-global-propylene-capacity-2026/> (accessed 2022-11-02).
- (94) Najari, S.; Saeidi, S.; Gallucci, F.; Drioli, E. Mixed Matrix Membranes for Hydrocarbons Separation and Recovery: A Critical Review. *Rev. Chem. Eng.* **2021**, *37* (3), 363–406. <https://doi.org/10.1515/revce-2018-0091>.
- (95) Peplow, M. How Fracking Is Upending the Chemical Industry. *Nature* **2017**, *550* (7674), 26–28. <https://doi.org/10.1038/550026a>.

- (96) *Global propylene prices 2022*. Statista. <https://www.statista.com/statistics/1170576/price-propylene-forecast-globally/> (accessed 2022-11-02).
- (97) Shafei, E. N.; Albahar, M. Z.; Aljishi, M. F.; Aljishi, A. N.; Alnasir, A. S.; Al-Badairy, H. H.; Sanhoob, M. A. Naphtha Catalytic Cracking to Olefins over Zirconia–Titania Catalyst. *React. Chem. Eng.* **2021**, *7* (1), 123–132. <https://doi.org/10.1039/D1RE00290B>.
- (98) Sadrameli, S. M. Thermal/Catalytic Cracking of Hydrocarbons for the Production of Olefins: A State-of-the-Art Review I: Thermal Cracking Review. *Fuel* **2015**, *140*, 102–115. <https://doi.org/10.1016/j.fuel.2014.09.034>.
- (99) *Enhancing the Production of Light Olefins by Catalytic Cracking of FCC Naphtha over Mesoporous ZSM-5 Catalyst* | SpringerLink. <https://link.springer.com/article/10.1007/s11244-010-9598-1> (accessed 2022-10-31).
- (100) National Academies of Sciences, E. *The Changing Landscape of Hydrocarbon Feedstocks for Chemical Production: Implications for Catalysis: Proceedings of a Workshop*; 2016. <https://doi.org/10.17226/23555>.
- (101) Farshi, A.; Shaiyegh, F.; Burogerdi, S. H.; Dehgan, A. FCC Process Role in Propylene Demands. *Pet. Sci. Technol.* **2011**, *29* (9), 875–885. <https://doi.org/10.1080/10916460903451985>.
- (102) Corma, A.; Wojciechowski, B. W. The Chemistry of Catalytic Cracking. *Catal. Rev.* **1985**, *27* (1), 29–150. <https://doi.org/10.1080/01614948509342358>.
- (103) Al-Khattaf, S.; Saeed, M. R.; Aitani, A.; Klein, M. T. Catalytic Cracking of Light Crude Oil to Light Olefins and Naphtha over E-Cat and MFI: Microactivity Test versus Advanced Cracking Evaluation and the Effect of High Reaction Temperature. *Energy Fuels* **2018**, *32* (5), 6189–6199. <https://doi.org/10.1021/acs.energyfuels.8b00691>.
- (104) Usman, A.; Siddiqui, M. A. B.; Hussain, A.; Aitani, A.; Al-Khattaf, S. Catalytic Cracking of Crude Oil to Light Olefins and Naphtha: Experimental and Kinetic Modeling. *Chem. Eng. Res. Des.* **2017**, *120*, 121–137. <https://doi.org/10.1016/j.cherd.2017.01.027>.
- (105) Aitani, A.; Yoshikawa, T.; Ino, T. Maximization of FCC Light Olefins by High Severity Operation and ZSM-5 Addition. *Catal. Today* **2000**, *60* (1), 111–117. [https://doi.org/10.1016/S0920-5861\(00\)00322-9](https://doi.org/10.1016/S0920-5861(00)00322-9).
- (106) Parthasarathi, R. S.; Alabduljabbar, S. S. HS-FCC High-Severity Fluidized Catalytic Cracking: A Newcomer to the FCC Family. *Appl. Petrochem. Res.* **2014**, *4* (4), 441–444. <https://doi.org/10.1007/s13203-014-0087-5>.
- (107) Frank, B.; Cotter, T. P.; Schuster, M. E.; Schlögl, R.; Trunschke, A. Carbon Dynamics on the Molybdenum Carbide Surface during Catalytic Propane Dehydrogenation. *Chem. Weinh. Bergstr. Ger.* **2013**, *19* (50), 16938–16945. <https://doi.org/10.1002/chem.201302420>.
- (108) Li, C.; Wang, G. Dehydrogenation of Light Alkanes to Mono-Olefins. *Chem. Soc. Rev.* **2021**, *50* (7), 4359–4381. <https://doi.org/10.1039/D0CS00983K>.
- (109) Teketel, S.; Erichsen, M. W.; Bleken, F. L.; Svelle, S.; Lillerud, K. P.; Olsbye, U. Chapter 6: Shape Selectivity in Zeolite Catalysis. The Methanol to Hydrocarbons (MTH) Reaction. In *Catalysis*; 2014; pp 179–217. <https://doi.org/10.1039/9781782620037-00179>.
- (110) Ilias, S.; Bhan, A. Mechanism of the Catalytic Conversion of Methanol to Hydrocarbons. *ACS Catal.* **2013**, *3* (1), 18–31. <https://doi.org/10.1021/cs3006583>.
- (111) Zhang, C.; Ng, K. L. A.; Yan, L.; Feng, X.; Jiang, B.; Liao, Z.; Wang, J.; Yang, Y. Kinetic Perspective on Methanol to Propylene Process via HZSM-5 Catalyst: Balancing between Reaction and Diffusion. *Ind. Eng. Chem. Res.* **2022**, *61* (5), 2055–2067. <https://doi.org/10.1021/acs.iecr.1c04589>.
- (112) *Deactivation and Regeneration of HZSM-5 Zeolite in Methanol-to-Propylene Reaction*. <http://www.whxb.pku.edu.cn/EN/10.3866/PKU.WHXB201604152> (accessed 2022-09-21).
- (113) Mol, J. C. Industrial Applications of Olefin Metathesis. *J. Mol. Catal. Chem.* **2004**, *213* (1), 39–45. <https://doi.org/10.1016/j.molcata.2003.10.049>.

- (114) Eivgi, O.; Phatake, R. S.; Nechmad, N. B.; Lemcoff, N. G. Light-Activated Olefin Metathesis: Catalyst Development, Synthesis, and Applications. *Acc. Chem. Res.* **2020**, *53* (10), 2456–2471. <https://doi.org/10.1021/acs.accounts.0c00495>.
- (115) Amghizar, I.; Vandewalle, L. A.; Van Geem, K. M.; Marin, G. B. New Trends in Olefin Production. *Engineering* **2017**, *3* (2), 171–178. <https://doi.org/10.1016/J.ENG.2017.02.006>.
- (116) D'Angelo, S. C.; Dall'Ara, A.; Mondelli, C.; Pérez-Ramírez, J.; Papadokonstantakis, S. Techno-Economic Analysis of a Glycerol Biorefinery. *ACS Sustain. Chem. Eng.* **2018**, *6* (12), 16563–16572. <https://doi.org/10.1021/acssuschemeng.8b03770>.
- (117) Lari, G. M.; Pastore, G.; Haus, M.; Ding, Y.; Papadokonstantakis, S.; Mondelli, C.; Pérez-Ramírez, J. Environmental and Economical Perspectives of a Glycerol Biorefinery. *Energy Environ. Sci.* **2018**, *11* (5), 1012–1029. <https://doi.org/10.1039/C7EE03116E>.
- (118) Quispe, C. A. G.; Coronado, C. J. R.; Carvalho Jr., J. A. Glycerol: Production, Consumption, Prices, Characterization and New Trends in Combustion. *Renew. Sustain. Energy Rev.* **2013**, *27*, 475–493. <https://doi.org/10.1016/j.rser.2013.06.017>.
- (119) *Glycerol Manufacturing Process and Different Methods Involved*. <https://kumarmetal.com/glycerol-manufacturing-process-methods-grades/> (accessed 2023-01-24).
- (120) Bideaux, C.; Alfenore, S.; Cameleyre, X.; Molina-Jouve, C.; Uribe Larrea, J.-L.; Guillouet, S. E. Minimization of Glycerol Production during the High-Performance Fed-Batch Ethanolic Fermentation Process in *Saccharomyces Cerevisiae*, Using a Metabolic Model as a Prediction Tool. *Appl. Environ. Microbiol.* **2006**, *72* (3), 2134–2140. <https://doi.org/10.1128/AEM.72.3.2134-2140.2006>.
- (121) Ciriminna, R.; Pina, C. D.; Rossi, M.; Pagliaro, M. Understanding the Glycerol Market. *Eur. J. Lipid Sci. Technol.* **2014**, *116* (10), 1432–1439. <https://doi.org/10.1002/ejlt.201400229>.
- (122) *Glycerol Market Share, Trends | Industry Analysis 2031*. Allied Market Research. <https://www.alliedmarketresearch.com/glycerol-market-A16434> (accessed 2022-11-02).
- (123) *OECD-FAO Agricultural Outlook 2018-2027 : BIOFUEL - OECD-FAO Agricultural Outlook 2018-2027*. <https://stats.oecd.org/index.aspx?queryid=84952> (accessed 2022-09-07).
- (124) OECD; Food and Agriculture Organization of the United Nations. *OECD-FAO Agricultural Outlook 2018-2027*; OECD-FAO Agricultural Outlook; OECD, 2018. https://doi.org/10.1787/agr_outlook-2018-en.
- (125) Singh, D.; Sharma, D.; Soni, S. L.; Inda, C. S.; Sharma, S.; Sharma, P. K.; Jhalani, A. A Comprehensive Review of Biodiesel Production from Waste Cooking Oil and Its Use as Fuel in Compression Ignition Engines: 3rd Generation Cleaner Feedstock. *J. Clean. Prod.* **2021**, *307*, 127299. <https://doi.org/10.1016/j.jclepro.2021.127299>.
- (126) Kayode, B.; Hart, A. An Overview of Transesterification Methods for Producing Biodiesel from Waste Vegetable Oils. *Biofuels* **2019**, *10* (3), 419–437. <https://doi.org/10.1080/17597269.2017.1306683>.
- (127) Alptekin, E.; Canakci, M.; Sanli, H. Biodiesel Production from Vegetable Oil and Waste Animal Fats in a Pilot Plant. *Waste Manag.* **2014**, *34* (11), 2146–2154. <https://doi.org/10.1016/j.wasman.2014.07.019>.
- (128) Toldrá-Reig, F.; Mora, L.; Toldrá, F. Trends in Biodiesel Production from Animal Fat Waste. *Appl. Sci.* **2020**, *10* (10), 3644. <https://doi.org/10.3390/app10103644>.
- (129) Kumar Tiwari, A.; Kumar, A.; Raheman, H. Biodiesel Production from *Jatropha* Oil (*Jatropha Curcas*) with High Free Fatty Acids: An Optimized Process. *Biomass Bioenergy* **2007**, *31* (8), 569–575. <https://doi.org/10.1016/j.biombioe.2007.03.003>.
- (130) Riayatsyah, T. M. I.; Sebayang, A. H.; Silitonga, A. S.; Padli, Y.; Fattah, I. M. R.; Kusumo, F.; Ong, H. C.; Mahlia, T. M. I. Current Progress of *Jatropha Curcas* Commoditisation as Biodiesel Feedstock: A Comprehensive Review. *Front. Energy Res.* **2022**, *9*, 815416. <https://doi.org/10.3389/fenrg.2021.815416>.

- (131) Zhang, S.; Zhang, L.; Xu, G.; Li, F.; Li, X. A Review on Biodiesel Production from Microalgae: Influencing Parameters and Recent Advanced Technologies. *Front. Microbiol.* **2022**, *13*, 970028. <https://doi.org/10.3389/fmicb.2022.970028>.
- (132) Dickinson, S.; Mientus, M.; Frey, D.; Amini-Hajibashi, A.; Ozturk, S.; Shaikh, F.; Sengupta, D.; El-Halwagi, M. M. A Review of Biodiesel Production from Microalgae. *Clean Technol. Environ. Policy* **2017**, *19* (3), 637–668. <https://doi.org/10.1007/s10098-016-1309-6>.
- (133) *Glycerin*. <https://webbook.nist.gov/cgi/cbook.cgi?Name=glycerol&Units=SI> (accessed 2022-09-20).
- (134) PubChem. *Glycerol*. <https://pubchem.ncbi.nlm.nih.gov/compound/753> (accessed 2022-11-03).
- (135) Hu, S.; Luo, X.; Wan, C.; Li, Y. Characterization of Crude Glycerol from Biodiesel Plants. *J. Agric. Food Chem.* **2012**, *60* (23), 5915–5921. <https://doi.org/10.1021/jf3008629>.
- (136) Chozhavendhan, S.; Karthiga Devi, G.; Bharathiraja, B.; Praveen Kumar, R.; Elavazhagan, S. Assessment of Crude Glycerol Utilization for Sustainable Development of Biorefineries. In *Refining Biomass Residues for Sustainable Energy and Bioproducts*; Elsevier, 2020; pp 195–212. <https://doi.org/10.1016/B978-0-12-818996-2.00009-0>.
- (137) Nanda et al., M. Purification of Crude Glycerol Using Acidification: Effects of Acid Types and Product Characterization. 7.
- (138) *Glycerine Market Size & Share | Global Research Report, 2028*. <https://www.fortunebusinessinsights.com/glycerine-market-102168> (accessed 2022-11-03).
- (139) Monteiro, M. R.; Kugelmeier, C. L.; Pinheiro, R. S.; Batalha, M. O.; da Silva César, A. Glycerol from Biodiesel Production: Technological Paths for Sustainability. *Renew. Sustain. Energy Rev.* **2018**, *88*, 109–122. <https://doi.org/10.1016/j.rser.2018.02.019>.
- (140) Checa, M.; Nogales-Delgado, S.; Montes, V.; Encinar, J. M. Recent Advances in Glycerol Catalytic Valorization: A Review. *Catalysts* **2020**, *10* (11), 1279. <https://doi.org/10.3390/catal10111279>.
- (141) SAURABH JYOTI SARMA. PRODUCTION D’HYDROGÈNE PAR BIOCONVERSION DU GLYCÉROL BRUT ET UTILISATION DURABLE DES REJETS LIQUIDES GÉNÉRÉS AU COURS DU PROCESSUS. *Université du Québec* **2014**, 1–473.
- (142) Athalye, S. K.; Garcia, R. A.; Wen, Z. Use of Biodiesel-Derived Crude Glycerol for Producing Eicosapentaenoic Acid (EPA) by the Fungus *Pythium Irregulare*. *J. Agric. Food Chem.* **2009**, *57* (7), 2739–2744. <https://doi.org/10.1021/jf803922w>.
- (143) Chi, Z.; Pyle, D.; Wen, Z.; Frear, C.; Chen, S. A Laboratory Study of Producing Docosahexaenoic Acid from Biodiesel-Waste Glycerol by Microalgal Fermentation. *Process Biochem.* **2007**, *42* (11), 1537–1545. <https://doi.org/10.1016/j.procbio.2007.08.008>.
- (144) Yang, F.; Hanna, M. A.; Sun, R. Value-Added Uses for Crude Glycerol--a Byproduct of Biodiesel Production. *Biotechnol. Biofuels* **2012**, *5* (1), 13. <https://doi.org/10.1186/1754-6834-5-13>.
- (145) Rodrigues, C. V.; Santana, K. O.; Nespeca, M. G.; Eduardo de Oliveira, J.; Maintinguer, S. I. Crude Glycerol by Transesterification Process from Used Cooking Oils: Characterization and Potentialities on Hydrogen Bioproduction. *Int. J. Hydrog. Energy* **2016**, *41* (33), 14641–14651. <https://doi.org/10.1016/j.ijhydene.2016.06.209>.
- (146) Chilakamarry, C. R.; Sakinah, A. M. M.; Zularisam, A. W.; Pandey, A. Glycerol Waste to Value Added Products and Its Potential Applications. *Syst. Microbiol. Biomanufacturing* **2021**, *1* (4), 378–396. <https://doi.org/10.1007/s43393-021-00036-w>.
- (147) *Contact us via LiveChat!* <https://secure.livechatinc.com/> (accessed 2022-11-03).
- (148) Chiu, C.-W. Catalytic Conversion of Glycerol to Propylene Glycol : Synthesis and Technology Assessment. Ph. D., University of Missouri--Columbia, 2006. <https://doi.org/10.32469/10355/4421>.

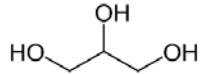
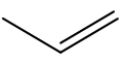
- (149) Kong, P. S.; Aroua, M. K.; Daud, W. M. A. W. Catalytic Esterification of Bioglycerol to Value-Added Products. *Rev. Chem. Eng.* **2015**, *31* (5), 437–451. <https://doi.org/10.1515/revce-2015-0004>.
- (150) Malleshham, B.; Sudarsanam, P.; Reddy, B. M. Production of Biofuel Additives from Esterification and Acetalization of Bioglycerol over SnO₂-Based Solid Acids. *Ind. Eng. Chem. Res.* **2014**, *53* (49), 18775–18785. <https://doi.org/10.1021/ie501133c>.
- (151) Kong, P. S.; Pérès, Y.; Wan Daud, W. M. A.; Cognet, P.; Aroua, M. K. Esterification of Glycerol With Oleic Acid Over Hydrophobic Zirconia-Silica Acid Catalyst and Commercial Acid Catalyst: Optimization and Influence of Catalyst Acidity. *Front. Chem.* **2019**, *7*, 205. <https://doi.org/10.3389/fchem.2019.00205>.
- (152) El Doukkali, M.; Iriondo, A.; Arias, P. L.; Requies, J.; Gandarías, I.; Jalowiecki-Duhamel, L.; Dumeignil, F. A Comparison of Sol–Gel and Impregnated Pt or/and Ni Based γ -Alumina Catalysts for Bioglycerol Aqueous Phase Reforming. *Appl. Catal. B Environ.* **2012**, *125*, 516–529. <https://doi.org/10.1016/j.apcatb.2012.06.024>.
- (153) Davda, R. R.; Shabaker, J. W.; Huber, G. W.; Cortright, R. D.; Dumesic, J. A. A Review of Catalytic Issues and Process Conditions for Renewable Hydrogen and Alkanes by Aqueous-Phase Reforming of Oxygenated Hydrocarbons over Supported Metal Catalysts. *Appl. Catal. B Environ.* **2005**, *56* (1), 171–186. <https://doi.org/10.1016/j.apcatb.2004.04.027>.
- (154) Katryniok, B.; Kimura, H.; Skrzyńska, E.; Girardon, J.-S.; Fongarland, P.; Capron, M.; Ducoulombier, R.; Mimura, N.; Paul, S.; Dumeignil, F. Selective Catalytic Oxidation of Glycerol: Perspectives for High Value Chemicals. *Green Chem.* **2011**, *13* (8), 1960–1979. <https://doi.org/10.1039/C1GC15320J>.
- (155) Walgode, P. M.; Faria, R. P. V.; Rodrigues, A. E. A Review of Aerobic Glycerol Oxidation Processes Using Heterogeneous Catalysts: A Sustainable Pathway for the Production of Dihydroxyacetone. *Catal. Rev.* **2021**, *63* (3), 422–511. <https://doi.org/10.1080/01614940.2020.1747253>.
- (156) Villa, A.; Dimitratos, N.; Chan-Thaw, C. E.; Hammond, C.; Prati, L.; Hutchings, G. J. Glycerol Oxidation Using Gold-Containing Catalysts. *Acc. Chem. Res.* **2015**, *48* (5), 1403–1412. <https://doi.org/10.1021/ar500426g>.
- (157) Katryniok, B.; Paul, S.; Bellière-Baca, V.; Rey, P.; Dumeignil, F. Glycerol Dehydration to Acrolein in the Context of New Uses of Glycerol. *Green Chem.* **2010**, *12* (12), 2079–2098. <https://doi.org/10.1039/C0GC00307G>.
- (158) Katryniok, B.; Paul, S.; Dumeignil, F. Recent Developments in the Field of Catalytic Dehydration of Glycerol to Acrolein. *ACS Catal.* **2013**, *3* (8), 1819–1834. <https://doi.org/10.1021/cs400354p>.
- (159) Abdullah, A.; Zuhairi Abdullah, A.; Ahmed, M.; Khan, J.; Shahadat, M.; Umar, K.; Alim, M. A. A Review on Recent Developments and Progress in Sustainable Acrolein Production through Catalytic Dehydration of Bio-Renewable Glycerol. *J. Clean. Prod.* **2022**, *341*, 130876. <https://doi.org/10.1016/j.jclepro.2022.130876>.
- (160) Wang, Y.; Zhou, J.; Guo, X. Catalytic Hydrogenolysis of Glycerol to Propanediols: A Review. *RSC Adv.* **2015**, *5* (91), 74611–74628. <https://doi.org/10.1039/C5RA11957J>.
- (161) Sun, D.; Yamada, Y.; Sato, S.; Ueda, W. Glycerol Hydrogenolysis into Useful C₃ Chemicals. *Appl. Catal. B Environ.* **2016**, *193*, 75–92. <https://doi.org/10.1016/j.apcatb.2016.04.013>.
- (162) Vasiliadou, E. S.; Lemonidou, A. A. Glycerol Transformation to Value Added C₃ Diols: Reaction Mechanism, Kinetic, and Engineering Aspects. *WIREs Energy Environ.* **2015**, *4* (6), 486–520. <https://doi.org/10.1002/wene.159>.
- (163) Mane, R.; Jeon, Y.; Rode, C. A Review on Non-Noble Metal Catalysts for Glycerol Hydrodeoxygenation to 1,2-Propanediol with and without External Hydrogen. *Green Chem.* **2022**, *24* (18), 6751–6781. <https://doi.org/10.1039/D2GC01879A>.

- (164) El Doukkali, M.; Iriondo, A.; Arias, P. L.; Cambra, J. F.; Gandarias, I.; Barrio, V. L. Bioethanol/Glycerol Mixture Steam Reforming over Pt and PtNi Supported on Lanthana or Ceria Doped Alumina Catalysts. *Int. J. Hydrog. Energy* **2012**, *37* (10), 8298–8309. <https://doi.org/10.1016/j.ijhydene.2012.02.154>.
- (165) Iriondo, A.; Barrio, V. L.; El Doukkali, M.; Cambra, J. F.; Güemez, M. B.; Requies, J.; Arias, P. L.; Sánchez-Sánchez, M. C.; Navarro, R.; Fierro, J. L. G. Biohydrogen Production by Gas Phase Reforming of Glycerine and Ethanol Mixtures. *Int. J. Hydrog. Energy* **2012**, *37* (2), 2028–2036. <https://doi.org/10.1016/j.ijhydene.2011.06.077>.
- (166) Sun, P.; Zhang, W.; Yu, X.; Zhang, J.; Xu, N.; Zhang, Z.; Liu, M.; Zhang, D.; Zhang, G.; Liu, Z.; Yang, C.; Yan, W.; Jin, X. Hydrogenolysis of Glycerol to Propylene Glycol: Energy, Technical, and Environmental Studies. *Front. Chem.* **2022**, *9*, 778579. <https://doi.org/10.3389/fchem.2021.778579>.
- (167) You, Y.-D.; Shie, J.-L.; Chang, C.-Y.; Huang, S.-H.; Pai, C.-Y.; Yu, Y.-H.; Chang, C. H. Economic Cost Analysis of Biodiesel Production: Case in Soybean Oil. *Energy Fuels* **2008**, *22* (1), 182–189. <https://doi.org/10.1021/ef700295c>.
- (168) De Paola, M. G.; Mazza, I.; Paletta, R.; Lopresto, C. G.; Calabrò, V. Small-Scale Biodiesel Production Plants—An Overview. *Energies* **2021**, *14* (7), 1901. <https://doi.org/10.3390/en14071901>.
- (169) Phillips, S.; Flach, B.; Lieberz, S.; Bolla, S. Biofuels Annual EU Biofuels Annual 2019. 52.
- (170) Campbell, S. M.; Bibby, D. M.; Coddington, J. M.; Howe, R. F.; Meinhold, R. H. Dealumination of HZSM-5 Zeolites: I. Calcination and Hydrothermal Treatment. *J. Catal.* **1996**, *161* (1), 338–349. <https://doi.org/10.1006/jcat.1996.0191>.
- (171) Marques, J. P.; Gener, I.; Ayrault, P.; Bordado, J. C.; Lopes, J. M.; Ribeiro, F. R.; Guisnet, M. Dealumination of HBEA Zeolite by Steaming and Acid Leaching: Distribution of the Various Aluminic Species and Identification of the Hydroxyl Groups. *Comptes Rendus Chim.* **2005**, *8* (3), 399–410. <https://doi.org/10.1016/j.crci.2005.01.002>.
- (172) Zhang, J.; Zhang, H.; Yang, X.; Huang, Z.; Cao, W. Study on the Deactivation and Regeneration of the ZSM-5 Catalyst Used in Methanol to Olefins. *J. Nat. Gas Chem.* **2011**, *20* (3), 266–270. [https://doi.org/10.1016/S1003-9953\(10\)60183-1](https://doi.org/10.1016/S1003-9953(10)60183-1).
- (173) Lee, W.-S.; Kumar, A.; Wang, Z.; Bhan, A. Chemical Titration and Transient Kinetic Studies of Site Requirements in Mo₂C-Catalyzed Vapor Phase Anisole Hydrodeoxygenation. *ACS Catal.* **2015**, *5* (7), 4104–4114. <https://doi.org/10.1021/acscatal.5b00713>.
- (174) Schaidle, J. A.; Blackburn, J.; Farberow, C. A.; Nash, C.; Steirer, K. X.; Clark, J.; Robichaud, D. J.; Ruddy, D. A. Experimental and Computational Investigation of Acetic Acid Deoxygenation over Oxophilic Molybdenum Carbide: Surface Chemistry and Active Site Identity. *ACS Catal.* **2016**, *6* (2), 1181–1197. <https://doi.org/10.1021/acscatal.5b01930>.
- (175) Liu, Y.; Tüysüz, H.; Jia, C.-J.; Schwickardi, M.; Rinaldi, R.; Lu, A.-H.; Schmidt, W.; Schüth, F. From Glycerol to Allyl Alcohol: Iron Oxide Catalyzed Dehydration and Consecutive Hydrogen Transfer. *Chem. Commun.* **2010**, *46* (8), 1238–1240. <https://doi.org/10.1039/B921648K>.
- (176) Yoshikawa, T.; Tago, T.; Nakamura, A.; Konaka, A.; Mukaida, M.; Masuda, T. Investigation of Reaction Routes for Direct Conversion of Glycerol over Zirconia–Iron Oxide Catalyst. *Res. Chem. Intermed.* **2011**, *37* (9), 1247. <https://doi.org/10.1007/s11164-011-0391-y>.
- (177) Burwell, R. L. Jr.; Pearson, R. G. The Principle of Microscopic Reversibility. *J. Phys. Chem.* **1966**, *70* (1), 300–302. <https://doi.org/10.1021/j100873a508>.
- (178) Krupka, R. M.; Kaplan, H.; Laidler, K. J. Kinetic Consequences of the Principle of Microscopic Reversibility. *Trans. Faraday Soc.* **1966**, *62* (0), 2754–2759. <https://doi.org/10.1039/TF9666202754>.
- (179) Canale, V.; Tonucci, L.; Bressan, M.; d’Alessandro, N. Deoxydehydration of Glycerol to Allyl Alcohol Catalyzed by Rhenium Derivatives. *Catal. Sci. Technol.* **2014**, *4* (10), 3697–3704. <https://doi.org/10.1039/C4CY00631C>.

- (180) Chai, S.-H.; Wang, H.-P.; Liang, Y.; Xu, B.-Q. Sustainable Production of Acrolein: Gas-Phase Dehydration of Glycerol over Nb₂O₅ Catalyst. *J. Catal.* **2007**, *250* (2), 342–349. <https://doi.org/10.1016/j.jcat.2007.06.016>.
- (181) Stošić, D.; Bennici, S.; Couturier, J.-L.; Dubois, J.-L.; Auroux, A. Influence of Surface Acid–Base Properties of Zirconia and Titania Based Catalysts on the Product Selectivity in Gas Phase Dehydration of Glycerol. *Catal. Commun.* **2012**, *17*, 23–28. <https://doi.org/10.1016/j.catcom.2011.10.004>.
- (182) Alhanash, A.; Kozhevnikova, E. F.; Kozhevnikov, I. V. Gas-Phase Dehydration of Glycerol to Acrolein Catalysed by Caesium Heteropoly Salt. *Appl. Catal. Gen.* **2010**, *378* (1), 11–18. <https://doi.org/10.1016/j.apcata.2010.01.043>.
- (183) García-Fernández, S.; Gandarias, I.; Requies, J.; Güemez, M. B.; Bennici, S.; Auroux, A.; Arias, P. L. New Approaches to the Pt/WO_x/Al₂O₃ Catalytic System Behavior for the Selective Glycerol Hydrogenolysis to 1,3-Propanediol. *J. Catal.* **2015**, *323*, 65–75. <https://doi.org/10.1016/j.jcat.2014.12.028>.
- (184) Gandarias, I.; Arias, P. L.; Requies, J.; El Doukkali, M.; Güemez, M. B. Liquid-Phase Glycerol Hydrogenolysis to 1,2-Propanediol under Nitrogen Pressure Using 2-Propanol as Hydrogen Source. *J. Catal.* **2011**, *282* (1), 237–247. <https://doi.org/10.1016/j.jcat.2011.06.020>.
- (185) Rousseau, R.; Dixon, D. A.; Kay, B. D.; Dohnálek, Z. Dehydration, Dehydrogenation, and Condensation of Alcohols on Supported Oxide Catalysts Based on Cyclic (WO₃)₃ and (MoO₃)₃ Clusters. *Chem. Soc. Rev.* **2014**, *43* (22), 7664–7680. <https://doi.org/10.1039/C3CS60445D>.
- (186) Xing, S.-K.; Wang, G.-C. Reaction Mechanism of Ethanol Decomposition on Mo₂C(100) Investigated by the First Principles Study. *J. Mol. Catal. Chem.* **2013**, *377*, 180–189. <https://doi.org/10.1016/j.molcata.2013.05.002>.
- (187) Yu, W.; Saliccioli, M.; Xiong, K.; Barteau, M. A.; Vlachos, D. G.; Chen, J. G. Theoretical and Experimental Studies of C–C versus C–O Bond Scission of Ethylene Glycol Reaction Pathways via Metal-Modified Molybdenum Carbides. *ACS Catal.* **2014**, *4* (5), 1409–1418. <https://doi.org/10.1021/cs500124n>.
- (188) Yfanti, V.-L.; Lemonidou, A. A. Mechanistic Study of Liquid Phase Glycerol Hydrodeoxygenation with In-Situ Generated Hydrogen. *J. Catal.* **2018**, *368*, 98–111. <https://doi.org/10.1016/j.jcat.2018.09.036>.
- (189) Bhasin, M. M.; McCain, J. H.; Vora, B. V.; Imai, T.; Pujadó, P. R. Dehydrogenation and Oxydehydrogenation of Paraffins to Olefins. *Appl. Catal. Gen.* **2001**, *221* (1), 397–419. [https://doi.org/10.1016/S0926-860X\(01\)00816-X](https://doi.org/10.1016/S0926-860X(01)00816-X).
- (190) He, S.; Krishnamurthy, K. R.; Seshan, K. Dehydrogenation of Long Chain N-Paraffins to Olefins – a Perspective. In *Catalysis*; 2017; pp 282–316. <https://doi.org/10.1039/9781788010634-00282>.
- (191) Hutchings, G. J.; Johnston, P.; Lee, D. F.; Warwick, A.; Williams, C. D.; Wilkinson, M. The Conversion of Methanol and Other O-Compounds to Hydrocarbons over Zeolite β. *J. Catal.* **1994**, *147* (1), 177–185. <https://doi.org/10.1006/jcat.1994.1128>.
- (192) Hutchings, G. J.; Johnston, P.; Lee, D. F.; Williams, C. D. Acetone Conversion to Isobutene in High Selectivity Using Zeolite β Catalyst. *Catal. Lett.* **1993**, *21* (1), 49–53. <https://doi.org/10.1007/BF00767370>.
- (193) Yang, M.; Han, B.; Cheng, H. First-Principles Study of Hydrogenation of Ethylene on a HxMoO₃(010) Surface. *J. Phys. Chem. C* **2012**, *116* (46), 24630–24638. <https://doi.org/10.1021/jp308255a>.
- (194) El Doukkali, M.; Iriondo, A.; Gandarias, I. Enhanced Catalytic Upgrading of Glycerol into High Value-Added H₂ and Propanediols: Recent Developments and Future Perspectives. *Mol. Catal.* **2020**, *490*, 110928. <https://doi.org/10.1016/j.mcat.2020.110928>.

- (195) Nnabalu, C. R.; Falcone, G.; Bortone, I. The Role of Fluid Catalytic Cracking in Process Optimisation for Petroleum Refineries. **2019**, *13* (7), 7.
- (196) Xu, Y.; Li, X.; Ding, M. Techno-Economic Analysis of Olefin Production Based on Fischer-Tropsch Synthesis. *Chem* **2021**, *7* (8), 1977–1980. <https://doi.org/10.1016/j.chempr.2021.07.008>.
- (197) Zhao, Z.; Jiang, J.; Wang, F. An Economic Analysis of Twenty Light Olefin Production Pathways. *J. Energy Chem.* **2021**, *56*, 193–202. <https://doi.org/10.1016/j.jechem.2020.04.021>.
- (198) Volk, R.; Stallkamp, C.; Steins, J. J.; Yogish, S. P.; Müller, R. C.; Stapf, D.; Schultmann, F. Techno-Economic Assessment and Comparison of Different Plastic Recycling Pathways: A German Case Study. *J. Ind. Ecol.* **2021**, *25* (5), 1318–1337. <https://doi.org/10.1111/jiec.13145>.
- (199) Mohsenzadeh, A.; Zamani, A.; Taherzadeh, M. J. Bioethylene Production from Ethanol: A Review and Techno-Economical Evaluation. *ChemBioEng Rev.* **2017**, *4* (2), 75–91. <https://doi.org/10.1002/cben.201600025>.
- (200) Kim, H.; Lee, B.; Lim, D.; Choe, C.; Lim, H. What Is the Best Green Propylene Production Pathway?: Technical, Economic, and Environmental Assessment. *Green Chem.* **2021**, *23* (19), 7635–7645. <https://doi.org/10.1039/D1GC01791H>.
- (201) Babor, M.; Tišler, Z.; Kocík, J.; Hubáček, J.; Bačiak, M.; Herrador, J. M. H. Bioethylene and Biopropylene Production from Waste Fat and Rapeseed Oil via Catalytic Hydrodeoxygenation and Hydrocracking Followed by Pyrolysis. *Chem. Eng. Technol.* *n/a* (n/a). <https://doi.org/10.1002/ceat.202200256>.
- (202) Niziolek, A. M.; Onel, O.; Floudas, C. A. Municipal Solid Waste to Liquid Transportation Fuels, Olefins, and Aromatics: Process Synthesis and Deterministic Global Optimization. *Comput. Chem. Eng.* **2017**, *102*, 169–187. <https://doi.org/10.1016/j.compchemeng.2016.07.024>.
- (203) Kusenberg, M.; Fausson, G. C.; Thi, H. D.; Roosen, M.; Grilc, M.; Eschenbacher, A.; De Meester, S.; Van Geem, K. M. Maximizing Olefin Production via Steam Cracking of Distilled Pyrolysis Oils from Difficult-to-Recycle Municipal Plastic Waste and Marine Litter. *Sci. Total Environ.* **2022**, *838*, 156092. <https://doi.org/10.1016/j.scitotenv.2022.156092>.
- (204) Tripodi, A.; Belotti, M.; Rossetti, I. Bioethylene Production: From Reaction Kinetics to Plant Design. *ACS Sustain. Chem. Eng.* **2019**, *7* (15), 13333–13350. <https://doi.org/10.1021/acssuschemeng.9b02579>.
- (205) Ward, A. M.; Stevenson, S.; OPRINS, A.; ZHAO, Z.; Abbott, T.; LAWSON, K. F.; SCHROER, J. W.; HUCKMAN, M. E. Use of Renewable Energy in Olefin Synthesis. WO2020150244A1, July 23, 2020. <https://patents.google.com/patent/WO2020150244A1/fr?q=WO+2020%2f150244A1> (accessed 2022-09-19).
- (206) Beacham, W. *SABIC takes first steps into renewable polyolefins*. ICIS Explore. <https://www.icis.com/explore/resources/news/2014/06/10/9789706/sabic-takes-first-steps-into-renewable-polyolefins> (accessed 2022-09-28).
- (207) *Mitsui Chemicals Group's Bio-Polypropylene Adopted for Project Commissioned by Ministry of the Environment | 2019 | Press Release | MITSUI CHEMICALS, INC.* https://jp.mitsuichemicals.com/en/release/2019/2019_0926.htm (accessed 2022-09-28).
- (208) Hannula, I.; Arpiainen, V. Light Olefins and Transport Fuels from Biomass Residues via Synthetic Methanol: Performance and Cost Analysis. *Biomass Convers. Biorefinery* **2015**, *5* (1), 63–74. <https://doi.org/10.1007/s13399-014-0123-9>.

Table 1. Main characteristics of glycerol and propylene molecules ^{82,83,118,121,133,134}

Characteristics	Glycerol	Propylene
IUPAC name	Propane-1,2,3-triol	Propene
Synonyms	glycerin, 1,2,3-Trihydroxy propane, propanetriol, 1,2,3-Propanetriol, etc.	1-Propene, prop-1-ene, Methyl-ethylene, etc.
CAS Number	56-81-5	115-07-1
Short formula	C ₃ H ₈ O ₃	C ₃ H ₆
Semi-structure		
Molecular weight	92.09 g.mol ⁻¹	42.08 g.mol ⁻¹
Description, security & toxicity	viscous, colorless, odorless, nontoxic, and sweet tasting	gas, colorless, nearly aromatic, irritant, highly flammable, explosion limit; 1.8–11.2 vol%
Refraction index	1.47	1.35
Melting point	17.8 °C	-185.2 °C
Boiling point	290 °C	-47.6 °C
Solubility in water 20 °C, 1 atm)	Totally miscible	384 mg.l ⁻¹
Density (25 °C, 1 atm)	1.26 g/cm ³	1.74 kg/m ³
Viscosity	1.49 Pa.s (25 °C, 1.013 10 ⁵ Pa)	87.8 10 ⁻⁷ Pa.s (25 °C, 1.27 10 ⁵ Pa)
Enthalpy, Δ _f H ⁰ (25 °C)	liquid phase; -669.6 kJ.mol ⁻¹ liquid phase; 221.9 J.mol ⁻¹ .K ⁻¹	gas phase; 20.41 kJ.mol ⁻¹ gas phase; 63.79 J.mol ⁻¹ .K ⁻¹
1.8.6. Heat capacity, C_p⁰ (25 °C)		
Auto-ignition temperature	370 °C	485 °C
Flash point	177 °C	-108 °C
Saturated vapor pressure	0.0263 bar (183.25 °C)	11.68 bar (25 °C)

Main qualities	commercialized	Food/drug use~ 99.7 %, tallow-based~ 99.5 %, vegetable-based ~96 %, technical 95.5-98 %, oleochemicals ~80 %, unrefined grades (40-88 %)	Polymer use (99.5–99.8 %), chemicals use (92–95 %), refinery-grade (50-70 %),
----------------	----------------	--	---

Table 2. Summary of the catalysts and their main catalytic properties for the GTP reaction

Catalysts type, ref.	Preparation and activation*	Characterization*	Relevant catalytic properties
Commercial FCC1 (Y, Si/Al~13 & metals ~1 %), γ -Al ₂ O ₃ , USY (Si/Al~12), ECat (Si/Al ~20, Ni~ 1400 ppm, V ~4400 ppm), H-ZSM-5 (Si/Al ~ 50, clay ~ 15 wt%) ^{41,66}	HT, physical mixture, CAL at each reaction temperature (N ₂ ~50 mL/min, 0.5 h). FCC1 and USY steamed at 816 °C (4 h).	Elemental analysis, probe molecule adsorption	Aluminosilicate surface with pronounced Brønsted acidity and microporosity.
ZSM-5 (Si/Al=11.5-12.5), BEA, Pt or Pd (1 wt%)/ γ -Al ₂ O ₃ or α -Al ₂ O ₃ ⁵⁰	HT, IWI, ex situ CAL (air ~ 0.2 L/min, 500 °C, 2 h) to H-zeolites. In situ RED of metals (H ₂ /N ₂ ~50 vol%, ~ 0.2 L/min, 500 °C, 0.5 h).	NA	Zeolites pore shape directly affects olefins distribution.
ZSM-5 (~30 wt% Cr, Li, Ni, Al, Cu, Mg or Ca). ³⁸	HT, WI, ex situ CAL (static air, 550 °C, 5 h), in situ CAL (He~10 mL/min, 500 °C, 1 h)	N ₂ -ads., FTIR, NH ₃ -TPD, TPR, XRD.	Presence of CuO _x leads to a larger number of medium acid sites compared to the predominant character of strong acid sites over bare ZSM5
Commercial ZSM-5 (~2.5 wt% Fe, Mo or Nb) ⁴⁵	HT, IMP, in situ CAL (airflow~ 50 mL/min, 600 °C, 2 h)	N ₂ -Ads., TPO, NH ₃ -TPD, XRD, SEM, EDX	Metals loading onto ZSM-5 change both its total acidity and distribution.
Commercial ZSM-5 (Si/Al~127), BEA. and Pt (0.3 wt%) or Cu. (20.2 wt%)/ZSM-5 (Si/Al~15) ²⁸	HT, IWI, ex situ CAL (static air, 500 °C, 6 h) to H-format. In situ CAL (air ~100 ml/min, 400 °C, 3 h), in situ RED (H ₂ /N ₂ ~10 %, ~100 ml/min, reaction temperature)	ICP, N ₂ -ads., NH ₃ -TPD.	Double-beds [bifunctional Pt/H-ZSM-5(Si/Al (15) + soft-acid HZSM-5 (127)] avoid coke and enhance C ₂₋₃ olefins.
Pt or Pd (5 wt%)/ZSM-5 (Si/Al = 40) ⁴⁴	HT, IWI, ex situ CAL (static air, 500 °C, 4 h) to form H-format. in situ RED (H ₂ /N ₂ ~25 vol%, 400 °C, 4 h).	ICP, N ₂ -ads., H ₂ -O ₂ titration, TEM, XRD, XPS, NH ₃ -TPD.	Bifunctional Pt/H-ZSM-5 (metallic/acid sites ratio ~7.7) fully hydrogenate glycerol-to-propane, while Pd/H-ZSM-5 (metallic/acid sites ratio ~1.7) promotes glycerol-to-olefins and avoids aromatization.
1 wt% of Ir, Pd, Rh, Pt or Ru loaded on ZrO ₂ and 1 wt% of Ir loaded on Al ₂ O ₃ , TiO ₂ , SiO ₂ , Carbon or ZrO ₂ .	PR, IWI, in situ RED (5 % H ₂ /Ar, 80 mL/min, 400 °C, 2 h)	ICP, N ₂ -Ads., H ₂ chemisorption, NH ₃ -TPD, TGA,	Highly dispersed Ir/ZrO ₂ (76 %, 1.6 nm) features pronounced hydrogenolysis, while H-ZSM-5

ZSM-5 (Si/Al~30-200), MCM-41, Al ₂ O ₃ , SAPO-11. ⁵³		XANES, XRD, TEM	(Si/Al~30) instead prompts a dehydration function.
3 wt% of Pt, Rh, Ru, Re, Ir or Cu on SiO ₂ , MoO ₃ -Ni ₂ P (10-30 wt%)/Al ₂ O ₃ , and ZSM-5 ⁴⁹	HT, IWI, ex situ CAL (air~ 30 mL/min, 350 °C, 2 h), RED (H ₂ /N ~9 %, 60 mL/min, 350 °C, 2 h), and passivation (O ₂ /He ~0.5 %, ~100 mL/min, 27 °C, 1 h). In situ RED (H ₂ ~20 mL/min, 345 °C, 1 h).	NA	Well-dispersed MoO _x -Ni ₂ P/Al ₂ O ₃ (21 %, 3 nm) coupled to acid H-ZSM-5 features synergic hydrogenolysis-dehydration sites.
0-12.3 wt% of WO ₃ , H ₃ PO ₄ , MoO ₃ or V ₂ O ₅ loaded on N242 or on T317. Amorphous SiO ₂ -Al ₂ O ₃ ⁴²	SG, IWI, ex situ CAL (air, T ∈200-600°C, 3 h), in situ RED (H ₂ ~ 60 ml/min, 250 °C, 1 h).	N ₂ Ads., NH ₃ -TPD, H ₂ -TPR	Acidic substances and controlled calcination improve surface functionalities.
Bulk and supported Cu, MoO ₃ , H ₃ VO ₄ , WO ₃ , H ₃ PO ₄ , HBO ₃ , TiO ₂ , SiO ₂ , Al ₂ O ₃ , C, ZnO ₂ , ZrO ₂ , mordenite, Beta, ZSM-5 ⁶⁴	IMP	NA	Combined WO ₃ (10 wt%)/ZrO ₂ , Cu (10 wt%)/ZnO ₂ and WO ₃ (10 wt%)/ZrO ₂ offer multi-catalytic functionalities.
Groups VIII-B (M ₁ = Fe, Ni, etc.) and VI-A (M ₂ = Mo, W, Cr, etc.) metals supported on charcoal ⁶³	Slurry IMP, pH-adjusted IMP, CAL in inert gas, and in situ RED under confidential conditions	NA	Specific mixed phases (atomic ratio M ₁ /(M ₁ +M ₂) ~0.2-0.4) act as active HDO sites.
Bulk/supported mono-, bi- or tri-group VI-B and VIII-B metals or those from 1 st , 2 nd and 3 rd row of the periodic table. ⁶¹	IMP, confidential RED and SLF conditions	NA	CoMo, NiMo and NiW oxides or sulfides over alumina or silicas display relevant HDO functions.
Homogeneous halogen-based catalysts (i.e., I ₂ , HI, HIO ₃ , Lil or a combination thereof). ⁶⁵	In situ dissolution, reductive treatment (H ₂), non-reductive treatment (inert gas)	NA	HI catalyst, formed in situ from I ₂ and H ₂ co-feeding, displays promising dehydroxylation functions
Homogeneous Ru-complex; RuBr ₃ .xH ₂ O (4.0 mg), HBr (2 mg), Bu ₄ PBr (577 mg) mixtures ⁴³	In situ dissolution (CO or CH ₂ O), in situ RED (H ₂ ~40 bar, stirring, 180 °C, 0.5 h), recrystallization	FTIR	CO-rich medium forms more Ru-C carbonyl-bonds, acting as a hydrogenation site.
Homogeneous complex: Ru (H ₂ O) ₃ (4'-phenyl-terpyridine)] (OTf) ₂ , Ru(H ₂ O) ₃ (terpy)](OTf) ₂ Brønsted acid co-catalyst; HOTf ⁵⁷	Suspension, PR, filtration and vacuum evaporation, reductive manipulation in dry-box and direct transfers to reaction medium	Elemental analysis, MALDI-TOF, ¹ H-NMR, ¹³ C-NMR	HOTf acts as a Brønsted site, while Ru-C bands act as a hydrogenating site.

316SS walls/alloy powder, HOTf co-catalyst, Commercial Ru (5 wt%)/AC (EVONIK) ⁵⁴	chemical corrosion, in situ acid attack (HOTf, H ₂ ~55 bar, 250 °C)	centrifugation, ICP-MS, SEM/EDX and XRF	Cr ^{3+/5+} act as hydrogenation sites, while Fe or Ni prompt H ₂ spillover.
Fe ~2.7 wt% and Mo~19.3 wt% (Mo/Fe atomic ratio ~4:1)/BC or AC ^{47,48,59}	IMP, CP, ex situ CAL (N ₂ ~100 ml/min, 200 °C, 2 h), in situ RED (H ₂ ~40 ml/min, 500 °C, 0.5 h)	N ₂ -Ads., XRD, NH ₃ -TPD, He-TPD, TPR, TGA, XPS	Fe substituted Mo ⁴⁺ promotes Mo ⁶⁺ reduction to Mo ⁵⁺ /Mo ⁴⁺ states; responsible for HDO events.
Mo-M (i.e., Ni, Fe, Cu or Zn)/AC; atomic ratio M/(M+Mo) = 0.4. Mo-Fe/AC, atomic ratio Fe/(Mo+Fe) from 0 to 1. Pd (5 wt%)/AC and Ru (5 wt%)/AC ⁵⁵	IMP, CP, ex situ CAL (inert gas, 450 °C, 2 h). In situ RED (H ₂ ~40 mL/min, 550 °C, 0.5 h).	N ₂ -Ads., TPR, n-butylamine-TPD, XRF, XRD	Mo ⁴⁺ and Mo-C catalyze the GTP route, while combined NiMo leads instead to propane.
Bulk MoO ₃ ³⁷	Idealized MoO ₃ structure	DFT calculation	Mo defects lead to oxygen vacancies, which trigger C-O dissociation and H-H activation.
Bulk and dispersed MoO _x , β-Mo ₂ C or η-MoC (14.8 wt%) based OMS materials ⁶⁰	HT, MIF, ex situ CAL or in situ H ₂ -RED (~100 ml/min, 500 °C, 3 h), CAR (CH ₄ /H ₂ ~18 vol%, C ₃ H ₈ /H ₂ ~10 vol.%, T∈ 500-700°C, 3-13 h)	ICP, CHNOS, N ₂ -Ads., TPD, in situ CO-FTIR, TGA, DSC, XPS, XRD, TEM	Mo ⁵⁺ /Mo ⁶⁺ Mo ³⁺ /Mo ⁴⁺ , carbidic and oxycarbide states are keys for HDO events.
NiMoO _x /Al ₂ O ₃ NiMoS _x /Al ₂ O ₃ ⁴⁶	IMP, in situ RED (H ₂ ~18.6 bar, 400 °C, 1h), In situ SLF [H ₂ S/H ₂ (~2 vol%, GHSV~ 600 h ⁻¹) or DMDS-heptane (4 wt%, WHSV~2 h ⁻¹ , 25 °C(3 h), 250 °C(8 h) and 320 °C(6 h).]	N ₂ -Ads., TPO	Mo-S sites feature better stability in C-O cleavage than Mo-O ones but co-generate C-C breaking.
Mo (110) single crystal; Mo ₂ C, Fe/Mo ₂ C, Cu/Mo ₂ C and Pt/Mo ₂ C ^{39,58}	PVD, ex situ CAR (C ₂ H ₄ , 327 °C, 927 °C, Mo/C~ 2:1). Ne ⁺ sputtering-annealing, and O ₂ treatment to remove excess carbon. in situ RED (H ₂ ~5.10 ⁻⁶ Torr.s, 527 °C)	AES, TPD-MS, HREELS, DFT calculation	Mo ₂ C affinity towards oxygen can be stabilized by depositing fewer oxophilic metals such as Fe, Cu, etc.

* Abbreviations and terminology: see supplementary information.

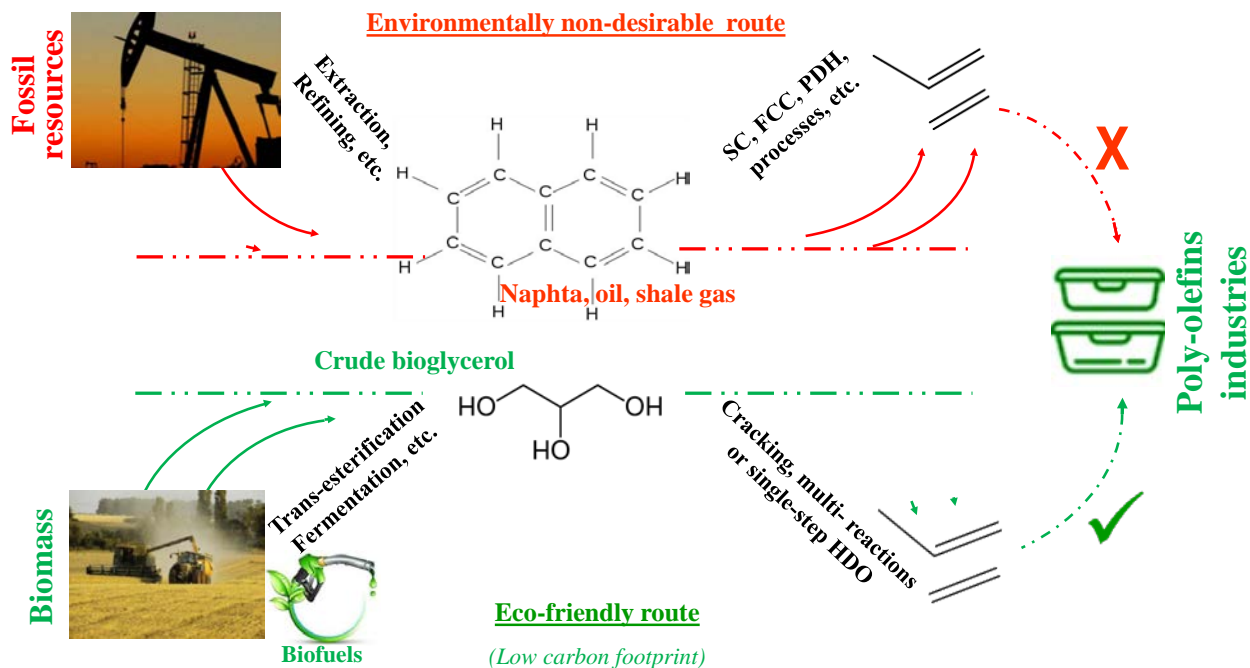
Table 3. Main GTP performance as function of reactor configurations, operating conditions, and most promising catalysts.

Bed configuration, relevant catalyst, ref.	Main operating conditions	Conv. (%)	Sel. (%)	Yield (%)
High-temperature MAT reactor; - HZSM-5(Si/Al ~50, binder ~ 15 wt%) - FCC1 (Y, Si/Al~13, metals ~1%) ^{41,66}	500-700 °C, 1 bar, N ₂ ~40 mL/min: - gly. in H ₂ O ~ 50-100 wt, cat./feed (<i>mass ratio</i>) ~1.5 – 6 - gasoil:glycerol (<i>mol.</i>) ~31:1 -7:1, WHSV~ 20-60 h ⁻¹ , TOS~ 30 min	100 100	- -	- C ₂₋₄ olefins~ 31 %. - C ₂₋₄ olefins ~13.3 %
High-temperature fixed-bed; Cu/ZSM-5 ^{38,51} Equilibrium Gibbs conditions ^{51,56}	511.8–688.2 °C, 1 bar, N ₂ ~40 mL/min, gly. in H ₂ O ~12.4 – 47.6 wt%, WHSV~ 25.6-184.4 h ⁻¹ , TOS~ 25 min 300-1000 °C, gly. in H ₂ O ~7.7-66.7 wt%, 1-12 bar	97.5 100		2.53 (C ₂₋₃ olefins~17.7 %) CO ~62.5, C ₂ H ₄ ~0.02
High-temperature single fixed-bed; Fe (2.5 wt%) ZSM-5 ⁴⁵	T~ 450-600 °C, P~ 1 bar, F _{N₂} ~100 ml/min, gly. in H ₂ O ~ 10 wt%, Feed~ 0.4 mL/h, TOS~5 h	100	-	33.3
Single fixed-bed; ZSM-5 ²⁸ Two-stage beds; Pt/ZSM-5 (Si/Al ~15, 1 g) + ZSM-5 (Si/Al~127, 1 g) ²⁸	T~ 400-600 °C P~ 1 bar, H ₂ :gly. (<i>mol.</i>)~100:1, partial pressure of gly. ~ 21.9 kPa, H ₂ O~78.1 kPa, WHSV~1 h ⁻¹ , TOS~30 min T~ 250 °C, 500 °C, P~ 1 bar, H ₂ :gly. (<i>mol.</i>)~100:1, WHSV~1 h ⁻¹ , Partial P _{gly.} ~ 1.0 kPa, H ₂ O~3.4 kPa, and H ₂ ~ 95.6 kPa, TOS~ 30 min Partial P _{gly.} ~ 1.0 kPa, CH ₃ OH~ 1.2 kPa, H ₂ O~2.2 kPa, and H ₂ ~ 95.6 kPa, TOS~500 h	90 100 100	14 (C ₂ H ₄ ~22) 76 63.7	- -
Three-stage fixed-beds; H-ZSM-5 (1 g), Pd (1 wt%)/γ-Al ₂ O ₃ (1 g) and H-BEA (0.5) ⁵⁰	T~ 500 °C, 100-300 °C, 400-500 °C, P~ 1 bar, F _{H₂} ~ 0.5 L/min, F _{N₂} ~ 1.5 L/min, F _{Ar} ~ 0.2 L/min, gly. in H ₂ O~ 10 wt%, Feed~ 40 μL/min, WHSV~ 11.2 h ⁻¹ , TOS ~ 10 min to 2.67 h	-	-	C ₂₋₃ olefins ~46*, ~15**
Three steps; WO ₃ (10 wt%, 30 g)/ZrO ₂ , Cu/ZnO ₂ (12 g) and WO ₃ (10 wt%, 12 g) ⁶⁴	T~ 280 °C, 270 °C, 208 °C, P~ 2-10 bar, H ₂ :gly. (<i>mol.</i>) ~2.5:1-4:1, gly. in H ₂ O ~15-30 wt%, TOS ~ 20 h	-	-	C ₃ H ₆ ~ 46

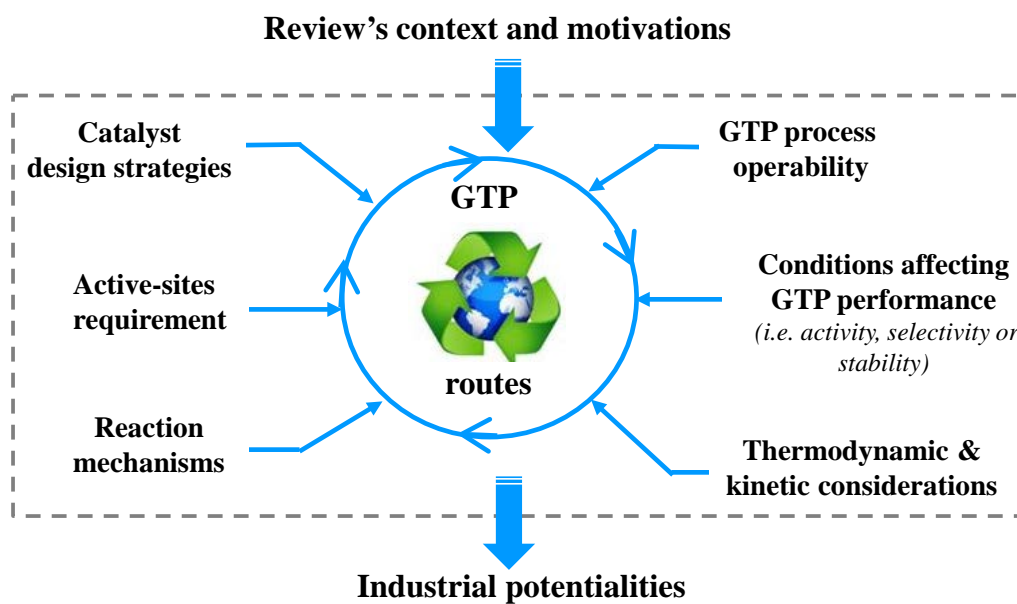
Two batch-reactors in series; I ₂ , HI, HIO ₃ , Lil catalysts or combinations thereof). ⁶⁵	T~ 50-250 °C, P _{H₂} or N ₂ ≤ 68.9 bar, crude gly./halogen ratio~ 4:1-8:1 Reductive TOS ~6 h Non-reductive TOS ~6.5 h	100 59 %	80 38 %	- -
Two separate steps: hydrogenolysis in batch Ir (1 wt%)/ ZrO ₂ (0.12 mol) and dehydration in fixed-bed HZSM-5 (2 g) ⁵³ Combined batch and fixed-bed; Ir (1 wt%)/ ZrO ₂ (2 g) + HZSM-5 (2 g). ⁵³	T~ 250 °C, gly. in H ₂ O ~ 30 wt%, P _{H₂} ~ 50 bar, H ₂ :gly. (<i>mol.</i>)~100:1, TOS~4 h, T~ 250 °C, propanol in H ₂ O ~ 10 wt%, P _{N₂} ~ 1 bar, N ₂ ~20 ml/min, WHSV~1 h ⁻¹ , TOS~2 h T~ 250 °C, H ₂ :gly. (<i>mol.</i>)~100:1, gly. in H ₂ O ~ 30 wt%, WHSV~1 h ⁻¹ , TOS~2 h P~ 50 bar P~ 5 bar	100 100 100 73	C ₃ H ₇ OH 94 %, C ₃ H ₆ 99* 67 88	- - - -
Single fixed-bed; WO ₃ (9.3 wt%)/T317(1 g) ⁴² Double fixed-beds; WO ₃ (9.3 wt%)/T317(1 g) + SiO ₂ -Al ₂ O ₃ (3 g) ⁴²	T~ 250, P~1 bar, F _{H₂} ~30-240 ml/min, gly. in H ₂ O~20 wt%, Feed~1.32 ml/h, WHSV~ 0.07 h ⁻¹ , TOS~ 2-5 h F _{H₂} ~ 240 ml/min F _{H₂} ~ 180 ml/min	100 100	57.8 84.8	- -
Double fixed-beds; MoO ₃ modified Ni ₂ P (20 wt%)/Al ₂ O ₃ + ZSM-5 ⁴⁹	T~ 250 °C, H ₂ : gly (<i>mol.</i>)~100 :1, WHSV~1 h ⁻¹ , gly. in H ₂ O ~ 59 wt%, TOS~ 2 h crude gly./CH ₃ OH (<i>mass</i>) ~ 85/15, TOS~550 h	100 100	88 71	- -
Single fixed-bed; Modified transition metals (Mo, Fe, Ni, etc.)/AC ^{55,63}	T~ 250-350 °C, P _{H₂} ~ 0.0098-9.8 bar, gly. in H ₂ O~30-100 wt%), WHSV~2-20 h ⁻¹ , H ₂ /gly.~30/1-240/1	100	90	-
One-pot fixed-bed; Modified Group VIII and VIb metal sulfides ⁶¹	T~ 175-500 °C, P _{H₂} ~83 bar, pure gly. steam, WHSV~2-20 h ⁻¹ , H ₂ :gly. (<i>mol.</i>) ratio up to 6.8:1. T~316 °C, H ₂ /gly. H ₂ :gly. ~ 2.3:1 T~254 °C, H ₂ /gly. H ₂ :gly. ~ 2.3:1 T~316 °C, H ₂ /gly. H ₂ :gly. ~ 6.8:1	> 99 85.9 > 99	59.2 82.1 C ₃ H ₈ ~76	
Single batch and fixed-bed reactors; Mo-based carbon ^{47,48,59,62}	T~ 240-300 °C, P~ 30-80 bar, H ₂ : gly (<i>mol.</i>) ~53:1, gly. in H ₂ O ~ 2 – 10 wt%, CT~7.2 h: 300 °C, TOS ~ 2 h/6 h	50/88.8	71/76.1	-

Single fixed-bed; NiMoS _x /Al ₂ O ₃ (130 mg) ⁴⁶	T~ 400 °C, P~ 18.6 bar, H ₂ excess, gly. in H ₂ O~ 72.5–80 wt%, TOS ~ 3 h CT~ 3 CT~360 s	<50 100	C ₃ H _y O _z 26.3	- -
Single fixed-bed; MoO _x (14.8 wt%)@SBA-15 β-Mo ₂ C (14.8 wt%)@SBA-15 ⁶⁰	T~ 318 °C, P~ 50 bar, gly. in H ₂ O~ 10 wt%, H ₂ :gly (mol.)~ 98:1, WHSV ~ 1.7 h ⁻¹ , TOS~14.5 h H ₂ :gly (mol.)~78:1, WHSV~2.35 h ⁻¹ , TOS~9.7 h H ₂ :gly (mol.)~78:1, WHSV~4.7 h ⁻¹ , TOS~9.7 h	100 100 100	- - -	~84.1-65.6 ~64.8-54.0 TOF _{C₃H₆} ~ 226.4- 153.1 h ⁻¹
One-pot batch; 316SS alloy powder and HOTf co-catalyst. ⁵⁴	T~ 100-250 °C, P H ₂ ~55 bar, gly. in H ₂ O~500 mmol/L T~ 250 °C, C _{co-cat} ~40 mmol/L, TOS ~ 24 h T~ 250 °C, C _{co-cat} ~60 mmol/L, TOS ~ 5 h	100 100	- -	96 96
One-pot batch; Homogeneous Ru-complex and HOTf as co-catalyst. ⁵⁷	T~ 250 °C, P H ₂ ~48.2 bar, gly. in H ₂ O~10-50 wt%, HOTf/Ru (mol.)~100, TOS ~ 24 h	100	-	C ₃ H ₈ ~100
One-pot batch; homogeneous Ru-complex (583 mg) ⁴³	T~ 220 °C, P H ₂ ~40 bar, P _{CO} ~10 bar, H ₂ excess, CT~ 285 s, TOS ~ 1 h: - pure gly. in H ₂ O (50-100 wt%), - crude gly. including H ₂ O, CH ₃ OH, NaCl, etc.	- -	- -	76 82

* Separate three-step reactions, ** Combined three-stage reactors. Abbreviations and terminology: see supplementary information.



Scheme 1. Expected eco-friendly GTP route (green) versus current fossil-based technologies (red). Abbreviations: see supplementary information.



Scheme 2. Overview of the approach for reviewing the topic of GTP catalysis.

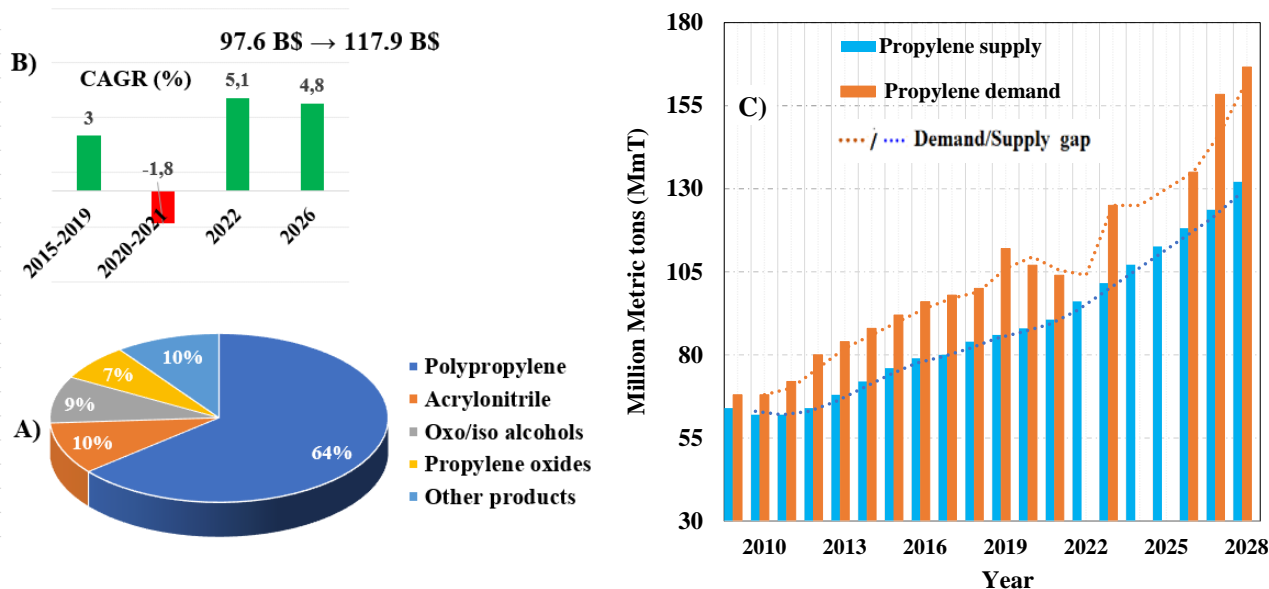


Fig. 1 A) Contribution of the main sectors for global propylene use (in %),⁸⁴⁻⁸⁶ B) current and projected compound annual growth rates (CAGR) for the propylene market (in billion dollars -B\$) and C) evolution of the gap between real production of propylene and its market demand during the period 2009–2022 (statistical data) and 2023–2028 (predicted data).^{8,85-88,91,92}

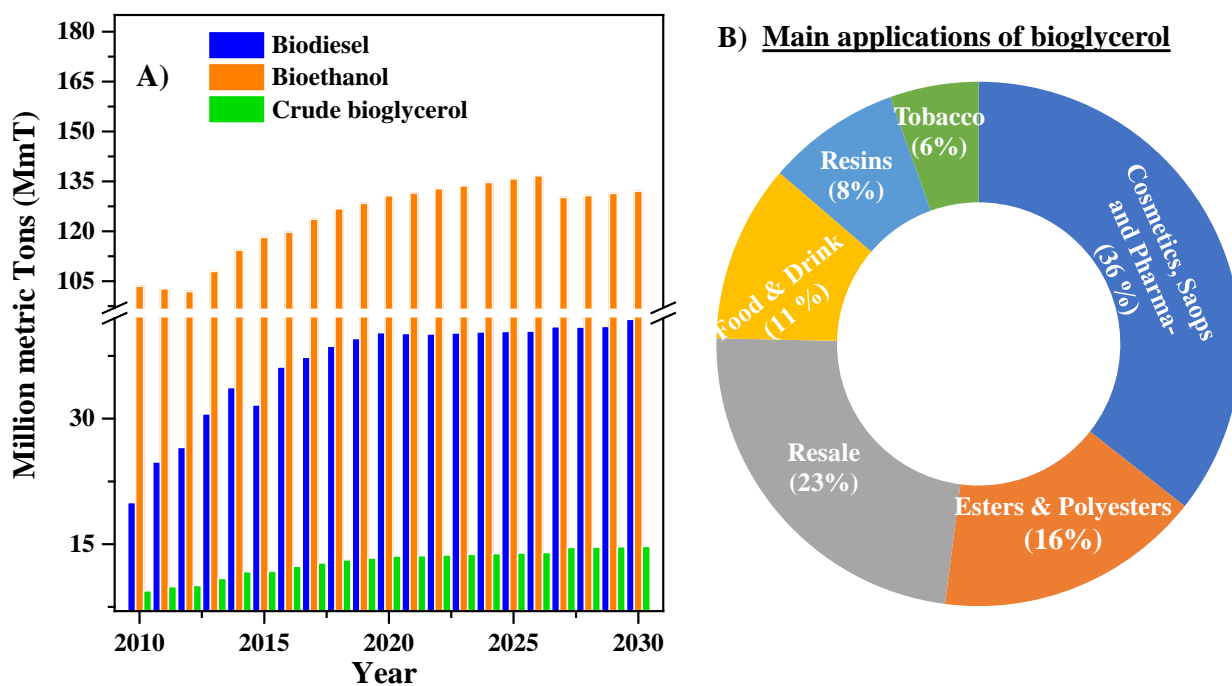


Fig. 2. A) Evolution of the global production of crude bioglycerol; mainly co-regenerated with biodiesel and to a lesser extent with bioethanol, for the period 2010–2022 (statistical data) and 2023–2030 (predicted data),^{123,124} and B) share of the main application sectors for bioglycerol.

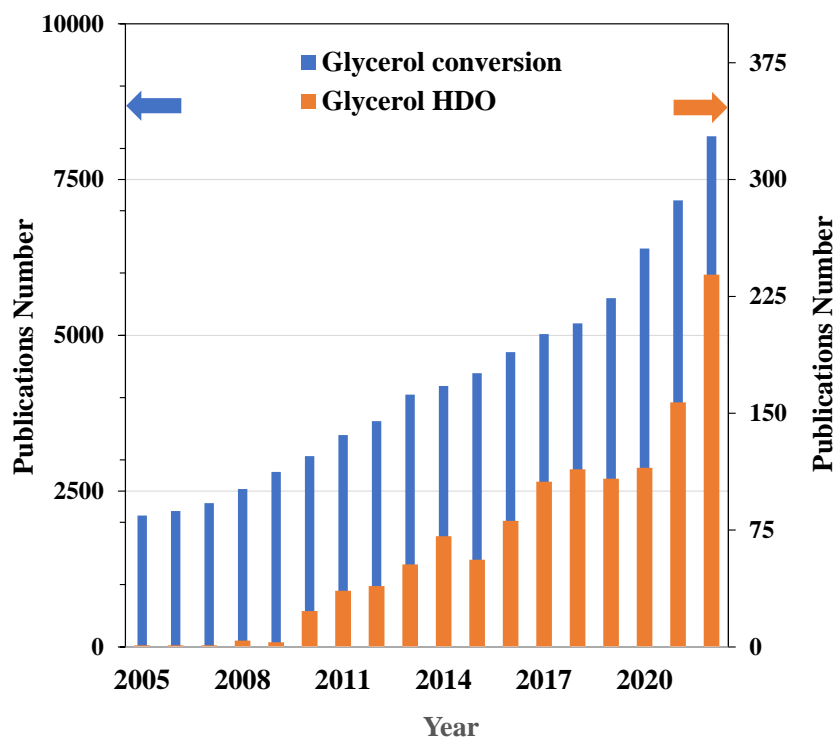
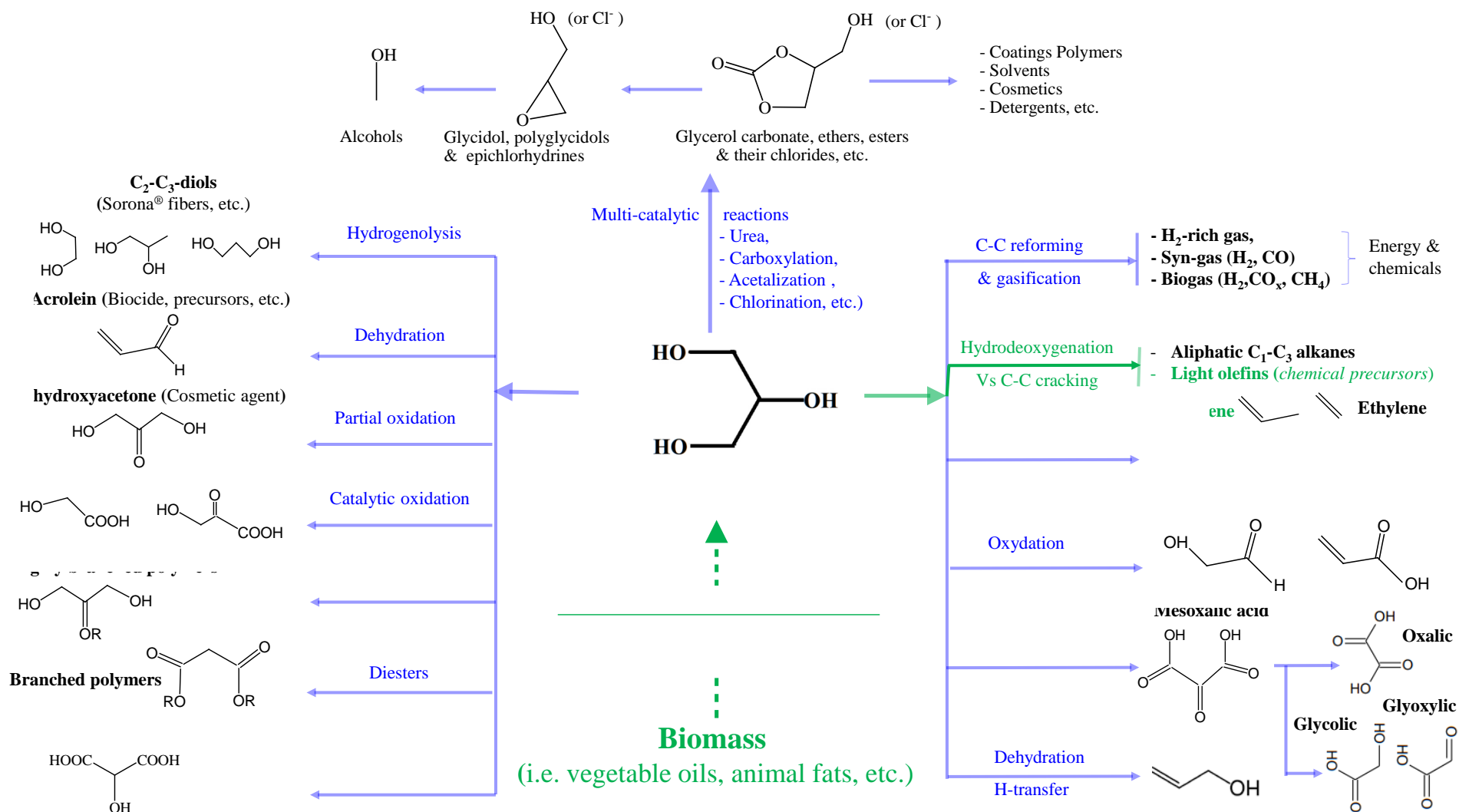


Fig. 3. Trends in publications dealing with the research topics of “*glycerol conversion*” and “*glycerol hydrodeoxygenation*”; data from Scopus (accessed 19 JAN 2023).



Scheme 3. Illustration of the most promising strategies for upgrading bioglycerol into added-value chemical intermediates. In *green*, the expected route for biomass to propylene.

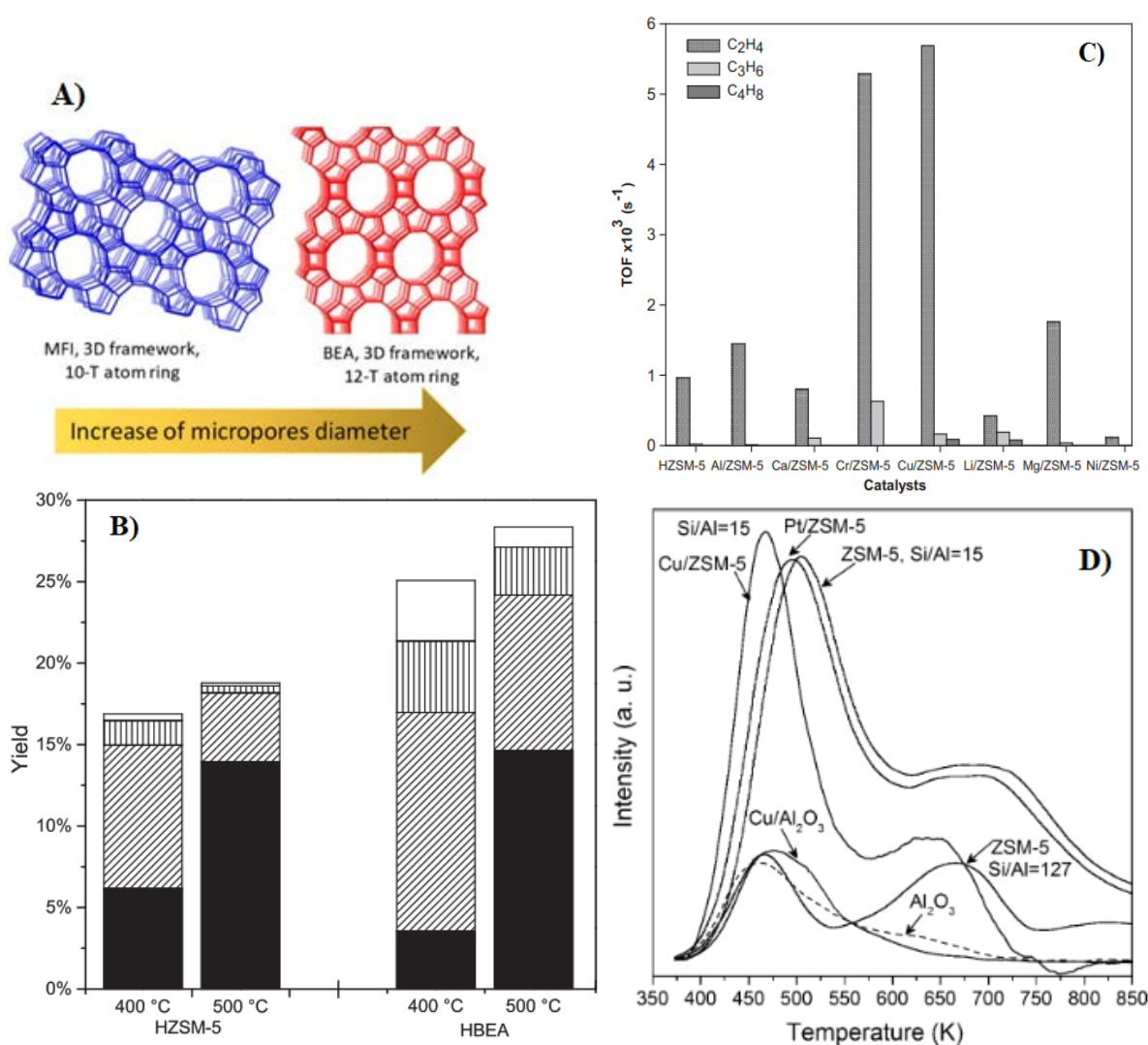


Fig. 4. **A)** Tri-dimensional (3D) structure of ZSM-5 and BEA zeolites. **B)** pore-shape effect on the formation of C₂₋₃ (■), C₄₋₅ (▨), C₆₋₇ (▧), and C₈₋₉ (□) olefins from glycerol conversion at 400 °C and 500 °C. Reproduced with permission from ref.⁵⁰ Copyright 2014 Elsevier. **C)** effect of metal-type modification of ZSM-5 on TOF_{olefins} distribution. Reproduced with permission from ref.³⁸ Copyright 2012 Elsevier. **D)** NH₃-TPD profiles reflecting the total amount/strength of acid sites over Al₂O₃, Cu/Al₂O₃, Cu/ZSM-5 (Si/Al=15), Pt/ZSM-5 (Si/Al=15), ZSM-5(Si/Al=15), and ZSM-5(Si/Al=127). Reproduced with permission from ref.²⁸ Copyright 2016 American Chemical Society.

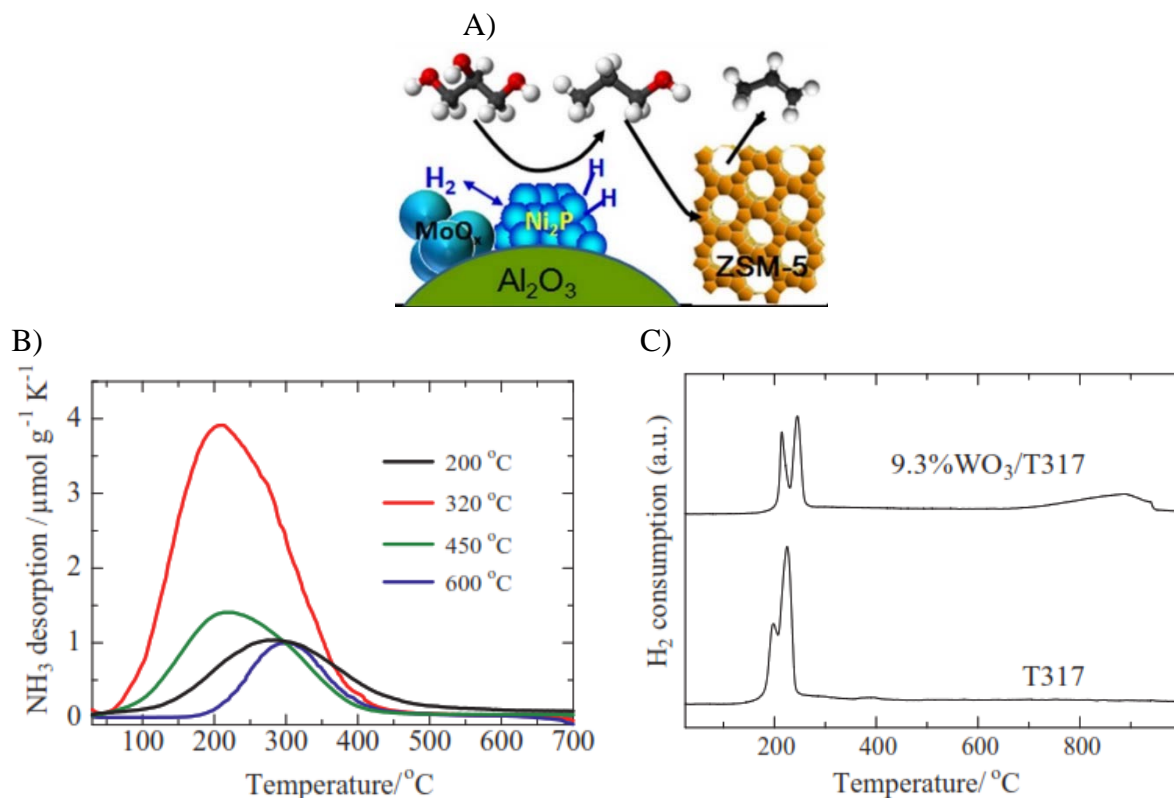


Fig. 5 A) Simplified illustration of the catalytic synergy between H_2 dissociation, hydrogenolysis, and dehydration events over a double-bed system; bifunctional Ni_2P/Al_2O_3 + acid ZSM-5. Reproduced with permission from ref. ⁴⁹ Copyright 2017 Elsevier. B) NH_3 -TPD profiles of $WO_x(9.3 \text{ wt}\%)/T317$ catalyst calcined at increasing temperatures. C) H_2 -TPR profiles of T317 and $WO_x(9.3 \text{ wt}\%)/T317$. Reproduced with permission from ref. ⁴² Copyright 2015 Elsevier.

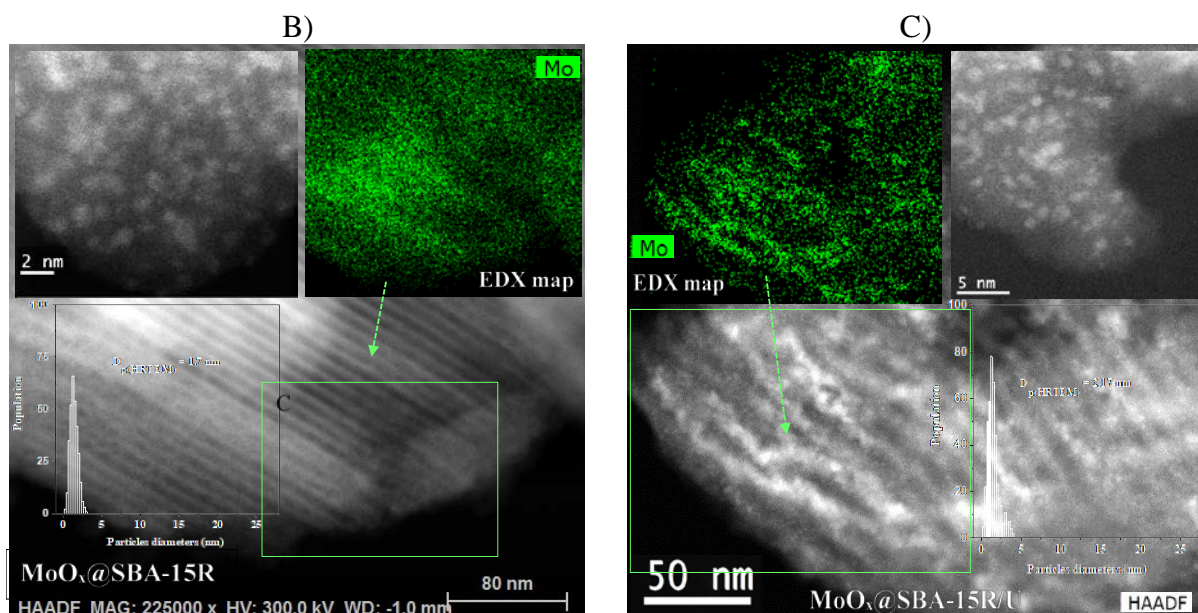
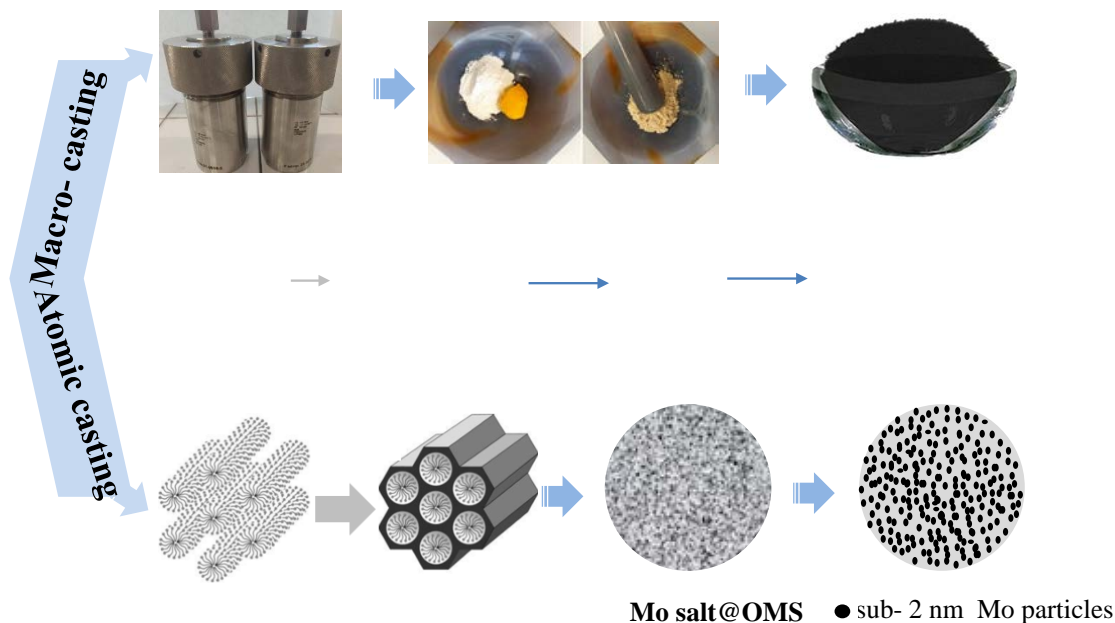
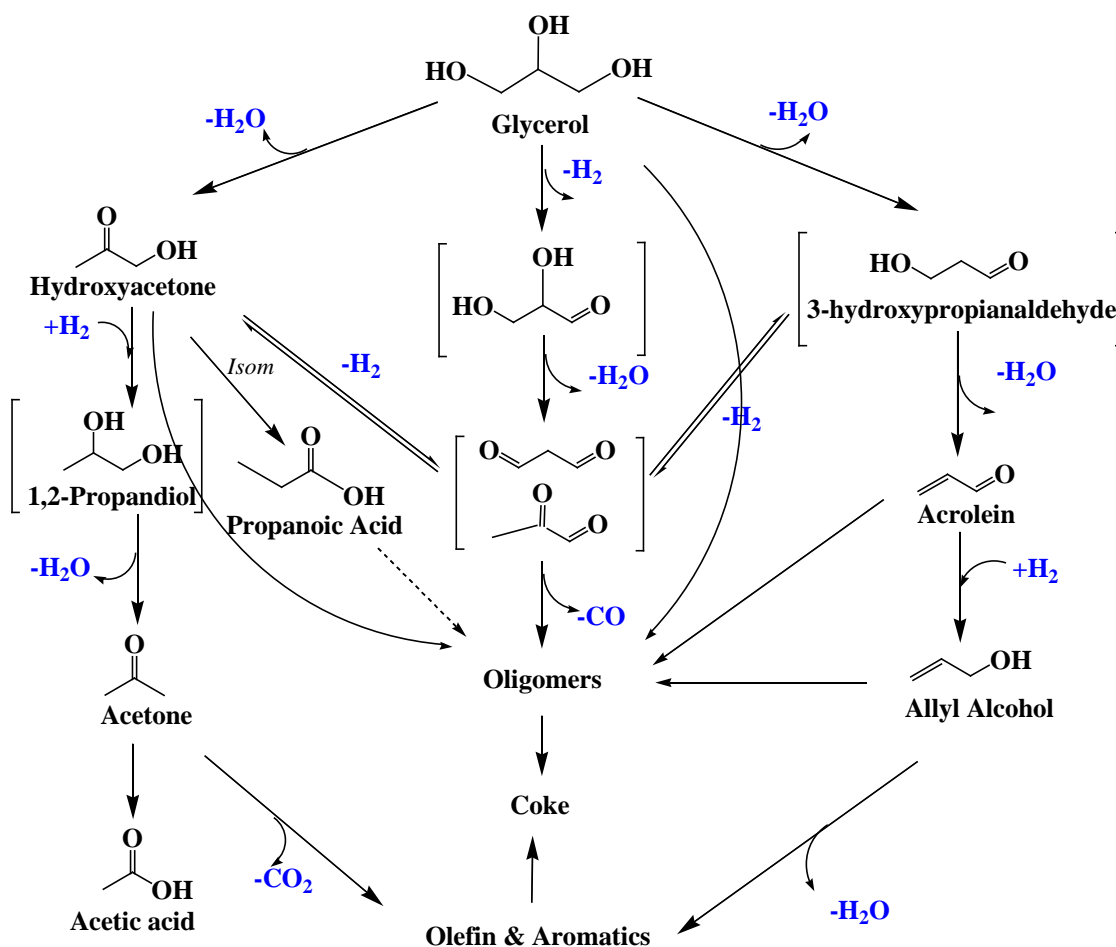
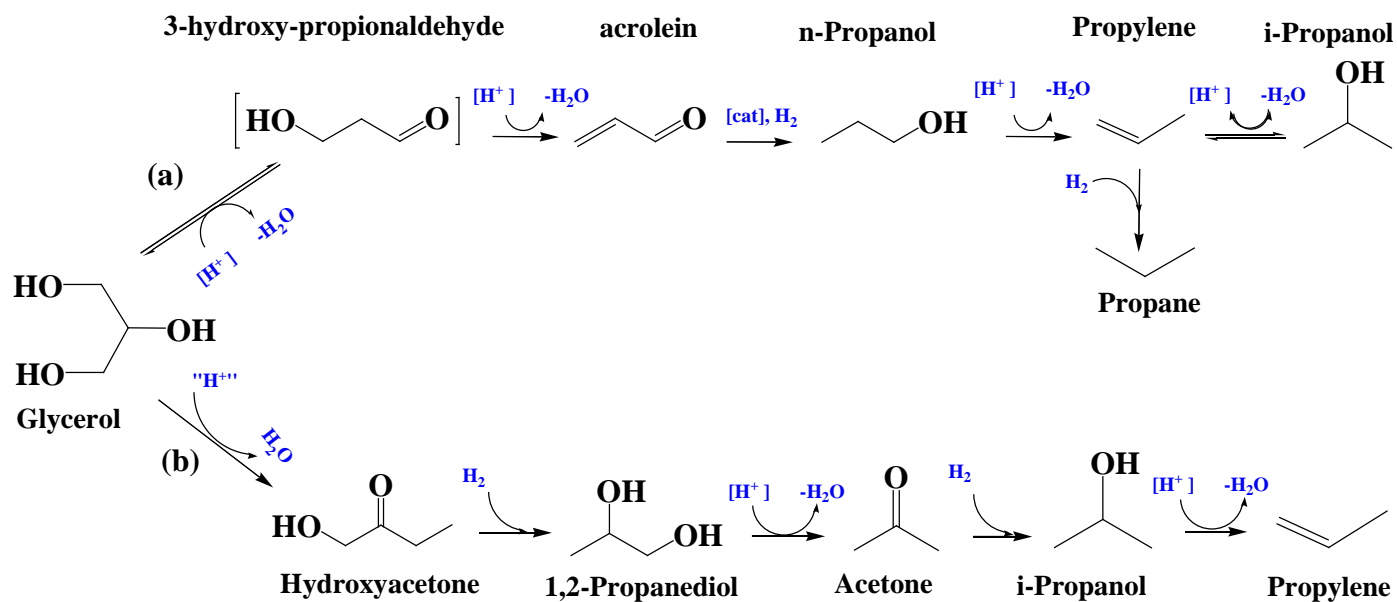


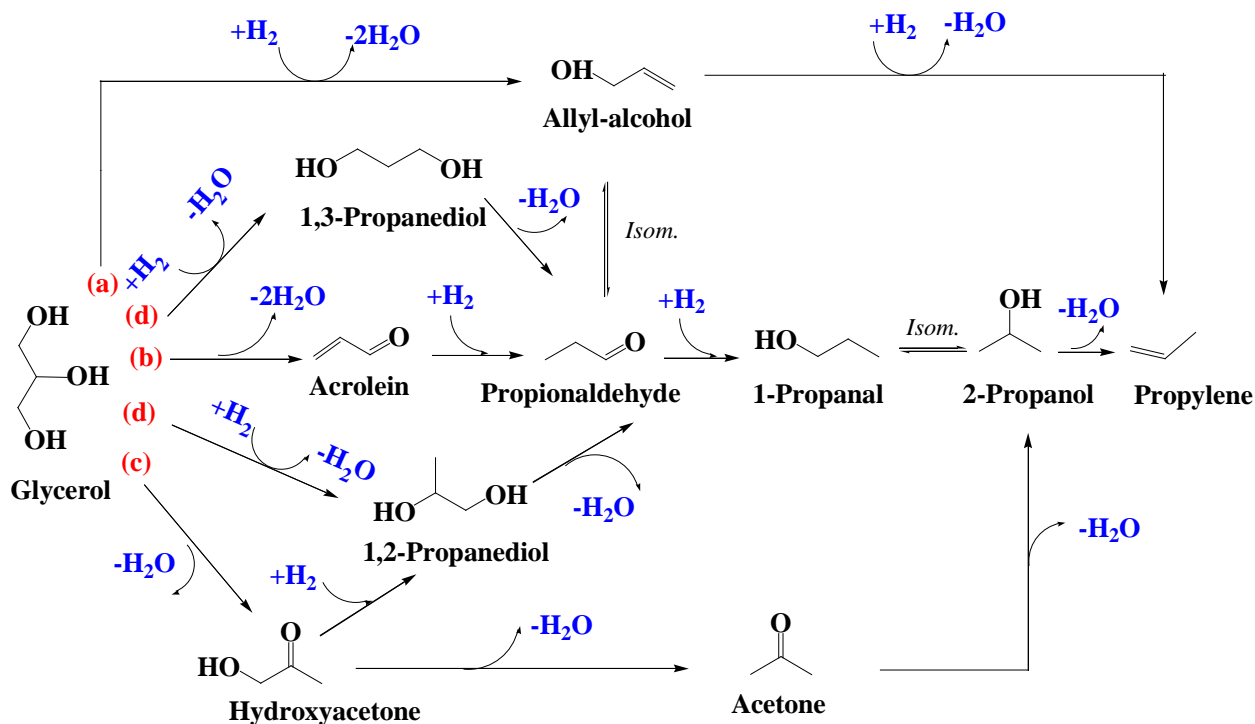
Fig. 6. A) Main steps of the combined preparation strategy involving hydrothermal synthesis, melt infiltration, and the reduction or carburization treatment of Mo oxides or carbide-based silica catalysts. B-C) TEM-HAADF images, including STEM-EDX mapping and histograms of Mo nanoparticle size distribution for fresh MoO_x@SBA-15 catalyst (left) and spent MoO_x@SBA-15R/U catalyst (right). Reproduced with permission from ref.⁶⁰ Copyright 2023 Elsevier.



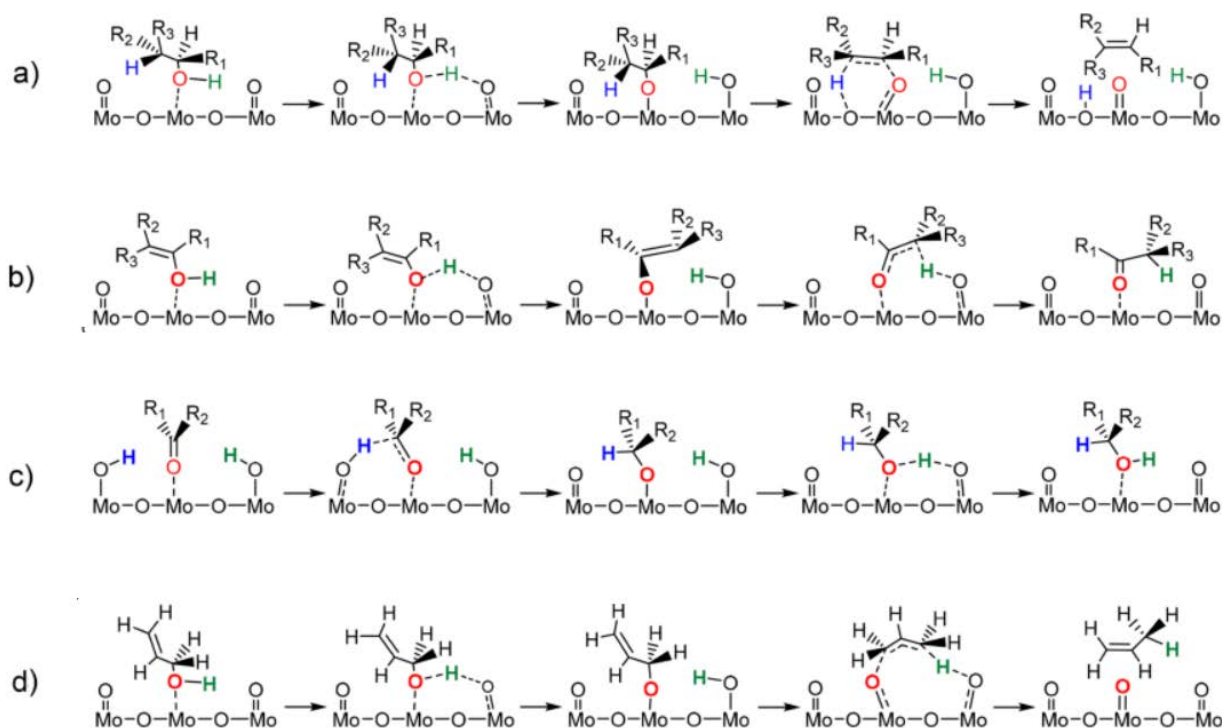
Scheme 4. Integral reaction pathways for the high-temperature catalytic cracking of glycerol conversion to olefins and the other main intermediates and co-products. Reproduced with permission from ref. ⁶⁶ Copyright 2008 Elsevier.



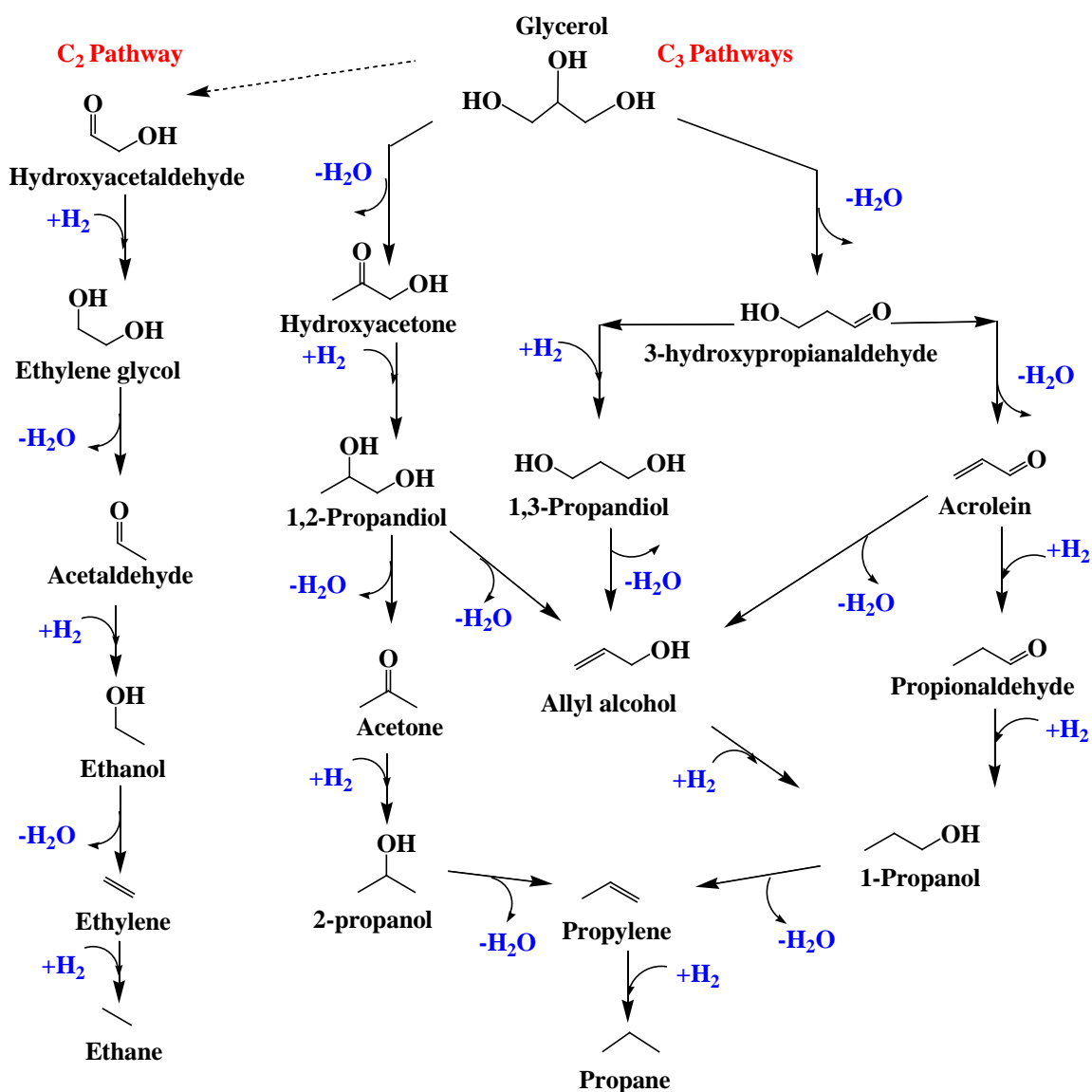
Scheme 5. a) Early cascade dehydration and hydrogenation events for the direct conversion of glycerol to propylene; b) updated glycerol-to-propylene pathway. Gathered with permission from ref.⁵⁵ Copyright 2016 Elsevier. from ref.⁵⁷ Copyright 2009 Wiley Online Library. from ref.⁵⁴ Copyright 2011 American Chemical Society.



Scheme 6. Four main reaction pathways for glycerol conversion to propylene over an MoO_x based catalyst *via* the following intermediates: a) allyl-alcohol, b) acrolein, c) hydroxyacetone, and d) C₃-diols. Gathered with permission from ref. ⁵⁹ Copyright 2018 Wiley Online Library



Scheme 7. Chemical rearrangements for forming the C=C bonds over uncoordinated Mo sites through the initial dehydration of glycerol (a), enol equilibrium (b), subsequent hydrogenation (c), and the final formation of an allyl-alcohol intermediate (d). Reproduced with permission from ref. ³⁷ Copyright 2018 American Chemical Society.



Scheme 8. Main C₃ and C₂ pathways for the complete HDO of glycerol to propylene or propane and ethylene or ethane over an NiMo-based catalyst operating under typical hydro-pyrolysis conditions. Reproduced with permission from ref. ⁴⁶ Copyright 2018 Wiley Online Library

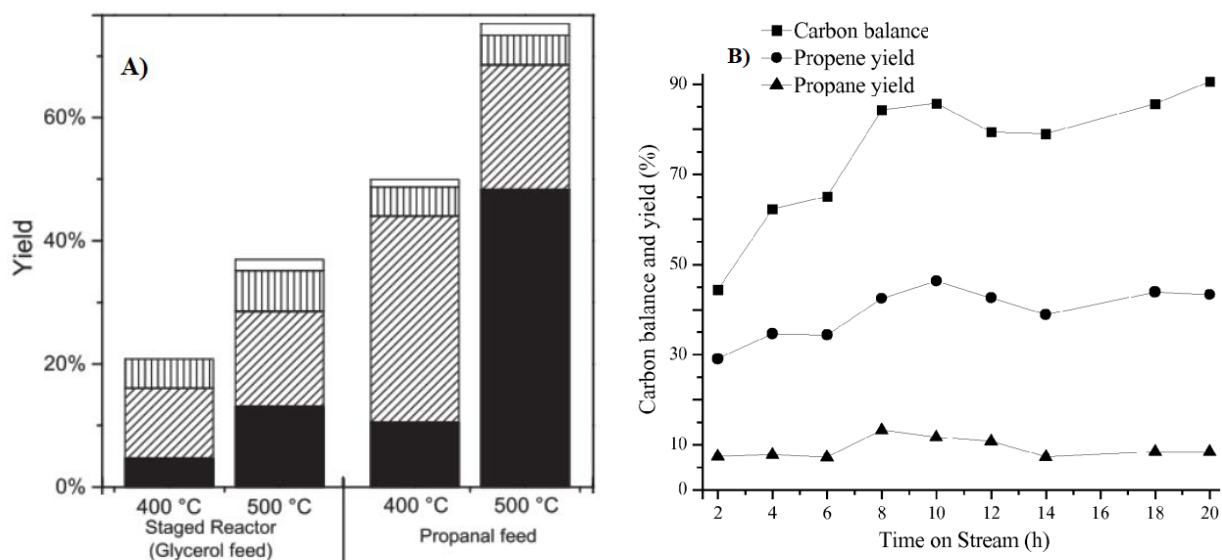


Fig. 7. A) Distribution of olefin yield; C₂₋₃ (■), C₄₋₅ (▨), C₆₋₇ (▧) and C₈₋₉ (□) formed during the feed of glycerol in staged three reactors, and of pure propanal in a single reactor (H-BEA zeolite) at 400 °C and 500 °C, WHSV ~11.2 h⁻¹, TOS ~10 min. Reproduced with permission from ref.⁵⁰ Copyright 2014 Elsevier. **B)** the yield of propylene and propane formed during the feed of glycerol through three separate catalytic steps involving WO₃/ZrO₂, Cu/ZnO₂ and WO₃/ZrO₂ catalysts tested at 280 °C, 270 °C, and 208 °C, respectively.⁶⁴

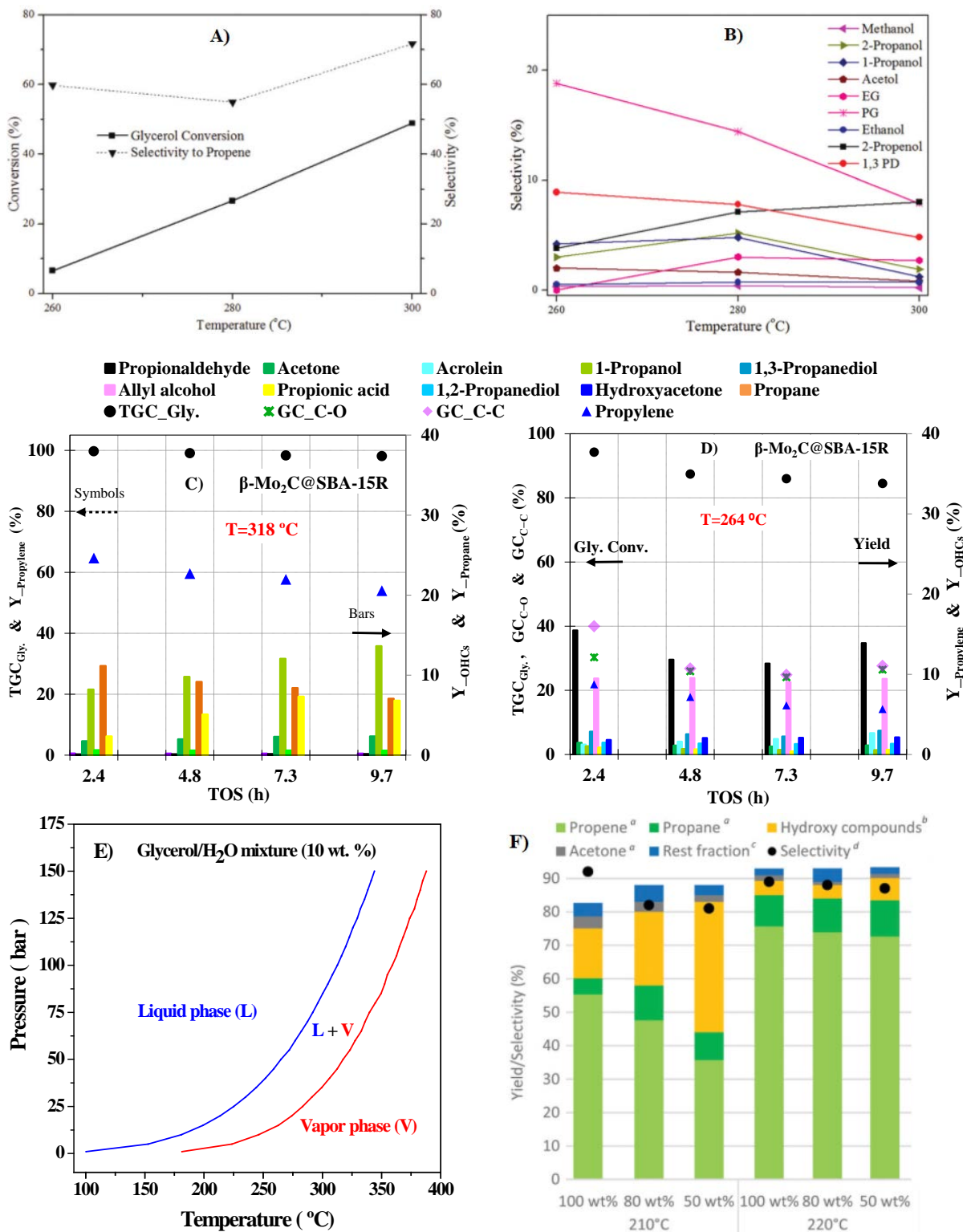


Fig. 8. Effect of temperature on glycerol conversion and propylene selectivity (A) and on oxygenate selectivity (B) over the FeMo/Carbon (80 bar, H₂/glycerol (*mol.*) ratio ~ 53:1, glycerol/H₂O ~ 2 wt%, TOS ~ 2 h). Reproduced with permission from ref.⁴⁸ Copyright 2015 Royal Society of Chemistry. Total glycerol conversion (TGC), deoxygenation (GC_{C-O}), hydrogenation (GC_{C-C}), and the yield of propylene and byproducts over an β -Mo₂C@SBA-15R catalyst tested at 318 °C (C) and 264 °C (D), glycerol/H₂O ~ 10 wt%, 50 bar, H₂/glycerol ~ 78 and WHSV ~ 2.35 h⁻¹. Existence of gas-liquid phases for glycerol/H₂O mixture ~ 10 wt% (E). Reproduced with permission from ref.⁶⁰ Copyright 2023 Elsevier. Yield^{a,b,c} and Selectivity^d provided by the single-step HDO of glycerol/H₂O mixture (50-100 wt%) over an Ru-based catalyst at 210 °C and 220 °C (F). Reproduced with permission from ref.⁴³ Copyright 2021 Royal Society of Chemistry.

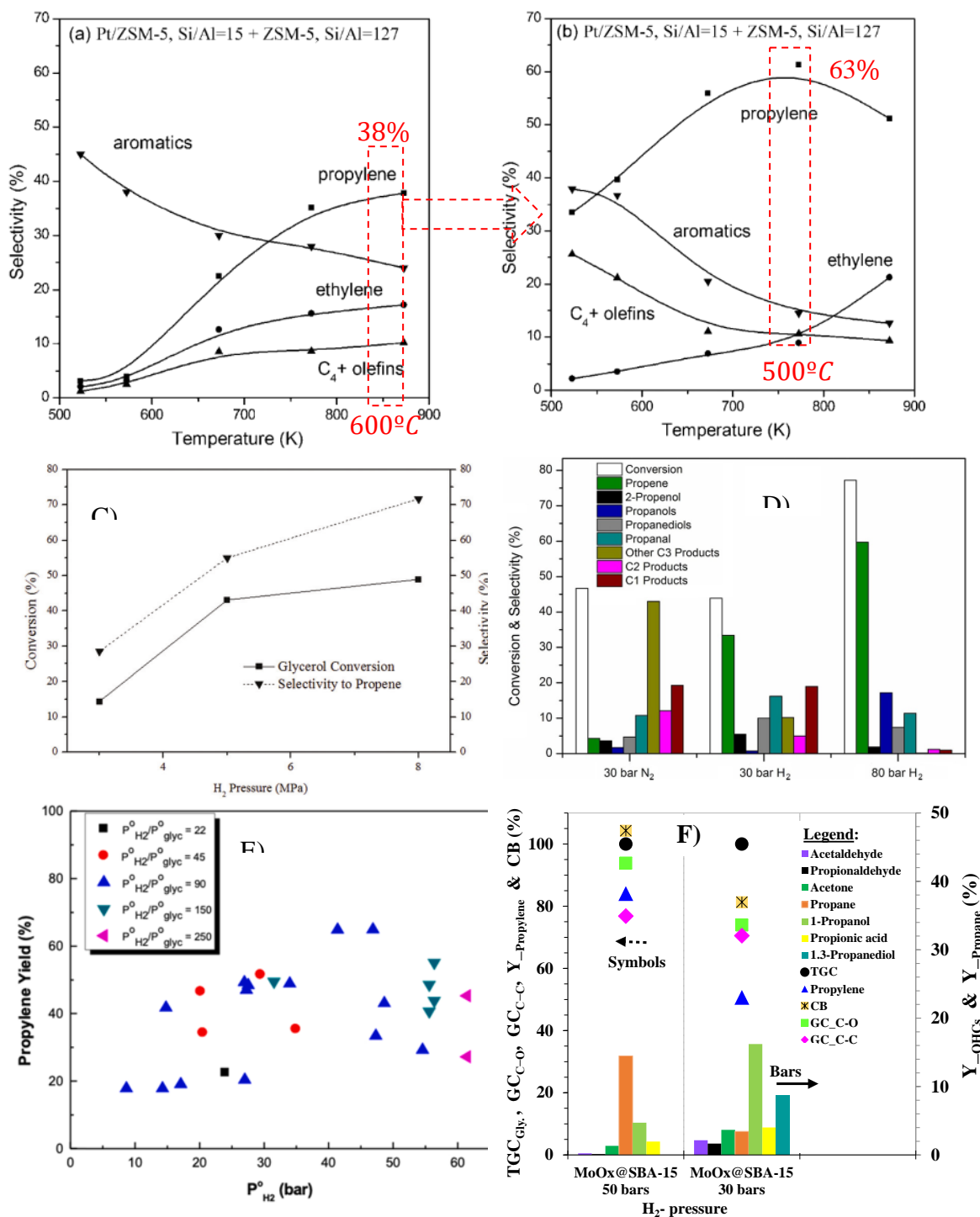
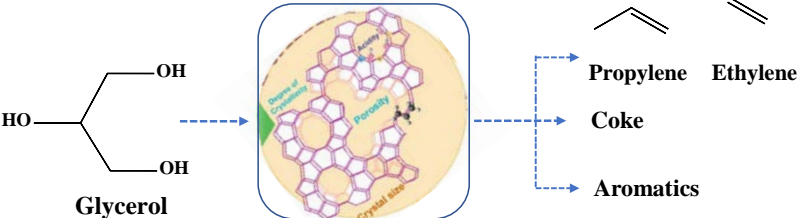
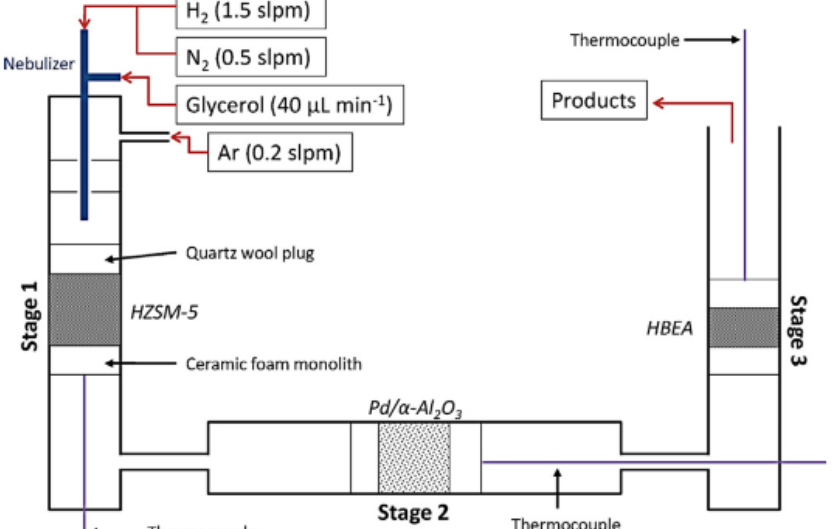
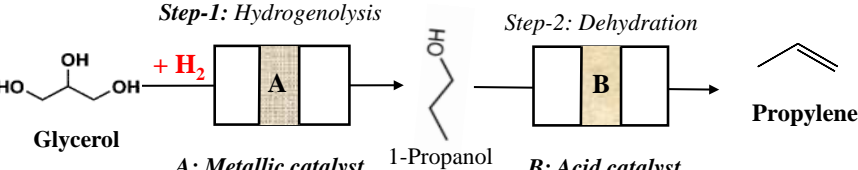
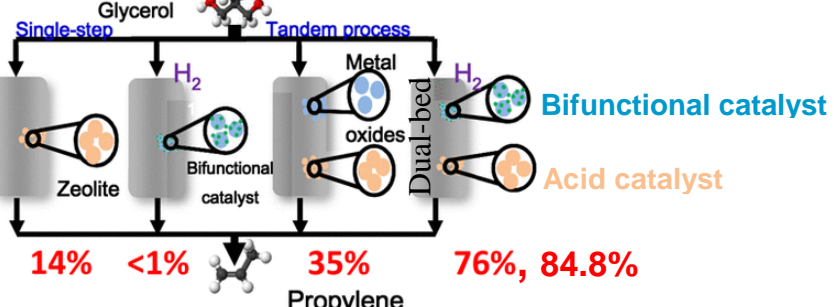
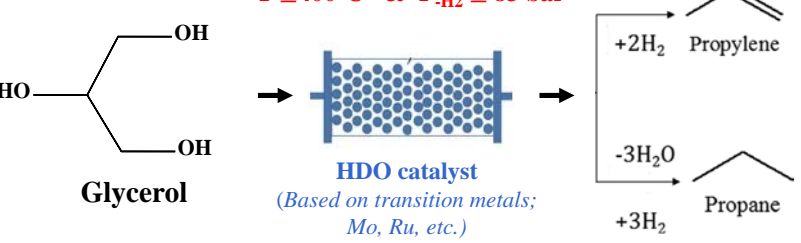


Fig. 9. Effect of H₂ partial pressure on the selectivity of olefins and aromatics over double-bed catalysts (Pt/ZSM-5 + ZSM-5); **A)** without H₂ (21.9 kPa glycerol, 28.1 kPa methanol, 50 kPa glycerol, WHSV = 1 h⁻¹, 30 min), and **B)** with H₂ (1.0 kPa glycerol, 1.2 kPa methanol, 2.2 kPa H₂O, 95.6 kPa H₂, WHSV = 0.5 h⁻¹, 30 min). Reproduced with permission from ref.²⁸ Copyright 2016 American Chemical Society. **C-D)** Effect of N₂ or H₂ atmosphere on glycerol conversion and product selectivity over FeMo/carbon (300 °C, glycerol/H₂O ~ 2 wt%, catalyst/Substrate ratio ~ 0.83, TOS ~ 2 h). Reproduced with permission from ref.⁴⁸ Copyright 2015 Royal Society of Chemistry. from ref.⁵⁹ Copyright 2018 Wiley Online Library. **E)** Effect of H₂ partial pressure on propylene yield as a function of H₂ to glycerol partial pressure ratio over Mo (8 wt%)-based Carbon catalyst (at 280 °C, glycerol/H₂O ~ 10 wt%, H₂/glycerol molar ratio ~ 22-250, total pressure ~ 70 bar, W/F ~ 195 g_{cat}/mol_{gly}.h, TOS ~ 4.8 h). Reproduced with permission from ref.⁶² Copyright 2022 Elsevier. **F)** effect of total H₂ pressure on the variation of total glycerol conversion (TGC) by deoxygenation (GC_{C-O}) and by hydrogenation (GC_{C-C}), carbon balance (CB), and on the yield of propylene and main byproducts over MoO_x (14.8 wt%)-based SBA-15 (318 °C, glycerol/H₂O ~ 10 wt%), H₂/glycerol molar ratio ~ 98, WHSV ~ 1.7 h⁻¹, TOS ~ 4.8 h). Reproduced with permission from ref.⁶⁰ Copyright 2023 Elsevier.

Description	Schematic illustration
<p>a) High-temperature GTP involving simultaneous dehydration, cracking, and hydrogen transfers over acid zeolites</p>	<p style="text-align: center;">$T > 400\text{ }^\circ\text{C}$ & inert atmosphere</p>  <p style="text-align: center;">Glycerol</p>
<p>b) Cascade GTP in triple-stage catalytic reactors. Reproduced with permission from ref.⁵⁰ Copyright 2014 Elsevier.</p>	
<p>c) GTP route in separate double steps involving 1st hydrogenolysis and 2nd dehydration</p>	<p style="text-align: center;"><i>Step-1: Hydrogenolysis</i></p>  <p style="text-align: center;"><i>Step-2: Dehydration</i></p> <p style="text-align: center;">A: Metallic catalyst B: Acid catalyst</p>
<p>d) Tandem or dual-bed GTP processes including bifunctional and acid catalysts. Reproduced with permission from ref.²⁸ Copyright 2016 American Chemical Society.</p>	 <p style="text-align: center;">14% <1% 35% 76%, 84.8%</p> <p style="text-align: center;">Propylene</p>
<p>e) Single-step GTP via simultaneous deoxygenation-hydrogenation</p>	<p style="text-align: center;">$T \leq 400\text{ }^\circ\text{C}$ & $P_{\text{H}_2} \leq 83\text{ bar}$</p>  <p style="text-align: center;">HDO catalyst (Based on transition metals; Mo, Ru, etc.)</p>

Scheme 9 (a-e). Main configuration strategies for converting glycerol to propylene

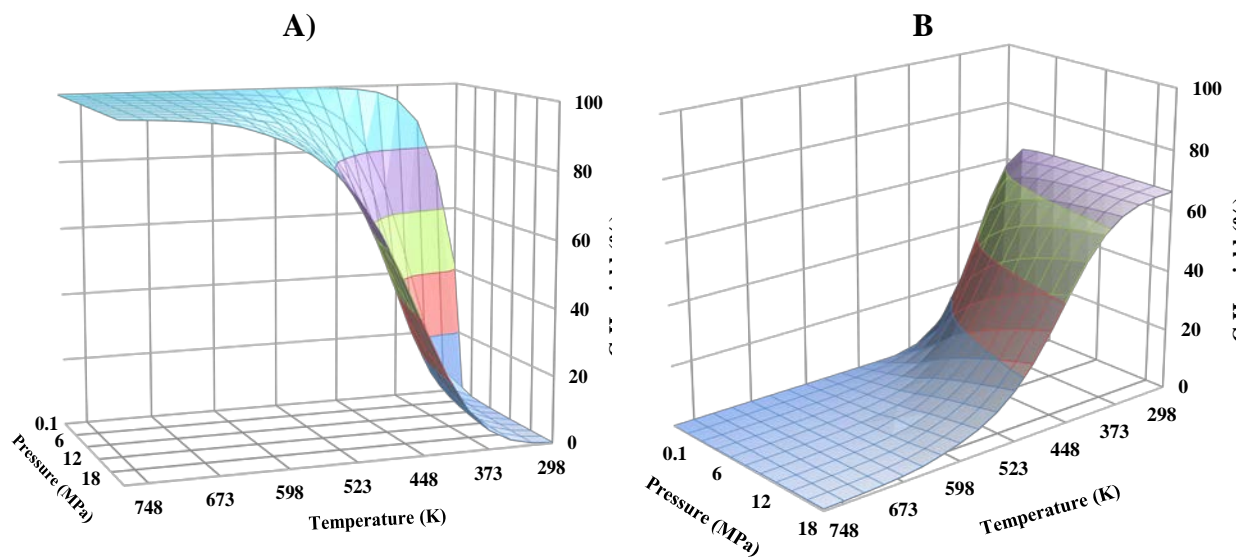


Fig. 10. Equilibrium yields of propylene (A) and propane (B) formed from the full HDO of glycerol as a function of temperature and total pressure. Calculation conditions: a Gibbs reactor (RGIBBS), Peng-Robinson equation of state (PENG-ROB), glycerol/H₂O mass ratio (10/90 wt%), and stoichiometric H₂/glycerol (*mol*) ratio.